

SILICON TETRACHLORIDE MEDIATED ASYMMETRIC ALDOL ADDITION REACTION

A THESIS SUBMITTED TO
GRADUATE SCHOOL OF NATURAL AND APPLIED SCIENCES
OF
MIDDLE EAST TECHNICAL UNIVERSITY

BY

DUYGU TAN

IN THE PARTIAL FULLFILMENT OF THE REQUIREMENTS
FOR
THE DEGREE OF MASTER OF SCIENCE
IN
CHEMISTRY

JANUARY 2013

Approval of the thesis:

SILICON TETRACHLORIDE MEDIATED ASYMMETRIC ALDOL ADDITION REACTION

submitted by **Duygu TAN** in partial fulfillment of the requirements for the degree of **Master of Science in Chemistry Department, Middle East Technical University** by,

Prof. Dr. Canan Özgen
Dean, Graduate School of **Natural and Applied Sciences**

Prof. Dr. İlker Özkan
Head of Department, **Chemistry**

Prof. Dr. Özdemir Doğan
Supervisor, **Chemistry Dept., METU**

Examining Committee Members:

Prof. Dr. Lemi Türker
Chemistry Dept., METU

Prof. Dr. Özdemir Doğan
Chemistry Dept., METU

Prof. Dr. Metin Zora
Chemistry Dept., METU

Assoc. Prof. Dr. Adnan Bulut
Chemistry Dept., Kırıkkale University

Assist. Prof. Dr. Akın Akdağ
Chemistry Dept., METU

Date: 23.01.2013

I hereby declare that all information in this document has been obtained and presented in accordance with academic rules and ethical conduct. I also declare that, as required by these rules and conduct, I have fully cited and referenced all material and results that are not original to this work.

Name, Last name: Duygu TAN
Signature:

ABSTRACT

SILICON TETRACHLORIDE MEDIATED ASYMMETRIC ALDOL ADDITION REACTION

TAN, Duygu

M.Sc., Department of Chemistry

Supervisor: Prof. Dr. Özdemir Doğan

January 2013, 92 Pages

Aldol addition reaction is one of the most important and most studied carbon-carbon bond forming reactions in organic chemistry. Recent studies focused on the catalytic version of this chemistry. Different from the classical Mukaiyama-type aldol reactions, chiral Lewis bases have been used as promoters. In the presence of SiCl_4 , these reactions proceed through a cyclic transition state leading to *anti* aldol product as a major product with moderate-to-good diastereo and enantioselectivities. Phosphoramidate derivatives, BINAPO, BINAPO derivatives, *N,N*-dioxides and *N*-oxides have been extensively used for this purpose.

Recently, our group has designed new phosphine oxy aziridinyl phosphonates (**POAP**) as chiral Lewis bases. These promoters were used for the asymmetric aldol addition reaction between cyclohexanone and different aldehydes in the presence of SiCl_4 . Moreover, our previously designed phosphine oxy ferrocenyl substituted aziridinyl methanol (**POFAM**) ligands were also tested as Lewis bases. Among these 6 potential promoters, **POAP-A** gave the best results, and the aldol product were obtained in moderate to good yields up to 80%, and with moderate enantioselectivities (the highest, 66%) after standard optimization studies. Aldehyde screening experiments provided the highest enantioselectivity (68%) with 2-naphthaldehyde.

Keywords: Asymmetric synthesis, Lewis base organocatalyst, aldol, silicon tetrachloride

ÖZ

SİLİKON TETRAKLORÜR VARLIĞINDA ASİMETRİK ALDOL KATILMASI TEPKİMESİ

TAN, Duygu

Yüksek Lisans, Kimya Bölümü

Tez Yöneticisi: Prof. Dr. Özdemir Doğan

Ocak 2013, 92 Sayfa

Aldol katılması organik kimyadaki en önemli ve en çok çalışılan karbon-karbon bağ oluşumu tepkimelerinden biridir. Son çalışmalar, bu kimyanın katalitik versiyonları üzerine odaklanmıştır. Klasik Mukaiyama tipi aldol tepkimelerinden farklı olarak, son zamanlarda kiral Lewis bazları katalizör olarak kullanılmaktadır. SiCl_4 varlığında bu tepkimeler *anti* ürünün iyi diastereo ve enantioseçicilikle ana ürün olarak oluşmasını sağlayan siklik geçiş ürünü ile ilerler. Fosforamid türevleri, BINAPO ve türevleri, *N,N'*-dioksitler ve *N*-oksitler bu amaç için yaygın olarak kullanılmıştır.

Grubumuz son zamanlarda yeni fosfin oksit aziridinil fosfonatları (**POAP**) organokatalizör olarak tasarlamıştır. Bu organokatalizörler, SiCl_4 varlığında sikloheksanon ve farklı aldehitler arasında gerçekleşen asimetrik aldol katılması tepkimelerinde kullanılmıştır. Ayrıca, daha önceden tasarlanan fosfin oksit ferrosenil sübstitüe aziridinil metanol (**POFAM**) ligandları da Lewis bazı olarak test edilmiştir. Bu 6 potansiyel kiral Lewis bazlarının arasında, en iyi sonuçları **POAP-A** vermiştir, ve standart optimizasyon çalışmalarının ardından aldol ürünleri iyi verimlerle (%80'e kadar) ve iyi enantioseçiciliklerle (en yüksek %66) elde edilmiştir. Aldehit taraması çalışmaları en iyi enantioseçiciliği (%68) 2-naftaldehit ile sağlamıştır.

Anahtar kelimeler: Asimetrik sentez, Lewis bazı organokatalizör, aldol, silikon tetraklorür

To my family and my husband...

ACKNOWLEDGEMENTS

“ Learn from yesterday, live for today, hope for tomorrow. The most important thing is not stop questioning.”

Albert Einstein

This thesis describes my efforts that I have been spending over two years to be successful in finishing my studies and be in the place I am right now. I cannot explain the satisfaction of being in this position after taking responsibility of asking a scientific question and searching for the answer over two years. I strongly suggest undergraduate students to participate in such a scientific journey. Of course, without the helps, supports, encouragements, endorsements and inspirations of many people, this study would have never been completed. Herein, I wish to acknowledge them.

I would like to emphasize my gratitude to my supervisor Prof. Dr. Özdemir Doğan since he gave me the opportunity to improve myself, gain insights, and he allowed me to involve systematically in every aspects of scientific processes starting from very beginning to the end. Thanks to him, I learned critical thinking, being patient, being insistent, and how to overcome several difficulties that I have faced during my master studies.

I would like to thank to Assoc. Prof. Dr. Adnan Bulut for his valuable scientific discussions, and constructive recommendations. I am also thankful to Assist. Prof. Dr. Müjgan Özkütük since she created a warm environment in our laboratory with her maternal attitude towards us.

I would like to thank to TUBITAK (TBAG 110T073) and BAP for their financial support.

I would like to thank to D-block Organic Chemistry members, especially Yılmaz Kelgökmen and Yağız Ünver, due to their sincere friendships, helps, moral and technical supports. Moreover, I would like to thank to Sadullah Polat since he always helped me about thesis formatting and technical issues related to computer software without being sickened with it.

My greatest appreciations go to Muhammet İşci and Eda Çağlı since they have always been much more than a usual collaborator for me. They have always encouraged me to advance and finish my studies. Whenever I have been in trouble, they have always been with me. We laughed and cried together, we shared everything throughout two years. Everything became easy for me to handle thanks to their reinforcements, they have been my ‘catalysts’.

Furthermore, I wish to thank to my best friends, Nurcan Tozluyurt, Döndü Özütürk, Özge Özgen, Eda Karadeniz, Deniz Demirci and Muhammet Tanç for their interests on every stage of my master studies. Throughout the years, I have always felt their supports with me which enabled to draw me up. I cannot replace their precious friendship with anything since we ‘grew up’ together.

Last, but certainly not least, my most special and deepest appreciations and gratitude are devoted to the people who have the greatest impact on my life, my parents Sema Aksakal, Turgut Aksakal, my dear brother Kadir Oğuz Aksakal and my lovely husband Serkan Tan even because they are present in my life. I cannot explain my exact feelings about how they are special to me by using simple words. They have always believed in me expecting nothing. My ultimate desire has been to work to be worthy of their endless love, patience, encouragement, support, etc..., in the absence of which I would do nothing.

TABLE OF CONTENTS

ABSTRACT	v
ÖZ.....	vi
ACKNOWLEDGEMENTS	viii
TABLE OF CONTENTS	ix
LIST OF TABLES.....	xii
LIST OF FIGURES.....	xiii
LIST OF SCHEMES.....	xvi
LIST OF ABBREVIATIONS.....	xviii
CHAPTERS	
1. INTRODUCTION.....	1
1.1. Chirality.....	1
1.2. Asymmetric synthesis.....	2
1.2.1. Asymmetric catalysis	3
1.2.1.1. Metal ligand complexes	3
1.2.1.2. Organocatalysis	4
1.3. Hypervalent silicon species in asymmetric organocatalysis	4
1.3.1. Reactions involving hypervalent silicon species.....	7
1.3.1.1. Epoxide ring-opening reactions	7
1.3.1.2. Enantioselective addition of trialkylphosphites to aldehydes.....	9
1.3.1.3. Addition of allenylsilane and propargylsilane to aldehydes.....	11
1.3.1.4. Stereoselective C-C bond formation reaction.....	13
1.3.1.4.1. Asymmetric allylation	13
1.3.1.4.2. Asymmetric aldol addition.....	16
1.4. Aim of work.....	22
2. RESULTS AND DISCUSSION	23
2.1. The synthesis of POFAM ligands.....	23

2.2. The synthesis of POAP chiral Lewis bases	27
2.3. Silicon tetrachloride-mediated asymmetric aldol addition	29
2.3.1. Formation of silyl enol ether	29
2.3.2. Chiral Lewis base screening	30
2.3.3. Temperature, concentration and additive screening studies	34
2.3.4. Solvent screening studies	35
2.3.5. Further optimization studies	36
2.3.6. Aldehyde screening studies	39
3. CONCLUSION	43
4. EXPERIMENTAL	45
4.1. General procedure	45
4.2. Synthesis and characterization of acryloyl ferrocene	45
4.2.1. Synthesis and characterization of aziridino ketones 18 and 19	46
4.2.2. Synthesis and characterization of tosylated aziridino ketones 20 and 21	46
4.2.3. Synthesis and characterization of phosphino aziridines and phosphine oxy aziridines.....	47
4.2.4. Synthesis and characterization of PFAM and POFAM ligands from phosphino aziridine 22	48
4.2.5. Synthesis and characterization of PFAM and POFAM ligands from phosphino aziridine 24	49
4.3. Synthesis and characterization of 1,2-dibromoethyl phosphonate.....	50
4.3.1. Synthesis and characterization of aziridines 38 and 39	50
4.3.2. Synthesis and characterization of tosylated aziridines 40 and 41	51
4.3.3. Synthesis and characterization of phosphine oxy aziridines 42 and 43	51
4.4. Asymmetric studies.....	52
4.4.1. General procedure for silicon tetrachloride mediated asymmetric Aldol addition.....	52
4.4.1.1. 2-(Hydroxy(phenyl)methyl) cyclohexan-1-one	52
4.4.1.2. 2-(Hydroxy(4-methoxyphenyl)methyl) cyclohexan-1-one	53

4.4.1.3. 2-(Hydroxy(3-methoxyphenyl)methyl) cyclohexan-1-one.....	53
4.4.1.4. 2-(Hydroxy(2-methoxyphenyl)methyl) cyclohexan-1-one.....	53
4.4.1.5. 2-(Hydroxy(4-methylphenyl)methyl) cyclohexan-1-one.....	54
4.4.1.6. 2-(Hydroxy(naphthalen-2-yl)methyl) cyclohexan-1-one	54
4.4.1.7. 2-(Hydroxy(naphthalen-1-yl)methyl) cyclohexan-1-one	54
4.4.1.8. 2-(1-Hydroxy-3-phenyl-2-propenyl) cyclohexan-1-one.....	55
4.4.1.9. 2-(Hydroxy(4-trifluoromethyl)phenyl)methyl) cyclohexan-1-one.....	55
4.4.1.10. 2-(Hydroxy(4-nitrophenyl)methyl) cyclohexan-1-one	55
4.4.1.11. 2-(Hydroxy(3-nitrophenyl)methyl) cyclohexan-1-one	56
4.4.1.12. 2-(Hydroxy(2-nitrophenyl)methyl) cyclohexan-1-one	56
4.4.2. Preparation of racemic compounds.....	56
BIBLIOGRAPHY	57
APPENDIX.....	61
NMR SPECTRA AND HPLC CHROMATOGRAMS	61

LIST OF TABLES

TABLES

Table 1 Chiral Lewis base screening studies.....	33
Table 2 Results of temperature, concentration and additive screening studies	35
Table 3 Solvent screening studies	36
Table 4 Equivalency screening studies.....	37
Table 5 Results of concentration, benzaldehyde addition and time studies.....	38
Table 6 Aldehyde screening studies	40

LIST OF FIGURES

FIGURES

Figure 1 Some naturally occurring chiral compounds; morphine, heroine and taxol	1
Figure 2 Lewis base activation of Lewis acids	5
Figure 3 Participation of 3d orbitals in bonding	5
Figure 4 3-Center-4-Electron model for hypervalent bonding.....	6
Figure 5 Molecular orbital diagram for 3-center-4-electron hypervalent bonds	6
Figure 6 Chiral Lewis bases employed by Nakajima group	10
Figure 7 Hypervalent silicon based transition states.....	11
Figure 8 Catalytic cycle of asymmetric allylation reaction proposed by Denmark.....	13
Figure 9 Catalytic cycle for silicon tetrachloride mediated asymmetric aldol addition	18
Figure 10 Chiral <i>N</i> -oxides and <i>N,N'</i> -dioxides used by Nakajima and coworkers.....	19
Figure 11 Transition states leading to anti and syn aldol products	19
Figure 12 BINAPO derivatives tested by Kotani, Nakajima and their coworkers.....	21
Figure 13 FAM series ligands.....	26
Figure 14 X-ray structure of POAP-B	29
Figure 15 Two pathways of aldol addition.....	32
Figure 16 Reaction conditions adapted after standard optimization studies	36
Figure A. 1 ¹ H-NMR spectrum of compound 14	61
Figure A. 2 ¹ H-NMR spectrum of compound 18	62
Figure A. 3 ¹ H-NMR spectrum of compound 20	62
Figure A. 4 ¹ H-NMR spectrum of compound 22	63
Figure A. 5 ¹ H-NMR spectrum of compound 23	63
Figure A. 6 ¹ H-NMR spectrum of compound 26	64
Figure A. 7 ¹ H-NMR spectrum of compound 27	64

Figure A. 8 ^1H -NMR spectrum of compound 28	65
Figure A. 9 ^1H -NMR spectrum of compound 29	65
Figure A. 10 ^1H -NMR spectrum of compound 19	66
Figure A. 11 ^1H -NMR spectrum of compound 21	66
Figure A. 12 ^1H -NMR spectrum of compound 24	67
Figure A. 13 ^1H -NMR spectrum of compound 25	67
Figure A. 14 ^1H -NMR spectrum of compound 30	68
Figure A. 15 ^1H -NMR spectrum of compound 31	68
Figure A. 16 ^1H -NMR spectrum of compound 32	69
Figure A. 17 ^1H -NMR spectrum of compound 33	69
Figure A. 18 ^1H -NMR spectrum of compound 35	70
Figure A. 19 ^1H -NMR spectrum of compound 38	70
Figure A. 20 ^1H -NMR spectrum of compound 40	71
Figure A. 21 ^1H -NMR spectrum of compound 42	71
Figure A. 22 ^{13}C -NMR spectrum of compound 42	72
Figure A. 23 ^1H -NMR spectrum of compound 39	72
Figure A. 24 ^1H -NMR spectrum of compound 41	73
Figure A. 25 ^1H -NMR spectrum of compound 43	73
Figure A. 26 ^{13}C -NMR spectrum of compound 43	74
Figure A. 27 ^1H -NMR spectrum of compound 44	74
Figure A. 28 ^1H -NMR spectrum of compound 45	75
Figure A. 29 ^1H -NMR spectrum of compound 46	75
Figure A. 30 ^1H -NMR spectrum of compound 47	76
Figure A. 31 ^1H -NMR spectrum of compound 48	76
Figure A. 32 ^1H -NMR spectrum of compound 49	77
Figure A. 33 ^1H -NMR spectrum of compound 50	77
Figure A. 34 ^1H -NMR spectrum of compound 51	78

Figure A. 35 ¹ H-NMR spectrum of compound 52	78
Figure A. 36 ¹ H-NMR spectrum of compound 53	79
Figure A. 37 ¹ H-NMR spectrum of compound 54	79
Figure A. 38 ¹ H-NMR spectrum of compound 55	80
Figure A. 39 HPLC chromatogram of 44	80
Figure A. 40 HPLC chromatogram of racemic mixture of 44	81
Figure A. 41 HPLC chromatogram of 45	81
Figure A. 42 HPLC chromatogram of racemic mixture of 45	82
Figure A. 43 HPLC chromatogram of 46	82
Figure A. 44 HPLC chromatogram of racemic mixture of 46	83
Figure A. 45 HPLC chromatogram of 47	83
Figure A. 46 HPLC chromatogram of racemic mixture of 47	84
Figure A. 47 HPLC chromatogram of 48	84
Figure A. 48 HPLC chromatogram of racemic mixture of 48	85
Figure A. 49 HPLC chromatogram of 49	85
Figure A. 50 HPLC chromatogram of racemic mixture of 49	86
Figure A. 51 HPLC chromatogram of 50	86
Figure A. 52 HPLC chromatogram of racemic mixture of 50	87
Figure A. 53 HPLC chromatogram of 51	87
Figure A. 54 HPLC chromatogram of racemic mixture of 51	88
Figure A. 55 HPLC chromatogram of 52	88
Figure A. 56 HPLC chromatogram of racemic mixture of 52	89
Figure A. 57 HPLC chromatogram of 53	89
Figure A. 58 HPLC chromatogram of racemic mixture of 53	90
Figure A. 59 HPLC chromatogram of 54	90
Figure A. 60 HPLC chromatogram of racemic mixture of 54	91
Figure A. 61 HPLC chromatogram of 55	91
Figure A. 62 HPLC chromatogram of racemic mixture of 55	92

LIST OF SCHEMES

SCHEMES

Scheme 1 The first study of ring-opening of meso-epoxides	7
Scheme 2 <i>N</i> -oxide catalyzed epoxide ring-opening reaction	8
Scheme 3 Results of the studies of Nakajima and coworkers.....	8
Scheme 4 Reaction conditions and results of the study of Ready and coworkers.....	9
Scheme 5 Asymmetric Abramov type phosphonylation	9
Scheme 6 Results of Dogan and co-workers	10
Scheme 7 Selective synthesis of allenic and homopropargylic alcohols.....	11
Scheme 8 The first catalytic enantioselective allenylation of aldehydes	12
Scheme 9 Asymmetric allenylation and propargylation using chiral <i>N</i> -oxide	12
Scheme 10 Asymmetric allylation with phosphoramidate derivatives	14
Scheme 11 Asymmetric allylation in the presence of 5	14
Scheme 12 Asymmetric allylation with (<i>S</i>)-3,3'-dimethyl-2,2'-biquinoline <i>N,N'</i> -dioxide.....	15
Scheme 13 2,2'-bipyridine <i>N,N'</i> -dioxide catalyzed asymmetric allylation.....	15
Scheme 14 Asymmetric allylation with (<i>S</i>)-BINAPO.....	16
Scheme 15 Asymmetric allylation with (<i>S</i>)- <i>tetra</i> -Me-BITIOPO	16
Scheme 16 Synthesis of trichlorosilylenolate of cyclohexanone	17
Scheme 17 Asymmetric aldol addition with phosphoramidate derivatives.....	17
Scheme 18 Results of Nakajima and coworkers for the asymmetric aldol reaction.....	20
Scheme 19 Results obtained with SiCl ₃ OTf	21
Scheme 20 Results of asymmetric aldol reaction with (<i>S</i>)- <i>tetra</i> -Me-BITIOPO.....	22
Scheme 21 Synthesis of acryloyl ferrocene.....	23
Scheme 22 Bromination of acryloyl ferrocene	23
Scheme 23 Synthesis of aziridino ketones	24

Scheme 24 Synthesis of tosylated products	24
Scheme 25 Synthesis of PFAM 1 (22) and PFAM 2 (24) and their oxide forms	25
Scheme 26 Reduction of PFAM1 for the synthesis of PFAM3 (26) and PFAM4 (28) and their oxide forms	25
Scheme 27 Reduction of PFAM2 for the synthesis of PFAM5 (30) and PFAM6 (32) and their oxide forms	26
Scheme 28 Synthesis of 1,2-dibromoethyl phosphonate.....	27
Scheme 29 Synthesis of aziridines	27
Scheme 30 Synthesis of tosylated aziridines	28
Scheme 31 Synthesis of POAP-A and POAP-B	28
Scheme 32 Methods for the synthesis of silyl enol ether	30
Scheme 33 Corresponding aldol reaction and chiral Lewis bases	31

LIST OF ABBREVIATIONS

BINAPO	: Bis-(diphenylphosphanyl)-binaphthyl dioxide
br	: Broad singlet
δ	: Chemical shift in parts per million downfield from tetramethylsilane
J	: Coupling constant
d	: Doublet (spectral)
DABCO	: 1,4-Diazabicyclo [2.2.2] octane
1, 2-DCE	: 1,2-Dichloroethane
DIPEA	: Diisopropylethylamine
dr	: Diastereomeric ratio
dt	: Doublet of triplets (spectral)
dd	: Doublet of doublet (spectral)
Fc	: Ferrocenyl
FAM	: Ferrocenyl substituted Aziridiny Methanol
HMPA	: Hexamethylphosphoramide
m	: Multiplet (spectral)
PFAM	: Phosphino Ferrocenyl Aziridiny Methanol
POAP	: Phosphine oxy Aziridiny Ahosphonate
POFAM	: Phosphine oxy Ferrocenyl Aziridiny Methanol
Proton sponge	: 1,8-Bis(dimethylamino)naphthalene
q	: Quartet (spectral)
R_f	: Retention factor (TLC)

t_R : Retention time (in HPLC)
s : Singlet (spectral)
tbp : Trigonal bipyramidal
TMEDA : Tetramethylethylenediamine
TMS : Tetramethylsilane, also Trimethylsilyl
t : Triplet (spectral)

CHAPTER 1

INTRODUCTION

1.1. Chirality

In 1678, Huygens postulated that the light consists of longitudinal and transverse waves. It was in 1808 that the light was found to be polarized by reflection at specific angles from a polished surface. Following these findings, the first polarimeter was developed by Biot who was the first to show that natural products have had optical activities, meaning that they were able to rotate plane polarized light [1]. Pasteur related this property of molecules to the asymmetric grouping of atoms. After Kekulé stated that carbon has four valences, it was Van't Hoff and Le Bel who were arranged these four valences in a tetrahedral arrangement. These developments prepared a stage for the idea that the carbon having four different substituents was recognized to exist as non-superimposable mirror images which rotate the plane polarized light and named to be 'chiral' [1,2].

Nature provides the richest source of chiral compounds, and this source has been named as 'chiral pool' [2]. Some examples of naturally occurring compounds with chiral centers are given below (Figure 1) [3].

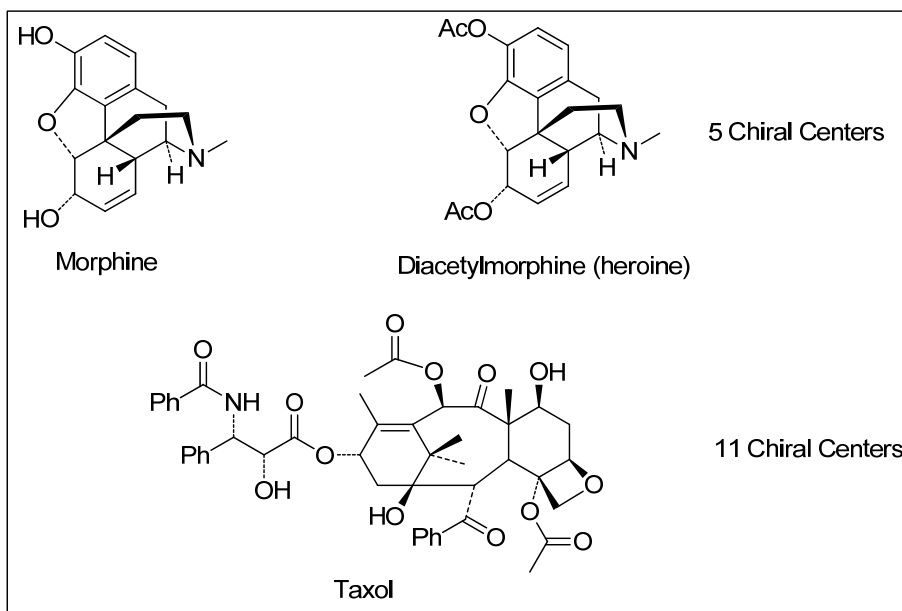


Figure 1 Some naturally occurring chiral compounds; morphine, heroine and taxol

The nature's chiral pool has a limited scope; thus, much effort has been spent to find new, simple and efficient methods to obtain these natural chiral products or their derivatives synthetically [4]. Thus, synthetic organic chemists wish to synthesize novel chiral molecules besides mimicking the natural products [3].

1.2. Asymmetric synthesis

Asymmetric synthesis has been one of the frontiers of organic chemistry. The earliest and most cited definition for the asymmetric synthesis was given by Willy Marckwald in 1904 [5]. He defines it as:

'Asymmetric synthesis are those reactions which produce optically active substances from symmetrically constituted compounds with the intermediate use of optically active materials but with the exclusion of all analytical processes.' [5]

His definition can be simplified by defining asymmetric synthesis as the conversion of an achiral substance into a chiral one by the action of a chiral reagent [5].

It has been the major promise of organic chemists to synthesize enantiopure amino acids, amino alcohols, amines, alkaloids, steroids, alcohols and epoxides which are crucial intermediates for pharmaceutical industry, and agrochemistry. Production of enantiopure substances with high purity and in high yields are required [6]. For this purpose, different methods have been utilized to synthesize such enantiopure substances, such as:

- Resolution of racemic mixture
- Chiral substrate
- Chiral reagents
- Chiral auxiliaries

- Enzymes
- Chiral catalysts
 - Metal-ligand complexes
 - Organocatalysts

Resolution of racemates was first performed by Louis Pasteur in 1848 who separated its D- and L- forms of tartaric acid. He formed the sodium ammonium salt of tartaric acid and the types of the crystals were so specific to each enantiomer that they were separated [7]. This type of resolution could not have widespread applicability since only a limited number of organic compounds can crystallize into such distinct types of crystalline forms for two different enantiomorphs [7]. The other method for the resolution of the racemates is kinetic resolution by enzymatic or non-enzymatic routes. Enantiomers have different chemical properties, as a result, they react with chiral substances at different rates [8]. By kinetic resolution technique, one can obtain both enantiomers of a racemate or single enantiomer or a further but structurally different chiral product, depending on the reaction employed [8].

Use of chiral substrates is another technique to bring about enantioselection. Enantiopure substances from nature's chiral pool such as steroids, terpenoids and amino acids, can also be used to induce enantioselectivity in the organic synthesis [9].

When a chiral reagent (eg: chiral borane reagents, chiral titanium reagents, etc...) is used, it will also match with specific enantiomer and react faster with it since the energy of the transition state is lower for that one [10]. Via using a stoichiometric or catalytic amount of a chiral reagent, enantiocontrol is brought about in a reaction [11,12].

It is noteworthy to mention about chiral auxiliaries which are also used for asymmetric synthesis. Diastereoselective transformations can occur by binding of a chiral auxiliary to the substrate via covalent interaction, and the active antipodes of the substrate can be recovered after the removal of auxiliary [13]. An ideal auxiliary should have high optical purity, can stand to the desired reaction conditions and should provide high diastereomeric ratio [14].

Resolution methods and methods with chiral precursors (chiral substrate, chiral reagents and chiral auxiliary) have serious drawbacks, the former in giving 50% yield for the target enantiomer, the latter in requiring stoichiometric amounts of a suitable precursor [15].

Enzymes are the natural catalysts derived from chirality pool and they have been also an alternative method for kinetic resolution. Some examples of enzymes used are hydrolytic enzymes such as pig liver esterase, porcine pancreatic lipase, and microbial lipases which are applicable to large number of substrates such as racemic acids and alcohols and catalyze their reactions with high enantioselectivity [16].

1.2.1. Asymmetric catalysis

Asymmetric catalysis, in which a molecule of chiral catalysts is used and continuously regenerated, is the best choice since the catalytic asymmetric reactions can proceed with high stereoselectivity resulting in the enantiopure compound in high yields and is also applicable for the synthesis of thousands of new chiral molecules [15,17,20]. The most important point is to design a ligand or an organocatalyst that will fit in a reaction as efficiently as possible to bring about enantioselection [17].

1.2.1.1. Metal ligand complexes

Many metal-ligand complexes have been able to catalyze various reactions with remarkable enantioselectivities [18]. In these reactions, enantioselectivity is induced by modification of the reactivity of metal center by the chiral ligand so that enantiocontrol is in the favor of one of the enantiomers [18].

Examples for the reactions that are mostly studied by metal ligand complexes involve hydrogenation, epoxidation, or dihydroxylation in which either a C-H or C-O bond is formed and enantioselectivity is brought about by differentiating the enantiotopic faces of a prochiral starting material such as a prochiral olefin or a carbonyl group [19].

In the early 1970s, W. Knowles and his coworkers showed that the rhodium complexes of chiral phosphine ligands worked well in the asymmetric hydrogenation of an olefinic substrate, giving high enantioselectivity. This major breakthrough was then commercialized to produce L-dopa, an antiparkinson drug [15]. In 2001, Knowles was given the Nobel Prize in chemistry for this achievement, and shared it with Ryoji Noyori, who also worked on asymmetric catalytic hydrogenation, and with K. Barry Sharpless for his work on asymmetric catalytic oxidation [15].

1.2.1.2. Organocatalysis

Use of small organic molecules, complementary to enzymes, and metal-ligand complexes, have been proved to be an extremely useful tool for asymmetric synthesis over the last decades [20]. Organocatalysis has been gaining attention continuously since it offers many advantages over other methods. Most organocatalysts are inert towards air and water, providing facile experimental procedures and easy handling. They are also readily available from nature's chiral pool, or easily prepared [21]. The most significant advantage of organocatalysis is metal-free environment which provides a route for green chemistry and also eliminates the drawbacks coming from the cost, toxicity and increasing deficiency of mostly used metals [21,22].

Organocatalysts can be divided into four major categories: Lewis bases, Lewis acids, Brønsted bases, and Brønsted acids. In each class, various types of activation modes are present, and different types of organocatalysts are able to utilize these properties to bring about the desired transformations [21].

1.3. Hypervalent silicon species in asymmetric organocatalysis

Silicon is the second most abundant element in the earth's crust (25.7%) [23]. Over the last three decades, employing silicon in asymmetric synthesis has been gaining importance for functional group modifications based on the fact that silicon has the ability to expand its valence shell up to two, resulting in penta or hexa-coordinated reactive intermediates [24]. This tendency of silicon for the valence expansion can be increased by substituting strong electron withdrawing groups on silicon atom [24]. Lewis bases can be employed in combination with silicon Lewis acids, forming hypervalent complexes which simultaneously activate the reactants along with giving possibility to enantioselective synthesis [25]. The change in the bonding and electronic properties in hypervalent silicate complexes which occurs after the attachment of Lewis base to silicon can be described by Gutmann's rules which are [26]:

1. As the intramolecular distance between the donor (D) and the acceptor (A) is getting smaller, the peripheral bonds (A-X) will lengthen more,
2. the long bond between D and A means the extent of the polarization of electron density will be more across D-A bond,
3. as the coordination number of an atom increases, the lengths of all the bonds originating from that coordination center will increase,
4. the bonds adjacent to D and A will either contract or elongate in order to compensate for the changes in electron density at D and A (*Figure 2*).

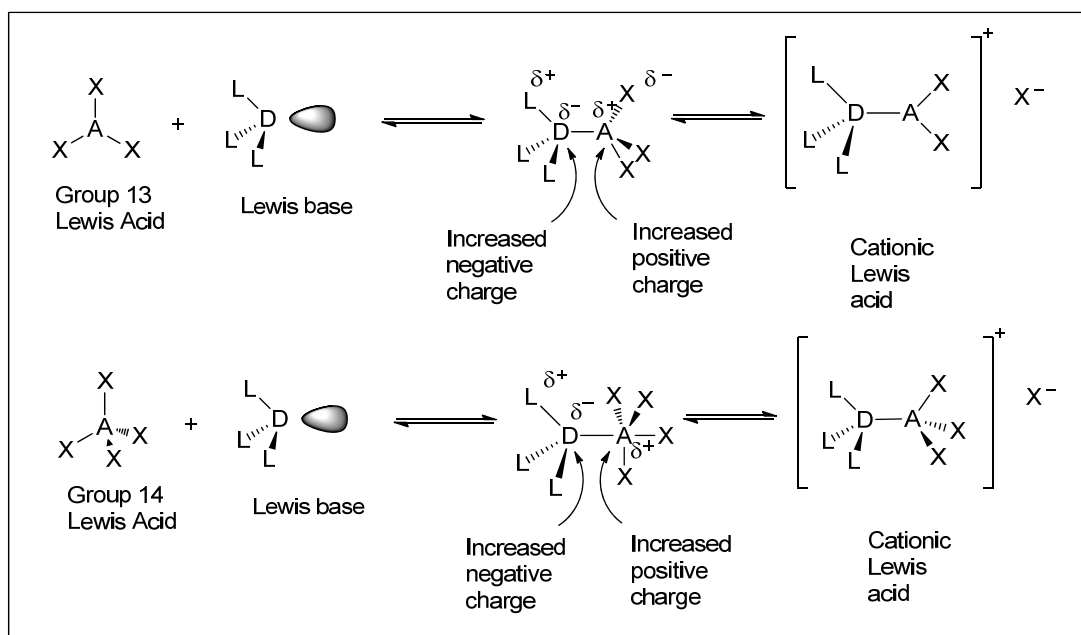


Figure 2 Lewis base activation of Lewis acids

Two theories based on the participation of 3d orbitals in bonding were constructed to explain this behavior of silicon, contrary to the behavior of carbon which is same group element with silicon [23].

The first theory suggests that the electronegative elements around silicon lowers the energy of 3d orbitals of silicon such that 3d orbitals engage in bonding by sp^3d and sp^3d^2 hybridization for the pentavalent and hexavalent species, respectively [23]. Since the s character of the silicon decreases, its Lewis acidity increases, and there is also a distribution of electron density towards the ligands around silicon atom [26]. This type of bonding is explained in *Figure 3*:

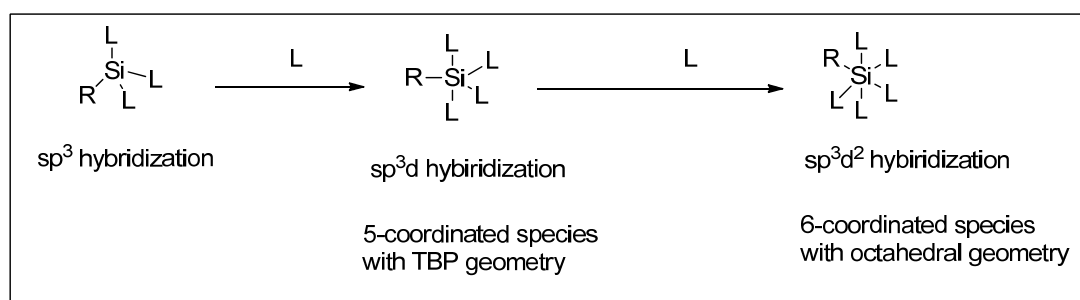


Figure 3 Participation of 3d orbitals in bonding

The second theory explains this situation with a term 'hypervalent bond'. It says that penta- or hexa-coordinated silicon species can be generated with one or two 3-center-4-electron molecular bonds formed by a silicon p orbital and two p orbitals of the electronegative ligands. The positions of the ligands are non-equivalent. The acceptor ligands prefer hypervalent bonds and the donor ligands form normal covalent bonds with the sp^2 (for pentavalent compounds) and sp (for hexavalent compounds) hybridization (Figure 4) [23].

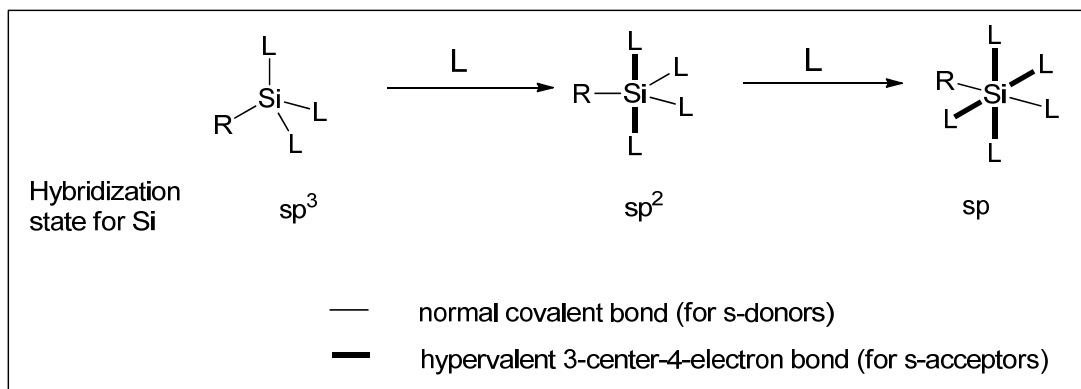


Figure 4 3-Center-4-Electron model for hypervalent bonding

In the second theory, central atom becomes electron deficient, and surrounding ligands are electron rich due to the inherent nature of these hypervalent bonds. By combining three atomic orbitals (AO), three molecular orbitals (MO) are generated (Figure 5). A pair of hybrid orbitals are generated by mixing of the filled σ orbital on the acceptor with the filled n orbital on the donor. There exists a node at the HOMO of the hybrid orbital (Ψ^2) at the central atom and the electron density is localized at the peripheral atoms. As a result, electrophilic and nucleophilic character are enhanced at different atoms in this adduct [26].

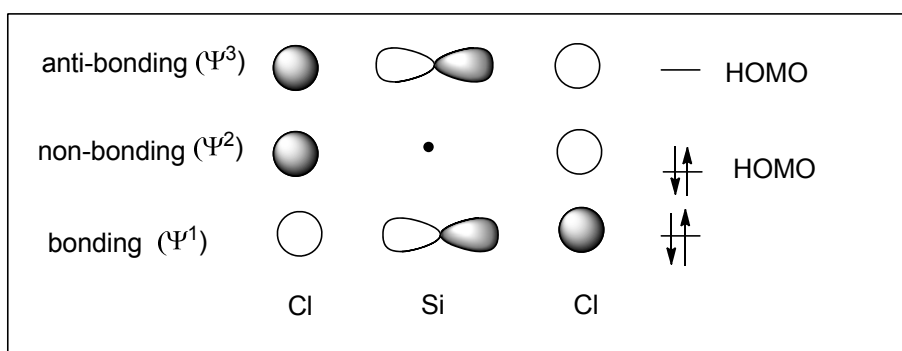


Figure 5 Molecular orbital diagram for 3-center-4-electron hypervalent bonds

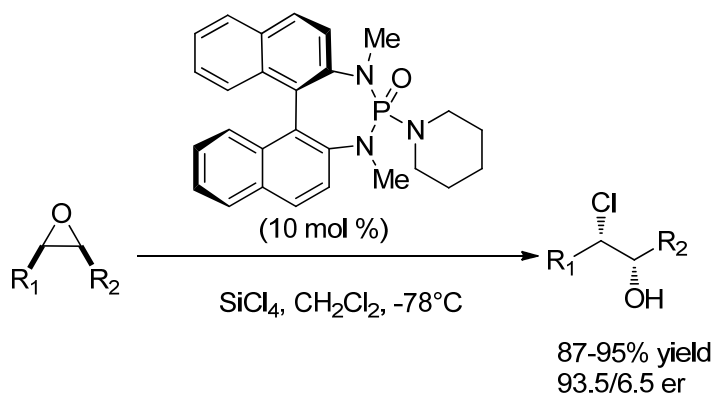
The enhanced reactivity of hypervalent silicate complexes can be explained by interpreting both theories which are helpful to comment on the increased Lewis acidity of silicon, distribution of electron density towards the ligands around silicon which gives them a nucleophilic character [23-26]. These hypervalent silicate complexes can be involved in asymmetric reactions after which Lewis base dissociates from silicon after the product is formed [23].

1.3.1. Reactions involving hypervalent silicon species

Using substoichiometric amounts of small organic molecules under metal-free conditions has been very attractive in terms of being nontoxic, cheap, and environment friendly. Indeed, these small organic molecules having low molecular weights and simple structures have been reported to catalyze reactions that worked with relatively expensive and toxic transition metal catalysts. Chiral Lewis base activated silicon based Lewis acids have been employed in wide variety of asymmetric reactions resulting in high chemical and stereochemical efficiency [23].

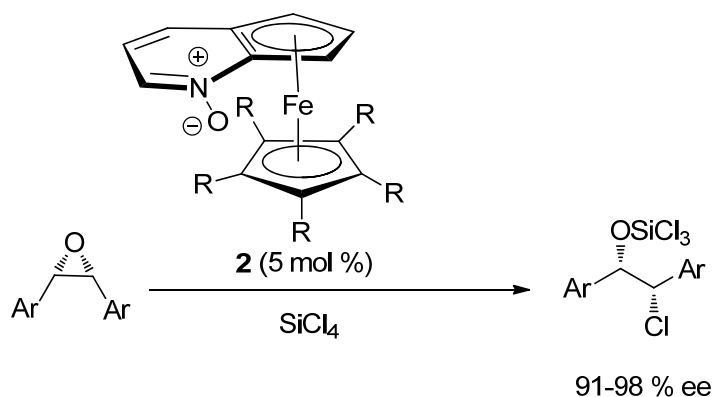
1.3.1.1. Epoxide ring-opening reactions

Enantioselective ring-opening of epoxides has been such a facile process that they have been significant intermediates. The first study was reported by Denmark and coworkers in 1998. In their study, they found out that catalytic amounts of phosphoramidate derivatives can effectively catalyze the reactions by activating the silicon tetrachloride which can be the source of chloride. After ensuring that silicon tetrachloride cannot be successful alone in this reaction (yield < 5%), they tested the efficiency of different Lewis bases. Among hexamethylphosphoramide (HMPA), 1,3-dimethyl-3,4,5,6-tetrahydro-2(1*H*)-pyrimidinone (DMPU) and pyridine, they found that HMPA was the best Lewis base having potential for the corresponding reaction [27]. However, after the survey of cyclic and acyclic epoxides, they concluded that the results solely depend on the structure of the epoxide, giving high enantioselectivity for acyclic epoxides whereas the enantioselectivity of the reactions of cyclic epoxides depend on ring size [27]. During the mechanistic studies, they reported that only SiCl_4 and HSiCl_3 were able to give the chlorohydrin product and only one of the chlorine of SiCl_4 is active. The results of this study was summarized in *Scheme 1* [28]:



Scheme 1 The first study of ring-opening of meso-epoxides

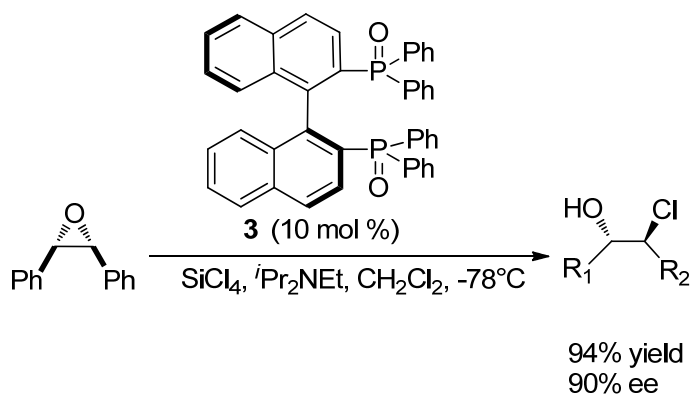
Following the study of Denmark and coworkers [27], Fu and coworkers were studied the epoxide ring-opening reactions with a planar-chiral heterocyclic Lewis base given in *Scheme 2* [29]:



Scheme 2 *N*-oxide catalyzed epoxide ring-opening reaction

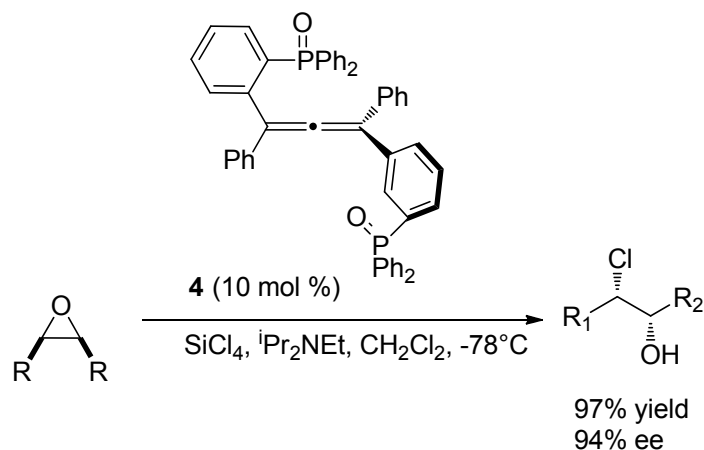
With the oxygen as being the nucleophilic site of their Lewis base, a number of epoxides were desymmetrized with very good yields and enantioselectivities by using 5 mol % of this planar-chiral catalyst designed by Tao et al. [29].

Under the lights of these pioneering works of Denmark and Fu, Nakajima and coworkers tested the effectiveness of (*S*)-BINAPO and got high yields and high enantioselectivities (*Scheme 3*) [30].



Scheme 3 Results of the studies of Nakajima and coworkers

Ready and coworkers reported their study in which they used allenes as chiral Lewis bases used to activate silicon tetrachloride [31]. With the same mole percent as in (*S*)-BINAPO (10 mol %) [30], allene catalyst of Ready et al. gave slightly better results in terms of yield and enantioselectivity (*Scheme 4*) [31].

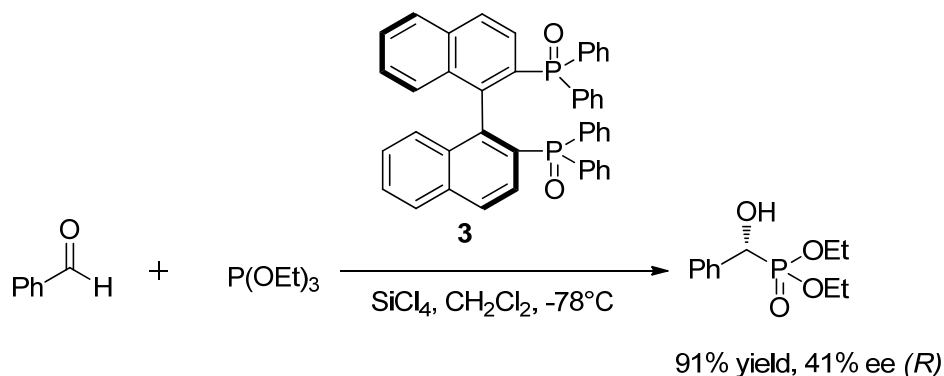


Scheme 4 Reaction conditions and results of the study of Ready and coworkers

1.3.1.2. Enantioselective addition of trialkylphosphites to aldehydes

Alpha-hydroxyphosphonates are biologically important molecules since they are known to be inhibitors of the enzymes such as renin (human medicinal enzyme) and HIV (human immunodeficiency virus) protease and polymerase. Moreover, they also exhibit antiviral and anticancer activities [32]. These important properties are possessed by single enantiomer of α -hydroxyphosphonates which makes their enantioselective synthesis attractive [33].

The first study based on the enantioselective synthesis of α -hydroxyphosphonates in the presence of SiCl_4 and substoichiometric amounts of chiral Lewis bases was reported by Sugiura, Nakajima and their coworkers, recently [33]. In their study, they used (*S*)-BINAPO to activate the weak Lewis acid, SiCl_4 and their results were summarized in *Scheme 5*:



Scheme 5 Asymmetric Abramov type phosphonylation

Sugiura, Nakajima and their coworkers screened different chiral Lewis bases. Higher enantioselectivities were obtained with triarylphosphine oxides while alkylarylphosphine oxides and bisquinoline *N,N'*-dioxides provided inferior results (*Figure 6*) [33].

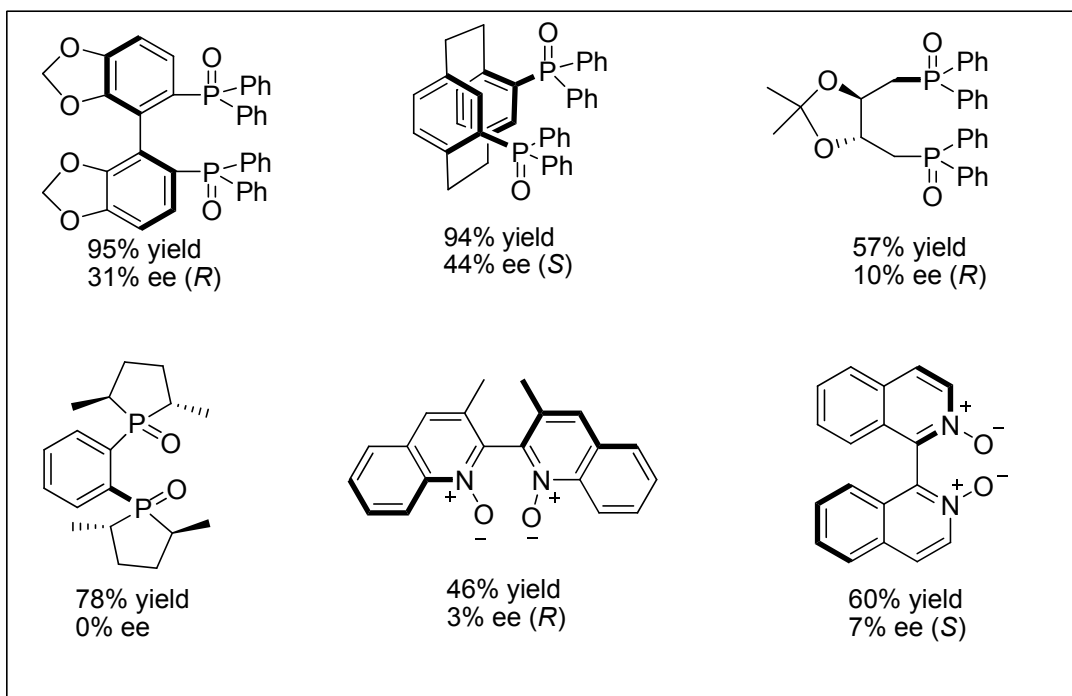
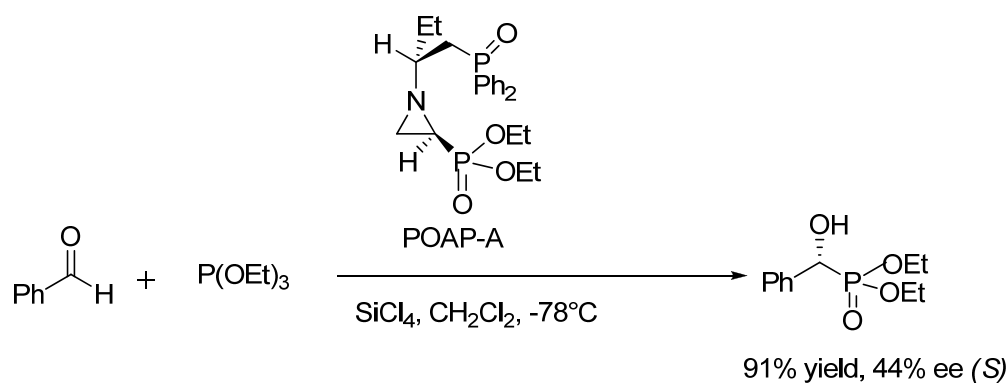


Figure 6 Chiral Lewis bases employed by Nakajima group

Following the study of Nakajima group, Dogan group has designed new phosphine oxy aziridinylphosphonates to perform enantioselective synthesis of α -hydroxyphosphonates [34]. By using POAP-A as the chiral Lewis base, they got acceptable results in terms of yield and enantioselectivity which are comparable with Nakajima and coworkers' results (Scheme 6) [34].

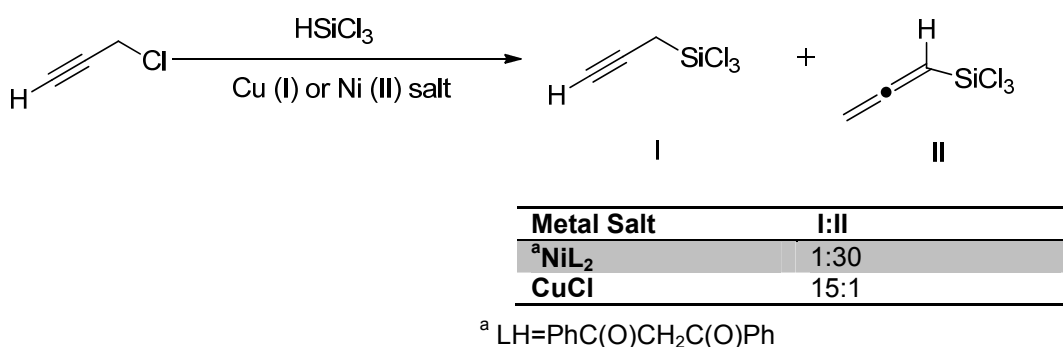


Scheme 6 Results of Dogan and co-workers

1.3.1.3. Addition of allenylsilane and propargylsilane to aldehydes

Allenic and propargylic alcohols constitute an important class of organic molecules that are versatile building blocks exhibiting many applications in organic synthesis [35]. However, in organometallic studies, chemoselectivity is so poor that mixture of allenic and propargylic alcohols are obtained [35,37].

Kobayashi and his coworker have reported a regioselective method where a Cu(I) salt selectively forms propargyltrichlorosilane and a Ni(II) salt selectively forms allenic trichlorosilane from the same intermediate which is propargyl chloride (*Scheme 7*) [35].



Scheme 7 Selective synthesis of allenic and homopropargylic alcohols

After obtaining allenyltrichlorosilane and propargyltrichlorosilane, the reactions of the former with aldehydes gave the homopropargylic alcohol while the reaction of the latter with aldehydes gave allenic alcohol with high regioselectivities via hypervalent silicates (*Figure 7*) [35].

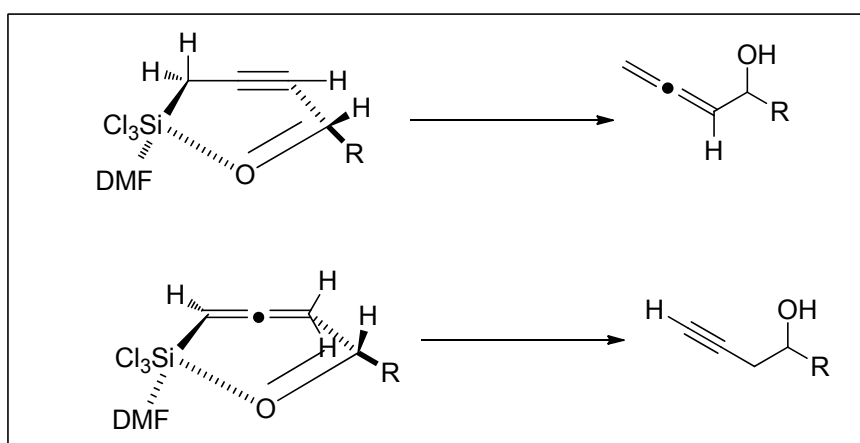
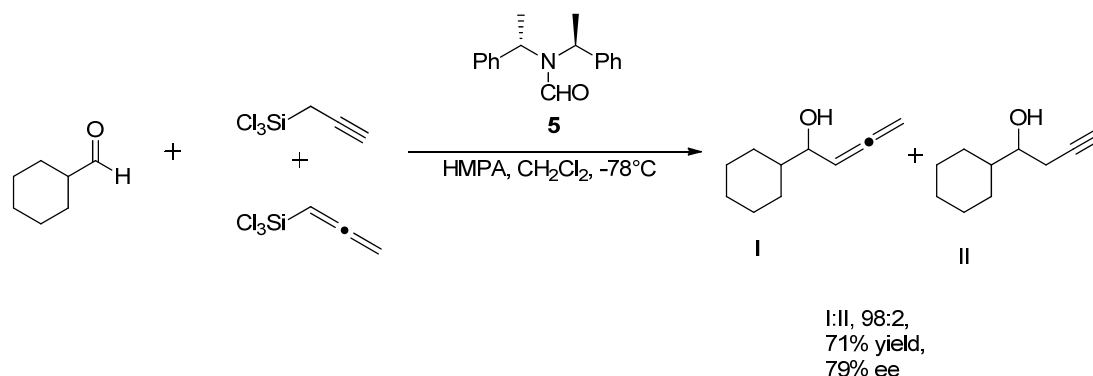


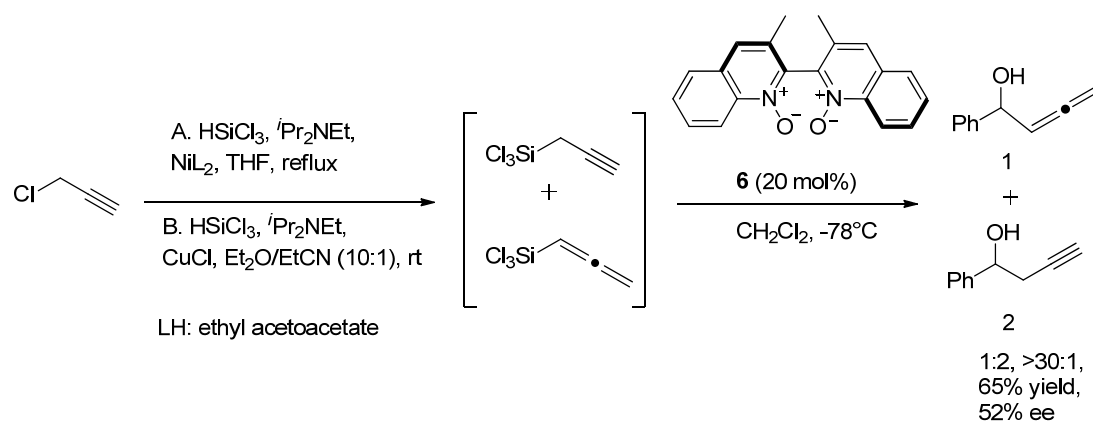
Figure 7 Hypervalent silicon-based transition states

Following the study of Kobayashi [35], Iseki and coworkers performed the first catalytic enantioselective allenylation of aldehydes in the presence of chiral DMF analog, (*S,S*)-*N,N*-bis(α -methylbenzyl)formamide **5** and additive HMPA [36]. After 14 days, they got the corresponding allenylation product selectively (98:2) with moderate yield and enantioselectivity (71% and 79%, respectively). Their conditions and results are summarized in *Scheme 8*:



Scheme 8 The first catalytic enantioselective allenylation of aldehydes

As a next study, Nakajima and coworkers have studied the same reaction with a different method. They performed the synthesis of allenyl and propargyltrichlorosilane selectively by using method of Kobayashi and his coworker. In the presence of HSiCl_3 and a Ni (II) salt, they formed the allenyltrichlorosilane in situ with a high preference (>30:1) and then, in the presence of their chiral *N*-oxide (20 mol%), the corresponding homopropargylic alcohol was afforded with a moderate enantioselectivity. On the other hand, when Cu (I) salt was used, in situ preparation of propargyltrichlorosilane was afforded preferentially (15:1). By using *N*-oxide (20 mol %), they got the corresponding allenic alcohol with moderate enantioselectivity [37]. Their results are summarized in *Scheme 9*:



Scheme 9 Asymmetric allenylation and propargylation using chiral *N*-oxide

1.3.1.4. Stereoselective C-C bond formation reactions

The formation of hypervalent silicate complexes results in the increased Lewis acidity of silicon. As a result, these hypercoordinated silicon species bear a strong electrophilic character at silicon and their ability to transfer a formally negatively charged group such as a carbon nucleophile or a hydride is improved. Thus, when a transformation occurs via formation of a hypervalent silicon complex, carbon-heteroatom bond formation as well as the carbon-carbon bond formation can occur [23].

1.3.1.4.1. Asymmetric allylation

The pioneering works based on the characteristics of allylation reaction in the absence of catalysts were performed by Hosomi [38] and Kobayashi [39].

In the asymmetric versions of allylation, binding of allyltrichlorosilane (the nucleophile) and the chiral Lewis base generates the hypervalent silicon species which further coordinates to aldehyde. The simultaneous activation gives rise to high yields and high enantioselectivities due to the closed transition state structure proposed by Denmark and his coworker (*Figure 8*) [40]. Due to the noncovalent nature of the binding between the nucleophile and the Lewis base, it is possible to use a substoichiometric amount of chiral promoter [40].

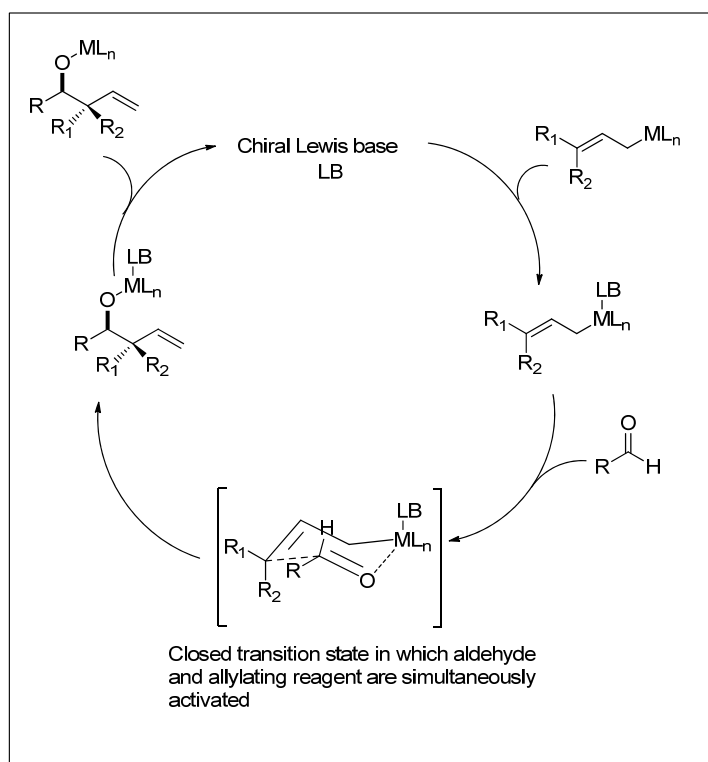
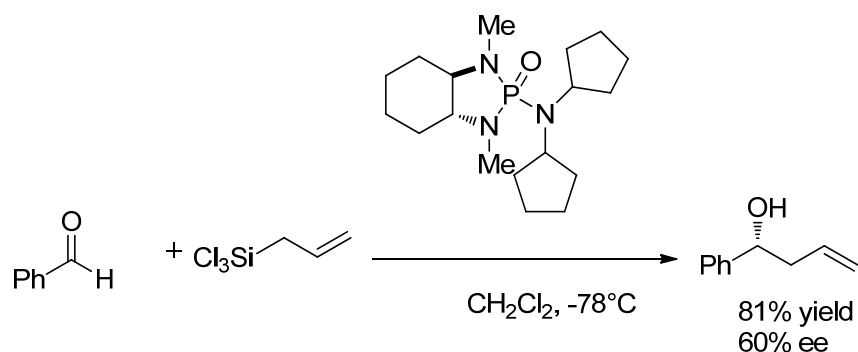


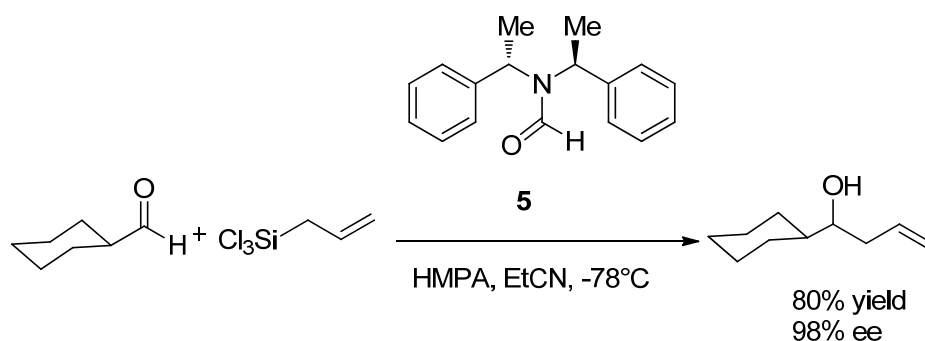
Figure 8 Catalytic cycle of asymmetric allylation reaction proposed by Denmark

The first catalytic version of allylation reaction was performed by Denmark and coworkers. With a piperidine derivative chiral Lewis base (10 mol %), they afforded the corresponding homoallylic alcohol in moderate yield and enantioselectivity (*Scheme 10*) [41].



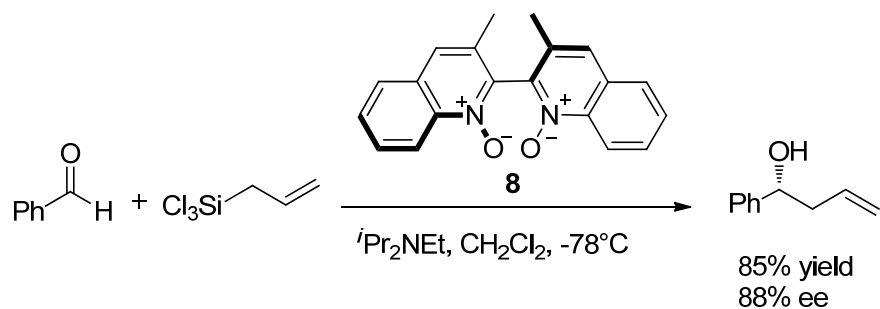
Scheme 10 Asymmetric allylation with phosphoramidate derivatives

Different from phosphoramidate derivatives, formamide derivative chiral Lewis bases were also employed in asymmetric allylation reactions. Iseki and coworkers prepared a chiral formamide **5**, (*S,S*)-(*N,N*)-bis(\square -methylbenzyl)formamide and tested the efficiency of this chiral Lewis base in asymmetric allylation of aliphatic aldehydes (*Scheme 11*) [42].



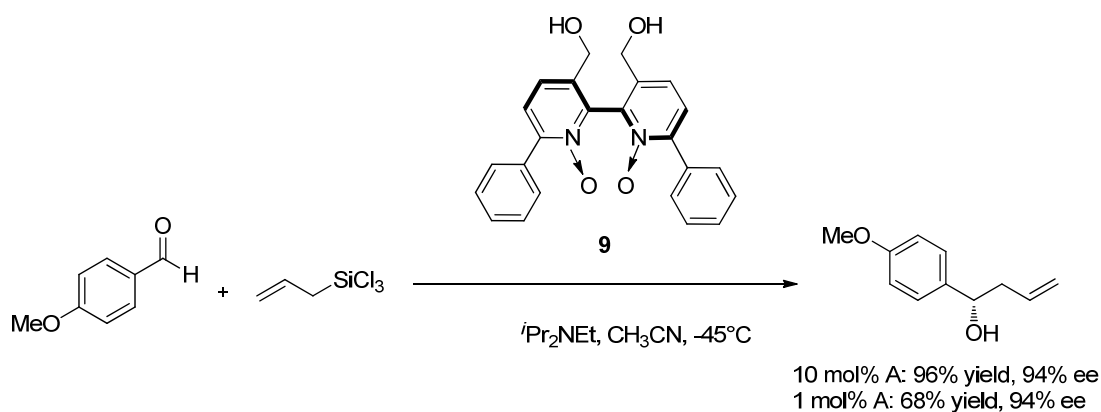
Scheme 11 Asymmetric allylation in the presence of **5**

In the same year with Iseki and coworkers, Nakajima group has performed the asymmetric allylation of aromatic aldehydes with their (*S*)-3,3'-dimethyl-2,2'-biquinoline *N,N'*-dioxide, **8** as the chiral Lewis base (*Scheme 12*) [43].



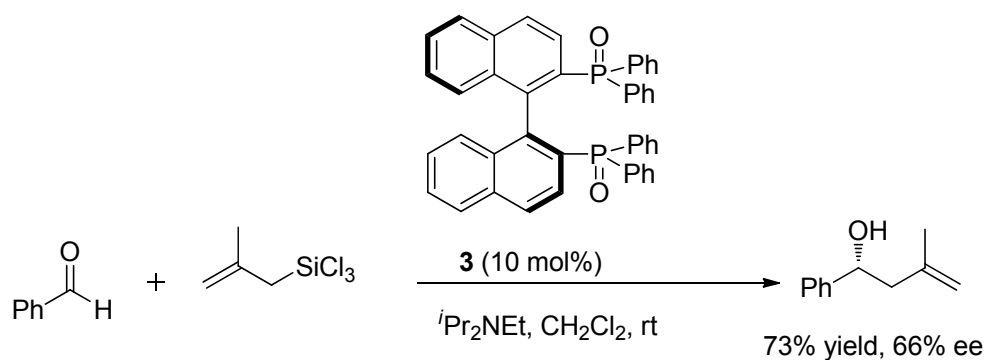
Scheme 12 Asymmetric allylation with (*S*)-3,3'-dimethyl-2,2'-biquinoline *N,N'*-dioxide

A novel catalyst 2,2'-bipyridine *N,N'*-dioxide, having extreme catalytic activity, was generated by Hayashi and coworkers. Even 1 mol % of the catalyst **9** provided excellent enantioselectivities for the corresponding homoallylic alcohols (Scheme 13) [44].



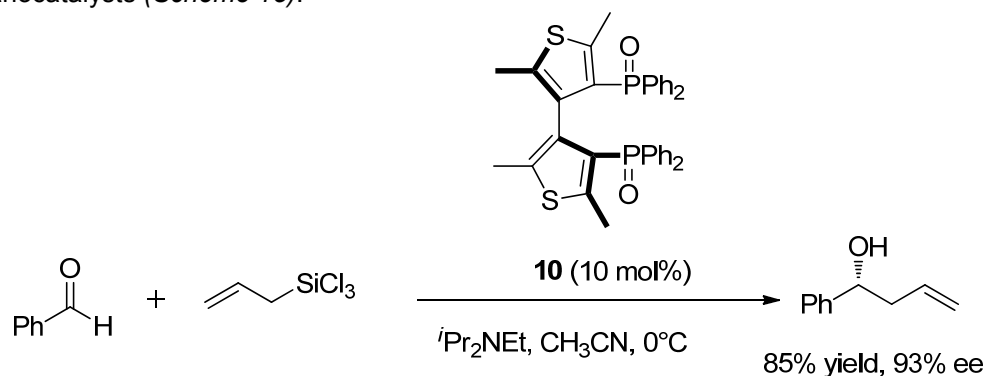
Scheme 13 2,2'-bipyridine *N,N'*-dioxide catalyzed asymmetric allylation

Nakajima and coworkers used (*S*)-BINAPO for the asymmetric allylation of aromatic aldehydes, and they obtained the corresponding homoallylic alcohol with high yields and moderate enantioselectivities (Scheme 14). To accelerate the catalytic cycle, they utilized a combination of two additives which are diisopropylethylamine and tetrabutylammonium iodide. This study was the first to show the effectiveness of a chiral phosphine oxide as a catalyst in the enantioselective reaction [45].



Scheme 14 Asymmetric allylation with (*S*)-BINAPO

The most prominent improvement based on the catalysis of allylation reactions was performed by Benaglia, Benincori and their coworkers [46]. Their catalyst, (*S*)-*tetra*-methylbithiophene phosphine oxide promoted the allylation of benzaldehyde giving a very high level of enantioselectivity, 93% ee, comparable to those obtained with the best known organocatalysts (Scheme 15).



Scheme 15 Asymmetric allylation with (*S*)-*tetra*-Me-BITIOPO

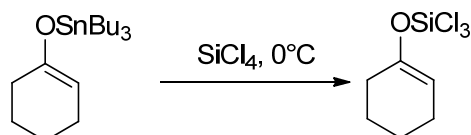
1.3.1.4.2. Asymmetric aldol addition

The design criteria of Denmark and coworkers were outlined in their published papers [47,48]. At first, Lewis base activates the enoxymetal forming a complex which is more reactive than free enolate and followed by the association of the aldehyde by the expansion of the valence of the metal by two, which generates an extremely reactive intermediate. After simultaneously activating the reactants in a closed-array, the reaction proceeds by closed-transition state to form the aldol addition product after the expulsion of the Lewis basic promoter [48].

It is crucial to select an appropriate metal which can expand its valence by two (eg: silicon, tin, titanium, zirconium, and aluminum) while balancing the nucleophilicity of the enolate with electrophilicity to coordinate both the Lewis basic aldehyde and the chiral Lewis basic group. Moreover, the ligands on the metal should be small and strongly electron-withdrawing such as halogen or carboxyl groups to provide valence expansion and accommodation of two Lewis basic groups.

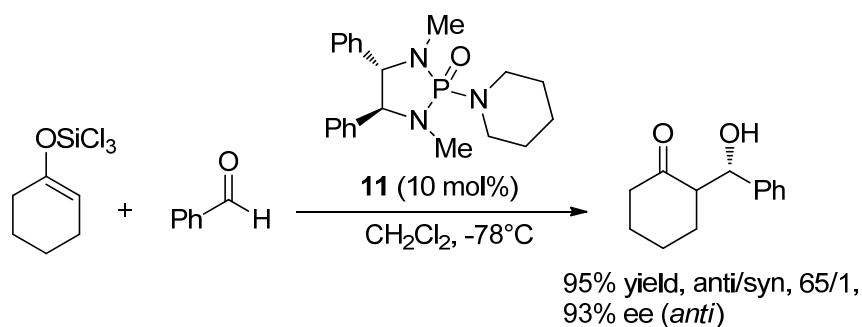
Second most important criteria is reported for the chiral Lewis basic group. It must be able to activate the addition without cleaving the oxygen-metal bond and provide an effective environment for the asymmetric aldol addition [48].

The milestone of the silicon mediated Lewis base catalyzed asymmetric aldol addition was performed by Denmark and coworkers [47]. They synthesized the trichlorosilyl enolate of cyclohexanone via metathesis of tributylstannyl derivatives (*Scheme 16*).



Scheme 16 Synthesis of trichlorosilylenolate of cyclohexanone

The trichlorosilyl enolate was reacted with benzaldehyde in the presence of catalytic amounts of chiral phosphoramidate **11** (10 mol %), and corresponding *anti* aldol addition product was obtained with excellent yield, diastereoselectivity and enantioselectivity (*Scheme 17*) [47].



Scheme 17 Asymmetric aldol addition with phosphoramidate derivatives

The catalytic cycle for this reaction is given in *Figure 9* [49]:

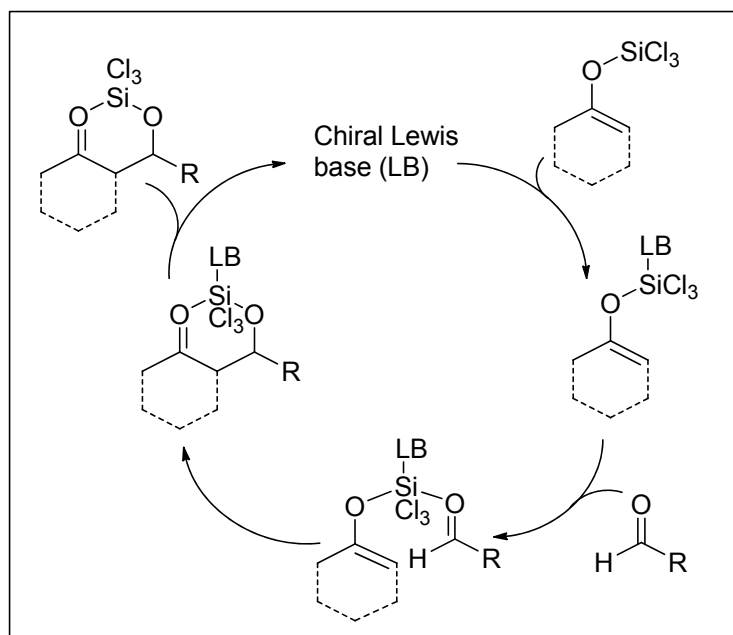


Figure 9 Catalytic cycle for silicon tetrachloride mediated asymmetric aldol addition

In 2004, Nakajima and coworkers tested the efficiency of the monodentate *N*-oxides and bidentate *N,N'*-dioxides as the chiral Lewis bases. They reported that two oxygens of an *N,N'*-dioxide can coordinate to silicon from two points via formation of octahedral intermediate resulting in *anti* aldol product. On the other hand, one oxygen of an *N*-oxide catalyst can coordinate to silicon, as a result reaction proceeds via trigonal bipyramidal intermediate leading to the *syn* aldol product. Their catalysts provided low diastereoselectivity (the largest one: *syn/anti* 30:1 for monodentate, 1:12 for bidentate catalysts), and enantioselectivities were all unsatisfactory. Addition of benzaldehyde to trichlorosilyl enolate of cyclohexanone catalyzed by (*R*)-7 catalyst gave the best results in terms of enantioselectivity (62% ee for *syn*, 66% ee for *anti*). The catalysts and the results of Nakajima group are given below (Figure 10) [50].

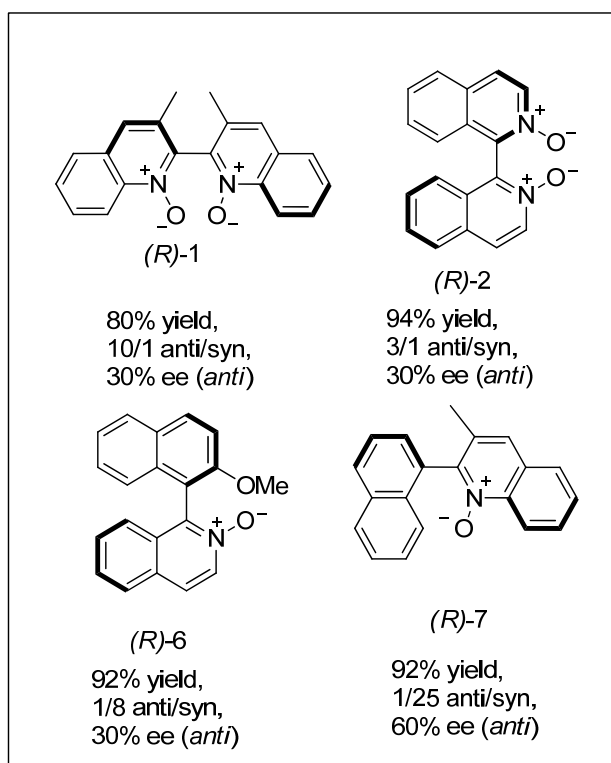


Figure 10 Chiral *N*-oxides and *N,N'*-dioxides used by Nakajima and coworkers

Transition state models based on the results of Denmark and Nakajima groups can be given as in Figure 11 [50]:

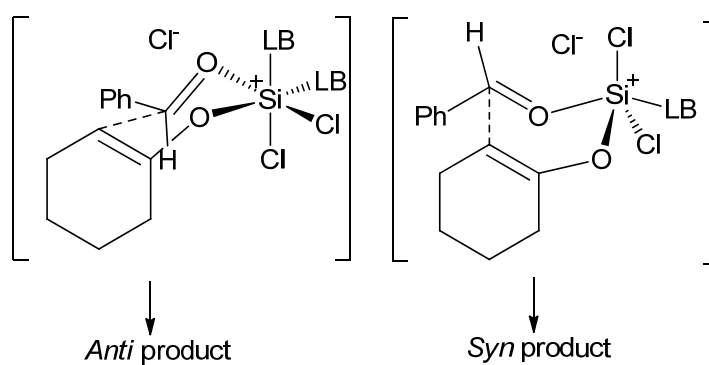
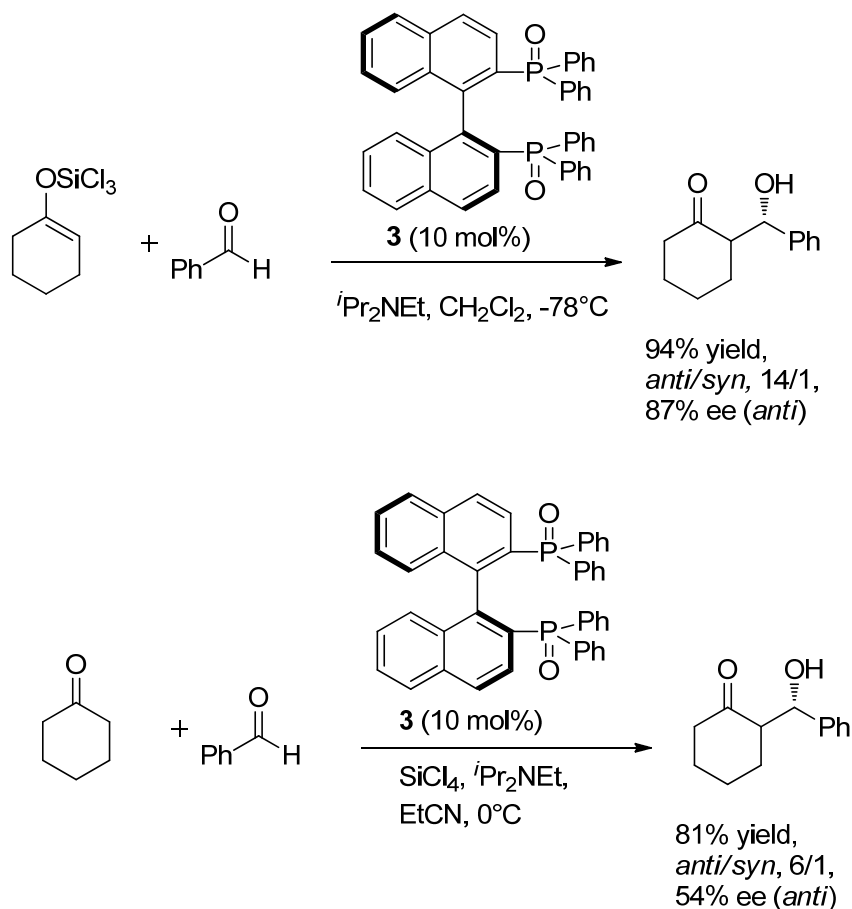


Figure 11 Transition states leading to *anti* and *syn* aldol products

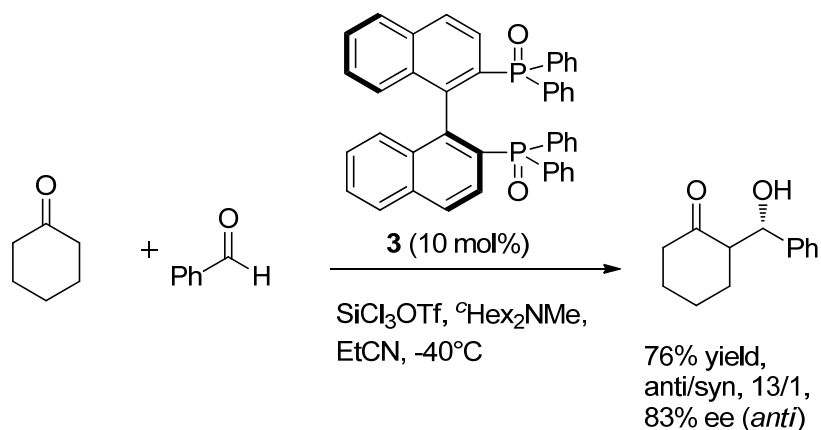
Nakajima and coworkers have studied the corresponding aldol reaction using (*S*)-bis-(diphenylphosphanyl)-binaphthyl dioxide, (*S*)-BINAPO. When they synthesized the trichlorosilyl enolate via starting from trimethylsilane derivative in the presence of mercuric

acetate, $\text{Hg}(\text{OAc})_2$, the yields, diastereomeric ratios and enantioselectivities were higher when compared to the yields of the study in which trichlorosilyl enolate was generated in situ with the use of tetrachlorosilane (*Scheme 18*) [51,52].



Scheme 18 Results of Nakajima and coworkers for the asymmetric aldol reaction

As a third and new approach, Kotani, Nakajima and their coworkers used trichlorosilyl triflate as the silicon-based Lewis acid and generated trichlorosilyl enolate in the reaction medium [53]. In this study, they tested the efficiencies of (*S*)-BINAPO and other phosphine oxide derivatives as the chiral Lewis bases and they obtained their best results in terms of diastereoselectivity and enantioselectivity with (*S*)-BINAPO (*Figure 12*). When compared with the results obtained with SiCl_4 , the yield was slightly decreased; however, the enantiomeric excess obtained after this Lewis acid change was superior (*Scheme 19*) [52,53].



Scheme 19 Results obtained with SiCl_3OTf

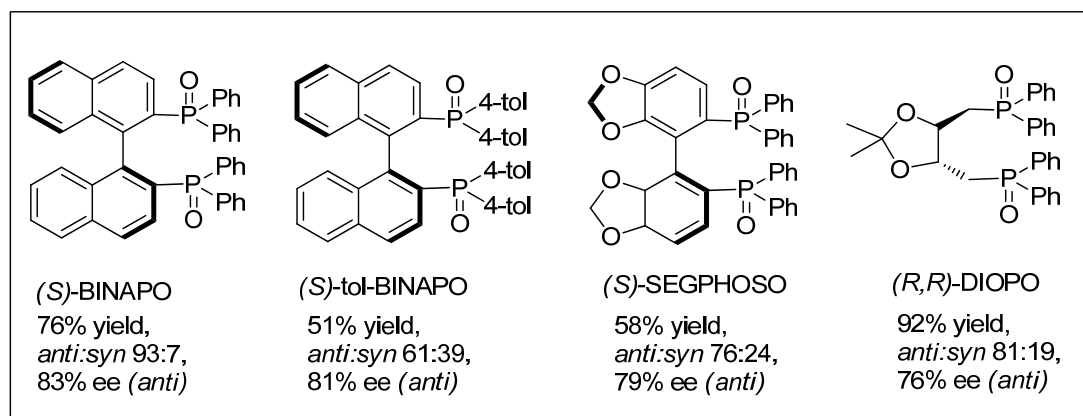
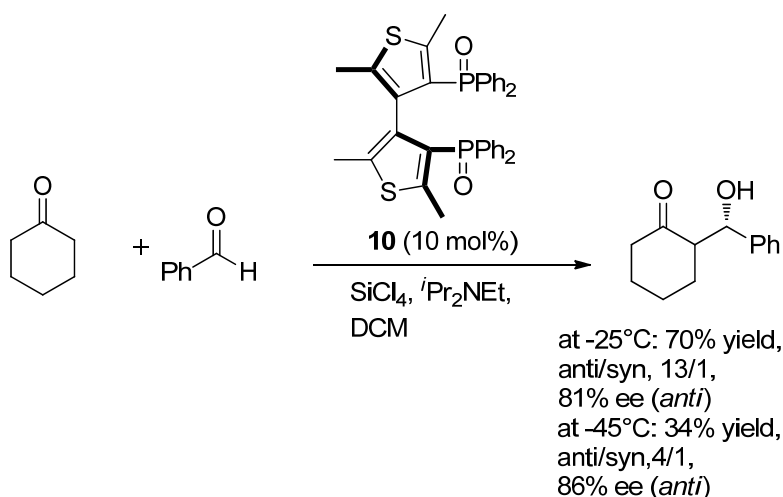


Figure 12 BINAPO derivatives tested by Kotani, Nakajima and their coworkers

Finally, Benaglia and coworkers studied the corresponding aldol reaction with a biheteroaryldiphosphine oxide *tetra*-Me-BITIOPO which was a very effective chiral Lewis base employed in asymmetric allylation reaction [46,54]. Under the same conditions with Kotani and coworkers, they afforded the aldol product with a lower yield, but higher enantioselectivity when compared to the results obtained with (*S*)-BINAPO (Scheme 20) [53, 54].



Scheme 20 Results of asymmetric aldol reaction with (*S*)-tetra-Me-BITIOPO

1.4. Aim of work

Aldol addition has been one of the most important C-C bond formation reactions. In aldol reactions, the subunits of polyol chains with 1,3-diol relationships can be obtained. In asymmetric versions of this chemistry, two new stereogenic centers are generated from the prochiral starting materials. Over 25 years, asymmetric versions of aldol reactions have been investigated in conjunction with hypervalent silicate complexes which have been providing good to excellent yields and enantioselectivities in the presence of chiral Lewis bases.

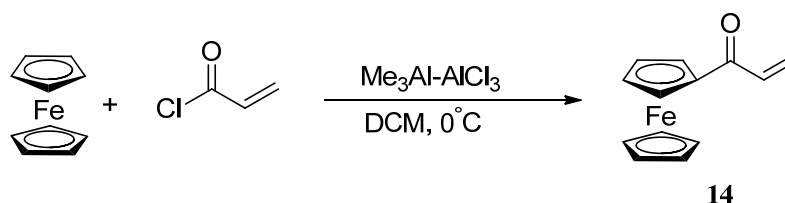
Among the different chiral Lewis bases summarized in the introduction part, chiral Lewis bases containing phosphine oxy groups have been the most pronounced ones since they provide good regioselectivities and stereoselectivities [47,51-54]. For this purpose, our chiral phosphine oxy ferrocenyl aziridiny methanol, **POFAM** series ligands have been synthesized according to the previous methods reported by our group by following acryloyl ferrocene synthesis, bromination, aziridination, tosylation, phosphonylation and reduction steps. Their catalytic activity has been tested for silicon tetrachloride mediated asymmetric aldol addition reactions. As a different family of chiral Lewis bases, our most recently developed phosphine oxy aziridiny phosphonates, **POAP** have also been tested for the asymmetric aldol reaction. Shortly, we aimed to test the performance of two different series of chiral Lewis bases **POFAM** and **POAP** for the asymmetric aldol reaction.

CHAPTER 2

RESULTS AND DISCUSSION

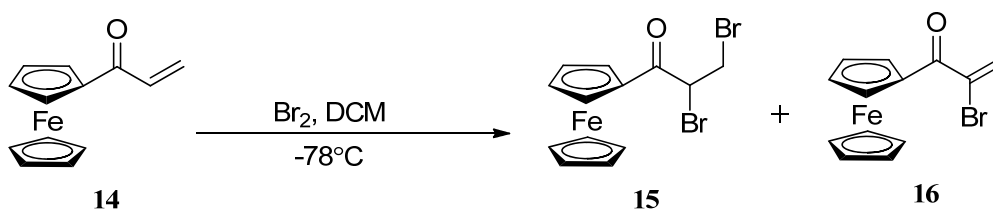
2.1. The synthesis of POFAM ligands

Acryloyl ferrocene was synthesized by starting from ferrocene and acryloyl chloride in the presence of Lewis acid mixture consisting of Me_3Al and AlCl_3 via Friedel-Crafts reaction. The product was obtained in excellent yields by the method developed in our group [56]. This method does not require extra purification, simple extraction is enough to get pure product.



Scheme 21 Synthesis of acryloyl ferrocene

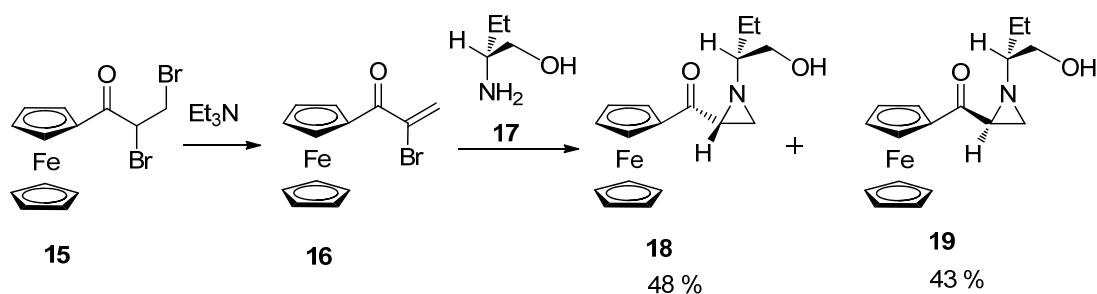
Bromination of acryloyl ferrocene was simply achieved by fast addition of bromine solution into the acryloyl ferrocene solution at -78°C as a result of which olefinic unit is brominated. In addition to dibromo compound, α -bromo compound was also afforded as a minor product, and the total yield of the reaction was 99%.



Scheme 22 Bromination of acryloyl ferrocene

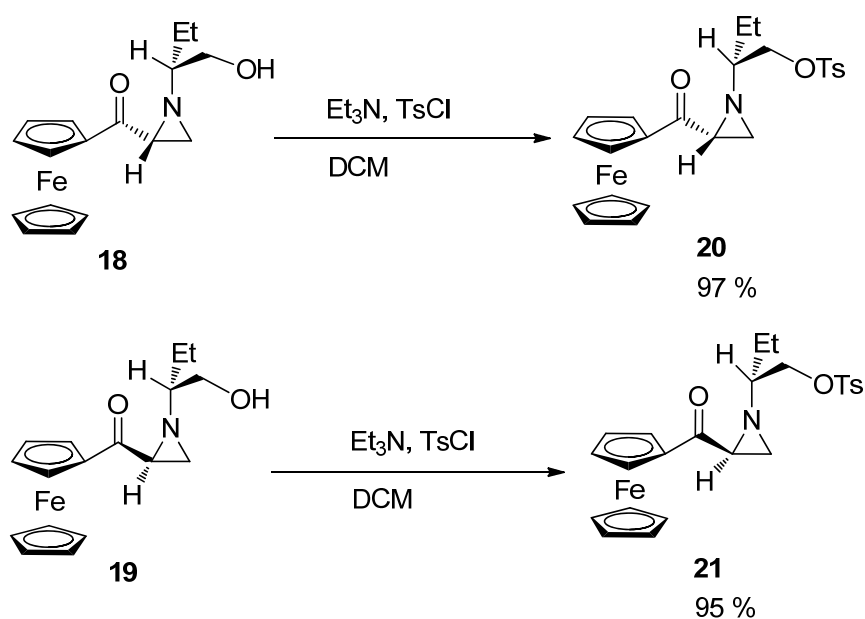
The next step for the synthesis of **POFAM** series ligands is the aziridination of the α -bromo compound **16** via Gabriel-Cromwell reaction [57]. In the presence of Et_3N and chiral amine,

17, (*R*)-(-)-2 amino-1-butanol, aziridination takes place and the aziridines **18** and **19** were obtained as a diastereomeric mixture in 91% total yield (*Scheme 23*). The products were separated and purified by flash column chromatography easily.



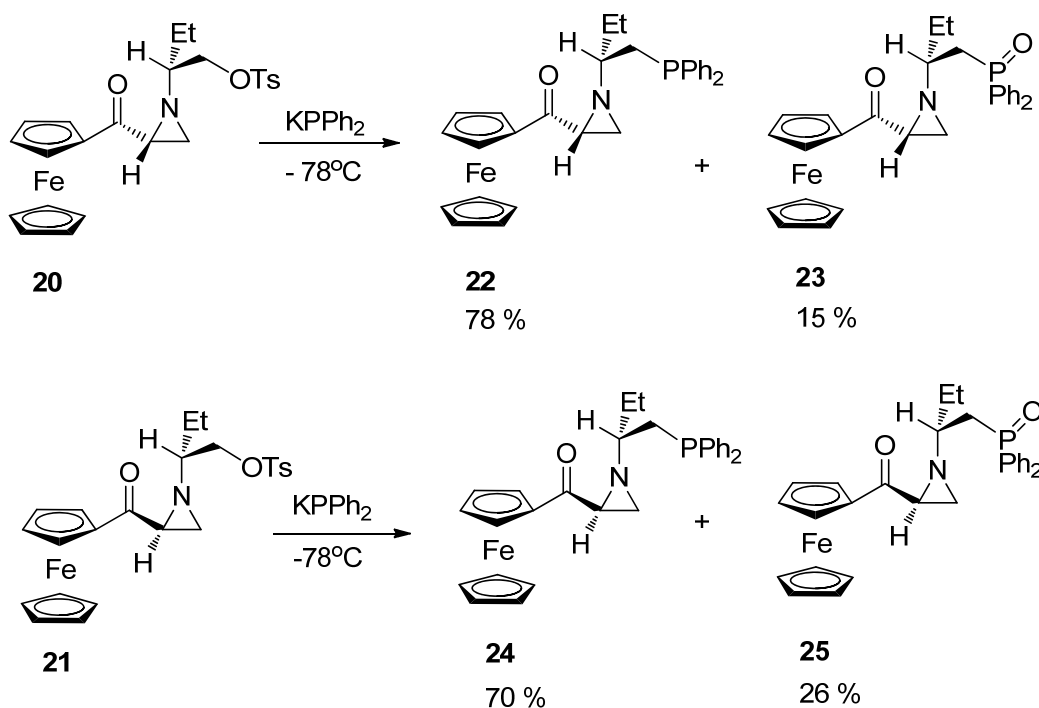
Scheme 23 Synthesis of aziridino ketones

After purification of the aziridines, hydroxyl group was converted to a better leaving group, which is tosylate. The tosylation product from the compound **18** was obtained in 97% yield while that of **19** was obtained in 95% yield (*Scheme 24*).



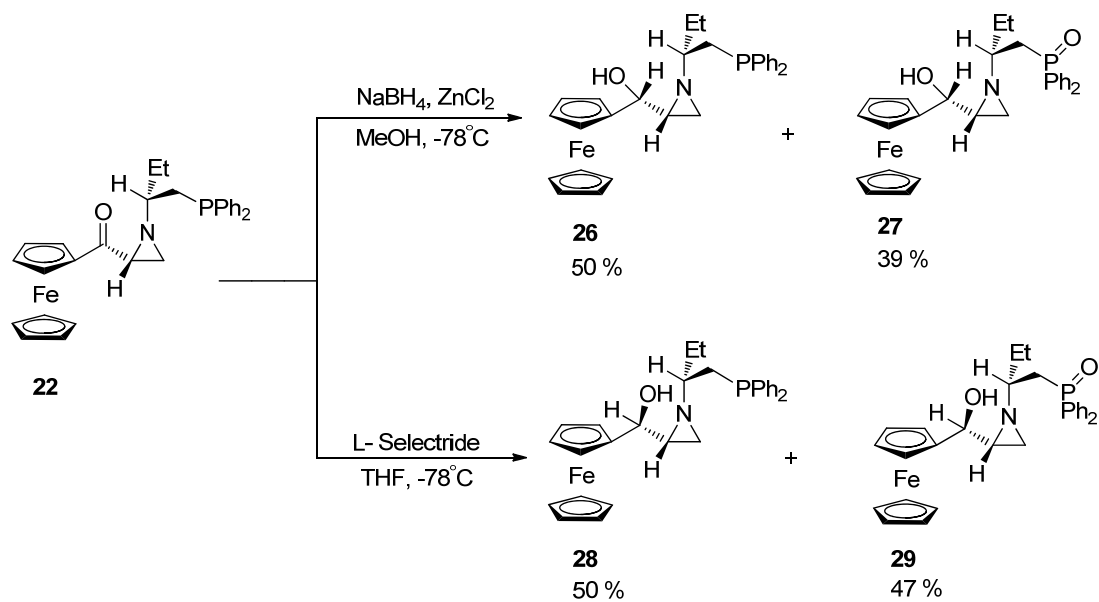
Scheme 24 Synthesis of tosylated products

To perform phosphonylation, our group adapted a procedure reported by Wills and coworkers [58]. Phosphonylation products were obtained in high yields via S_N2 reaction (*Scheme 25*).

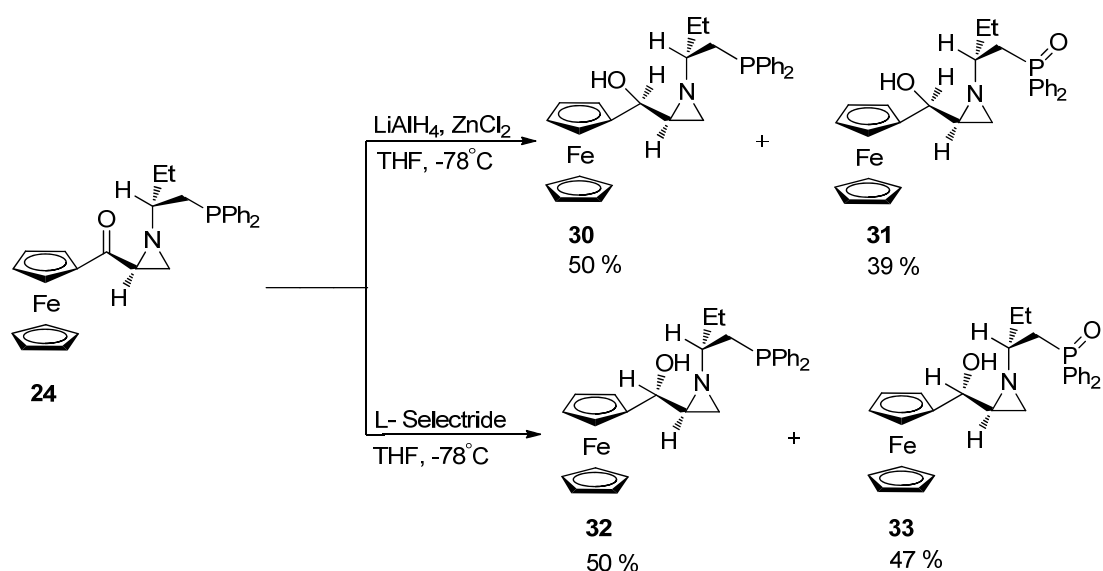


Scheme 25 Synthesis of **PFAM 1 (22)** and **PFAM 2 (24)** and their oxide forms

After obtaining **PFAM1** and **PFAM2**, the remaining **PFAM** series ligands were synthesized by reduction reactions via a literature procedure reported by Lee and coworkers [59].



Scheme 26 Reduction of **PFAM1** for the synthesis of **PFAM3 (26)** and **PFAM4 (28)** and their oxide forms



Scheme 27 Reduction of **PFAM2** for the synthesis of **PFAM5 (30)** and **PFAM6 (32)** and their oxide forms

The absolute configurations of **PFAM** ligands were not determined by X-ray analysis, rather an analogy was made between **PFAM** series ligands and our previously synthesized ferrocenyl aziridinyl methanol, **FAM** ligands. By this way, we assigned configuration of each ligand in **PFAM** series (Figure 13).

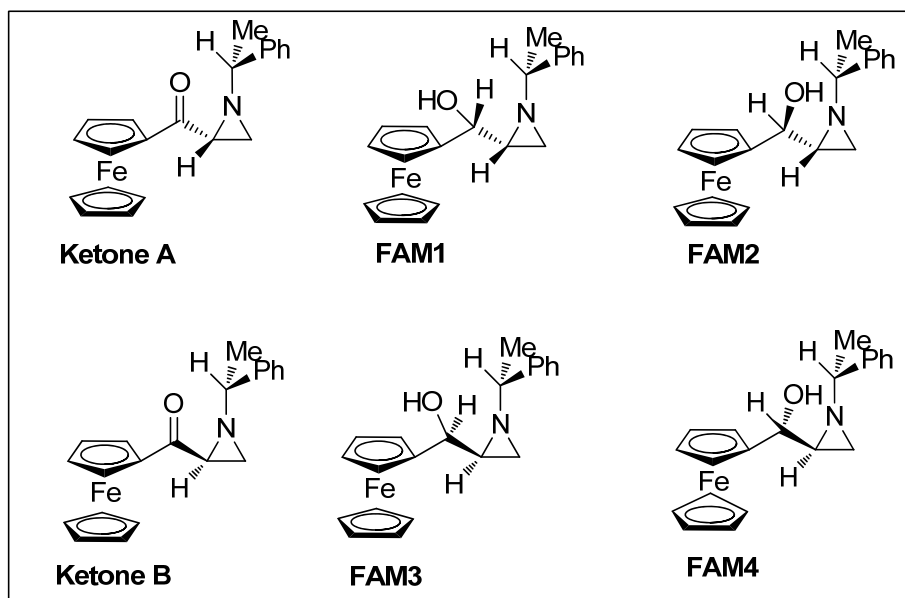
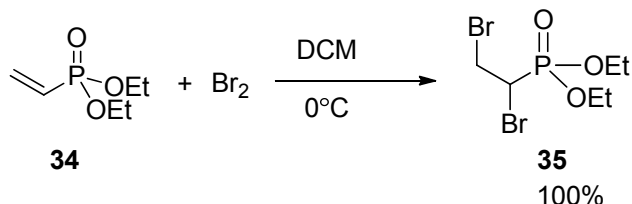


Figure 13 **FAM** series ligands

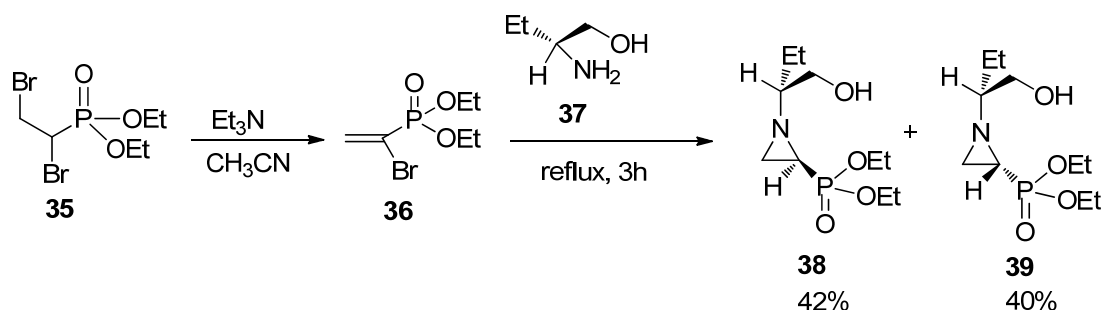
2.2. The synthesis of POAP chiral Lewis bases

To synthesize our newly designed chiral Lewis bases which are aziridinylphosphonates, we started from commercially available diethylvinylphosphonate. Bromination at 0°C provided dibromo compound **35** (Scheme 28) which was purified easily by flash column chromatography. Since this dibromo compound is not UV active, visualization of the TLC was performed by phosphomolybdic acid.



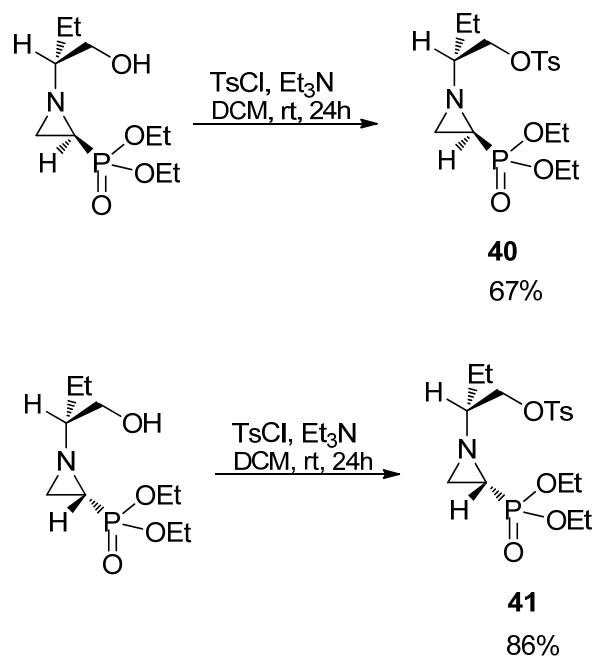
Scheme 28 Synthesis of 1,2-dibromoethyl phosphonate

The same synthetic pathway as in the synthesis of **PFAM** series aziridines were followed to synthesize phosphinoxy counterparts of the **PFAM** aziridines, **18** and **19**. 1,2-Dibromoethyl phosphonate was converted to corresponding α -bromo compound in the presence of Et₃N at room temperature. Then, in the presence of chiral amine *R*-(-)-2-amino-1-butanol, **37**, aziridination took place via Gabriel-Cromwell reaction. The aziridines **38** and **39** were separated and purified by flash column chromatography easily and obtained in 42% and 40% yields, respectively.



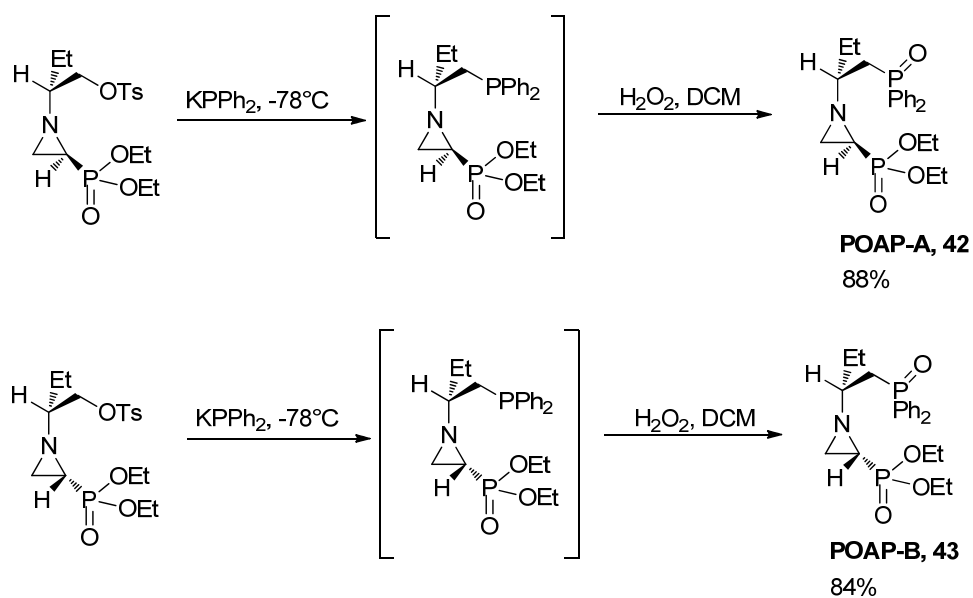
Scheme 29 Synthesis of aziridines

The next step for the synthesis of **POAP** Lewis bases is the tosylation as in the **POFAM** series. The tosylation products **40** and **41** were obtained with 90% and 85% yields (Scheme 30).



Scheme 30 Synthesis of tosylated aziridines

To perform phosphonylation, we adapted the same procedure reported by Wills and coworkers as in **POFAM** series [58]. The reaction proceeds via S_N2 reaction and, at -78°C , corresponding phosphonylation products **42** and **43** were afforded in high yields via dropwise addition of potassium diphenylphosphide. Corresponding phosphonylation products were oxidized in the presence of hydrogen peroxide to get the desired chiral Lewis bases (Scheme 31).



Scheme 31 Synthesis of **POAP-A** and **POAP-B**

The **POAP-B** organocatalyst was obtained as white crystals. Thus, to determine the absolute configuration, X-ray analysis was performed (*Figure 14*). We know the configuration of the chiral center labeled as C14 from the reagent, chiral amine, **37**. Then, we determined the absolute configuration of the center, C18. According to X-ray structure of **POAP-B** crystals, we determined the configuration as (*S,R*), then we assigned the configuration of the other diastereomer as (*R,R*).

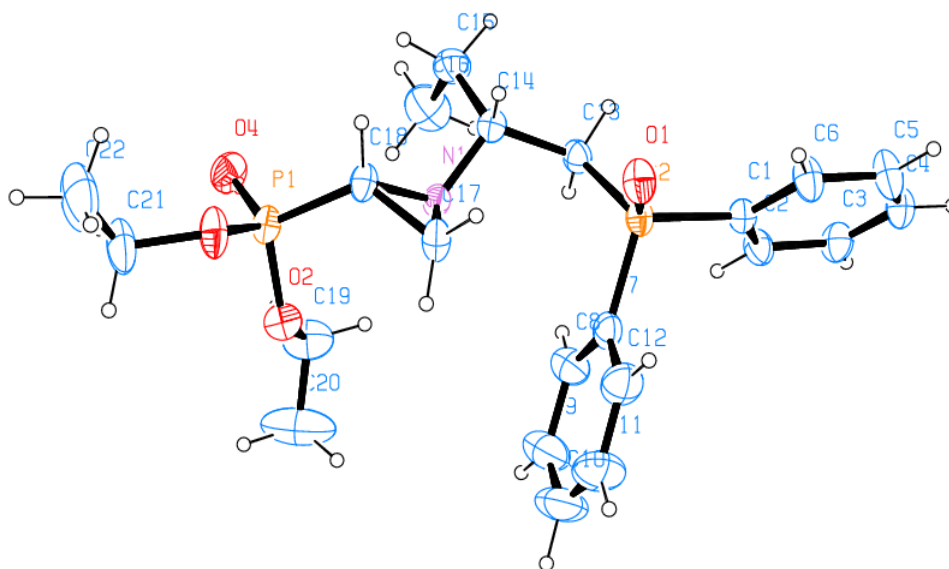


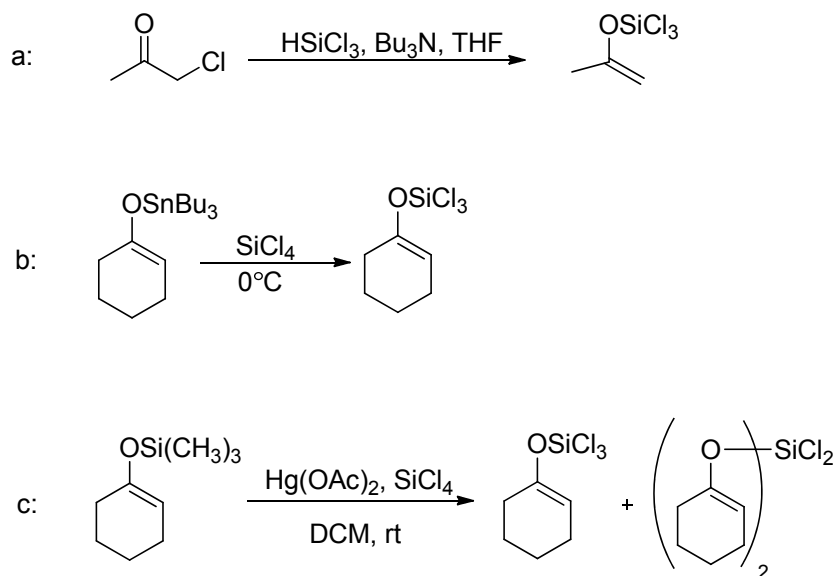
Figure 14 X-ray structure of **POAP-B**

2.3. Silicon tetrachloride mediated asymmetric aldol addition

2.3.1. Formation of silyl enol ether

Ketone-derived silyl enol ethers have been used as the starting materials for the asymmetric aldol addition reactions. There have been two basic approaches based on the formation of silyl enol ether as mentioned in the introduction part [47-54]. The first and the oldest approach involves the synthesis of silyl enol ether starting from α -chloroketones which makes this method impractical due to the limited availability of starting materials (*Scheme 32-a*). The second method involves the transmetalation between stannyl derivatives and SiCl_4 in which stoichiometric amounts of tin reagents are used and tributyltin chloride is formed as a side product (*Scheme 32-b*). Due to the fact that tin reagents are dangerous for our health, this method is not preferred, too. Third method involves the synthesis of silyl enol ether via either transilylation between trimethylsilyl derivative and silicon tetrachloride in the presence of catalytic amounts of mercuric acetate (*Scheme 32-c*). While this method has been an applicable method for the synthesis of various types of ketone-derived silyl enol ethers, it has disadvantageous in terms of formation of bis(enoxy)dichlorosilane as the side product which decreases the overall yield of the desired product [60]. Moreover, the last method involves the use of mercuric salts which is also environmentally unfriendly [61]. Thus, as a more efficient, direct and environmentally friendly procedure, silyl enol ether has

started to be synthesized from ketones in the presence of silicon tetrachloride *in situ* [52-54]. However, *in situ* formation of silyl enol ether results in the decrease in the yields and enantioselectivities, so this method needs to be improved and new catalytic systems should be generated to obtain better results. As a result of these, we selected our approach in favor of *in situ* formation of silyl enol ether.

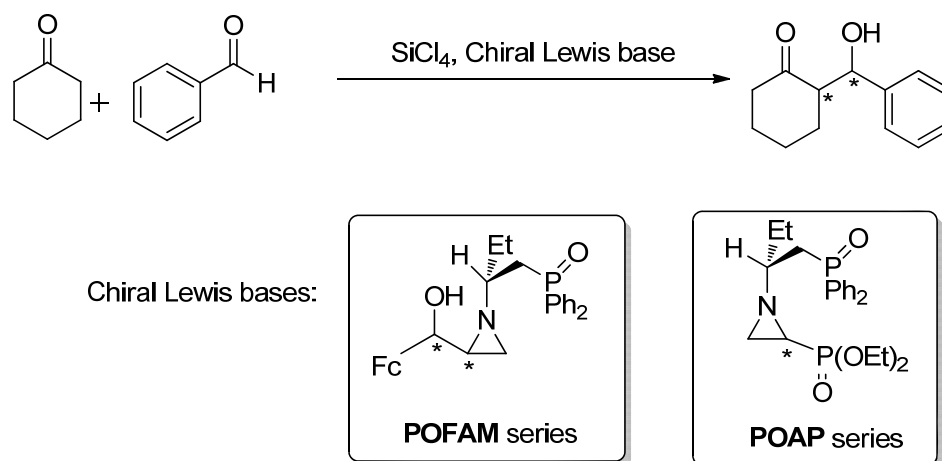


Scheme 32 Methods for the synthesis of silyl enol ether

2.3.2. Chiral Lewis base screening

Asymmetric aldol addition has been well studied with chiral Lewis bases bearing phosphine oxy groups as mentioned in the introduction part [47,51-54]. Phosphine oxy bearing chiral Lewis bases have been attractive candidates for the catalysis of silicon tetrachloride mediated asymmetric aldol reactions due to the high nucleophilicity of them as a result of polarization between P-O bonds compared to the amine analogues. Moreover, their nucleophilicity can be adjusted by the substituents on phosphorous [51,61].

For this purpose, we decided to test the catalytic activities of our **POFAM** ligands containing one phosphine oxy group as well as **POAP** Lewis bases with two phosphine oxy groups (*Scheme 33*).



Scheme 33 Corresponding aldol reaction and chiral Lewis bases

Our initial question was about the coordination of phosphine oxy groups in **POAP** series whether both of them coordinate to silicon or not. Actually, the reason for testing **POFAM** series chiral Lewis base was to answer this question. At -78°C , **POFAM** series chiral Lewis bases were ineffective in performing these diastereoselective and enantioselective transformations. Background reaction was also slow at -78°C , the corresponding aldol addition products were obtained in trace amounts (*Entries 3-6, Table 1*). Then, we thought that phenyl group bearing phosphine oxy part cannot be able to activate silicon, rather ethoxy substituted phosphine oxy group participates in this enantioselective transformation by activating the silicon. The results of the chiral Lewis base screening studies were summarized in *Table 1*.

Among the two phosphine oxy aziridinyl phosphonates, **POAP-A** was by far the most effective in terms of diastereoselection and enantioselection. Most probably, it is the outcome of the stereochemistry of the chiral Lewis base. For **POAP-B**, suitable approach and coordination of the Lewis base to silicon for sufficient activation of the center to induce diastereoselection and enantioselection was not the case. As a result, the chiral Lewis base of choice was **POAP-A**.

Malkov and Kocovsky mentioned in their reviews that the diastereoselectivity of the reaction largely depends on the structure of the catalyst [62]. In other words, bidentate and smaller monodentate catalysts were allowed to coordinate to silicon from two points, and thus reacted through a cationic chairlike transition state. In the case of a bulky monodentate catalyst, due to the steric reasons, coordination of the second catalyst molecule is prevented, as a result of which the diastereoselectivity of the reaction was reversed.

Aldol reactions can proceed in two distinct pathways which determines whether the reaction is *anti* or *syn* selective, ie. the diastereomeric ratio [63]. The preference of the *anti* diastereomer over *syn* diastereomer (*Entry 1, Table 1*) suggest that our reaction follows the first pathway in which two phosphine oxy groups coordinate to silicon and form hexavalent species (*Figure 15*).

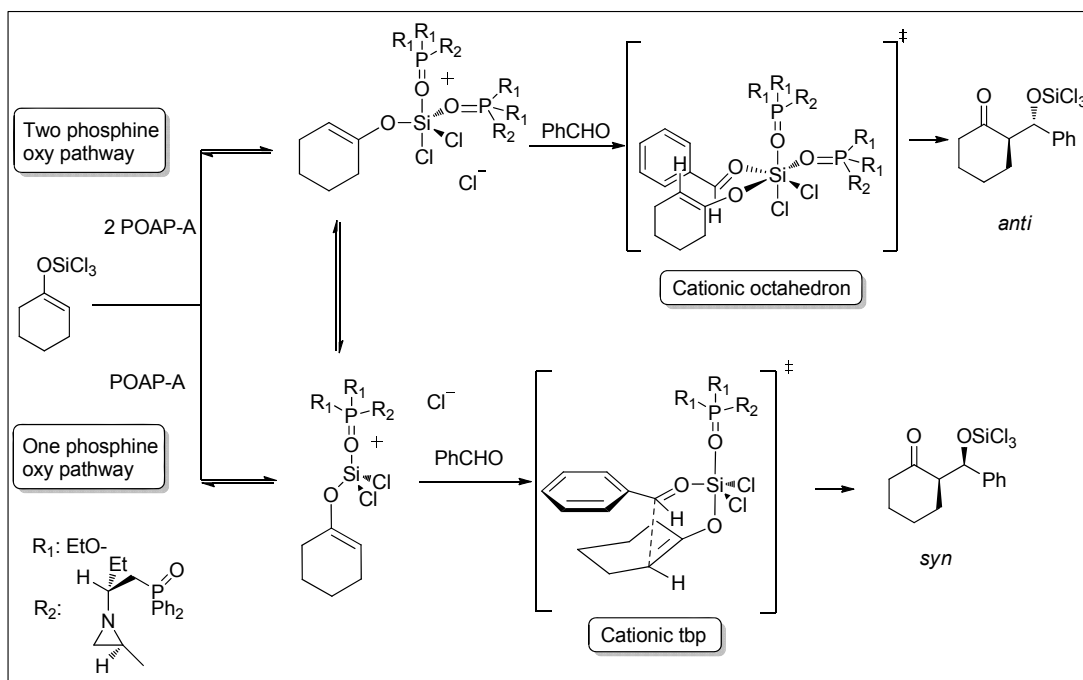
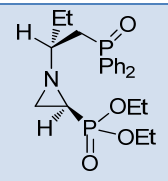
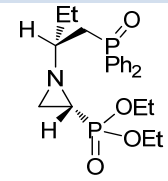
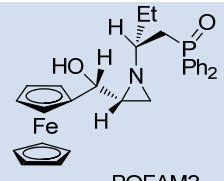
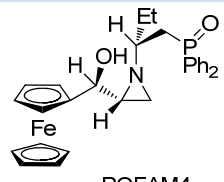
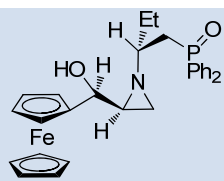
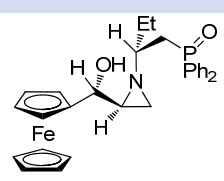


Figure 15 Two pathways of aldol addition

Table 1 Chiral Lewis base screening studies

Entry	Chiral catalyst	Yield ^a (%)	dr ^b (<i>anti</i> : <i>syn</i>)	ee ^c % <i>anti</i> (<i>syn</i>)
1	 POAP-A	26	92:8	37 (1)
2	 POAP-B	13	50:50	5 (2)
3	 POFAM3	<5	52:48	9 (2)
4	 POFAM4	<5	58:42	3 (7)
5	 POFAM5	<5	60:40	5 (rac)
6	 POFAM6	<5	63:37	3 (4)

^aIsolated yield ^bDetermined from crude ¹H-NMR spectrum ^cDetermined by HPLC using Chiralcel OD-H column

2.3.3. Temperature, concentration and additive screening studies

Following the chiral Lewis base screening studies, we conducted the temperature screening studies at four different temperatures. At room temperature, aldol condensation occurs with the elimination of water, so we did not perform our reaction at higher temperatures. At 0°C, poor diastereomeric ratio and racemic products were obtained which made us think that the rate of background reaction was faster than the chiral Lewis base catalyzed pathway. When the reaction was run at -20°C, sharp increase in the diastereoselectivity and enantioselectivity were achieved with little decrease in yield. As a result, we thought that if we decrease the temperature, the diastereoselectivity and enantioselectivity will improve. We performed the reaction at -50°C and -78°C degrees, and the results of these reactions satisfied our initial considerations about the enantioselectivity of the *anti* product (*Table 2*) whereas the reverse trend in diastereoselectivities were obtained. At lower temperatures, the yield of the reaction decreased as expectedly, but this decrease was not so critical and deterrent that we chose -78°C as our reaction temperature and continued with additive screening studies.

The rate and the diastereoselectivity of the aldol reactions depend on the additive, too. Use of additive minimizes the silyl cation promoted achiral pathway. Moreover, tertiary amines are not only used as acid scavengers to neutralize hydrogen chloride generated *in situ* during silyl enol ether formation, but also they are effective in catalyst turnover, and increase the reaction rate by promoting the dissociation of phosphine oxide from silicon [61,64].

Different tertiary amine additives were tested for the corresponding aldol reaction (*Entries 4-9, Table 2*). The diastereomeric ratios are comparable except the one obtained with *N,N*-dicyclohexylmethylamine. The reactions with DIPEA and proton sponge proceeded in favor of *syn* diastereomer (*Entries 5 and 6*), while the *anti* diastereomer predominates with Et₃N, DABCO or TMEDA (*Entries 4, 7 and 9*). With *N,N*-dicyclohexylmethylamine, no diastereomeric excess was observed (*Entry 8*). Moreover, the effect of additive on the yield of the reaction can be easily perceived from the *Table 2*. Unfortunately, aldol products were obtained in trace amounts when DIPEA, proton sponge and *N,N*-dicyclohexylmethylamine were used (*Entries 5, 6 and 8*) as well as DABCO which give only 7% yield (*Entry 7*). Under the same conditions, aldol products were obtained with the highest yield when TMEDA was used as the tertiary amine additive (*Entry 9*).

To make sure that whether we can increase the enantioselectivity of the reaction or not, we performed concentration screening studies. We thought that the background reaction would slow down, or its effect on the overall reaction can diminish upon dilution. As a result of dilution of the reaction mixture, the enantiomeric excess and the diastereomeric ratio were slightly increased, while the yield was decreased as expected, but it was not a crucial decrease (*Entries 9, 10 and 11*). Since the diastereomeric ratio was higher at the lower concentration, we prefer to perform the optimization studies at that concentration (*Entry 11*).

Table 2 Results of temperature, concentration and additive screening studies

Entry	T (°C)	Additive	M	Yield ^a (%)	dr ^b (anti:syn)	ee ^c % anti (syn)
1	0	Et ₃ N	1.12	28	67:33	2 (Rac)
2	-20	Et ₃ N	1.12	26	92:8	37 (1)
3	-50	Et ₃ N	1.12	20	75:25	55 (3)
4	-78	Et ₃ N	1.12	18	71:19	61 (19)
5	-78	DIPEA	1.12	<5	25:75	42 (17)
6	-78	Proton sponge	1.12	<5	27:73	23 (15)
7	-78	DABCO	1.12	7	76:24	61 (7)
8	-78	cHex ₂ NMe	1.12	<5	50:50	32 (10)
9	-78	TMEDA	1.12	52	78:22	60 (10)
10	-78	TMEDA	0.71	50	83:17	66 (15)
11	-78	TMEDA	0.35	46	88:12	66 (14)

^aIsolated yield ^bDetermined from crude ¹H-NMR spectrum ^cDetermined by HPLC using Chiralcel OD-H column

2.3.4. Solvent screening studies

Different solvents including polar and nonpolar, or protic and aprotic were also tested for the corresponding aldol reaction and the results are summarized in *Table 3*. It was reported by Denmark and coworkers that highly polar or protic solvents promote catalyst turnover [64].

Table 3 Solvent screening studies

Entry	T (°C)	Solvent	Yield ^a (%)	dr ^b (<i>anti:syn</i>)	ee ^c % <i>anti</i> (<i>syn</i>)
1	-78	Toluene	<5	6:94	12 (6)
2	-78	Et ₂ O	trace	nd	17 (6)
3	-78	EtCN	61	83:17	55 (rac)
4	-20	DCE	50	72:28	23 (23)
5	-20	CH ₃ CN	66	66:34	10 (42)
6	-78	DCM	50	83:17	66 (15)

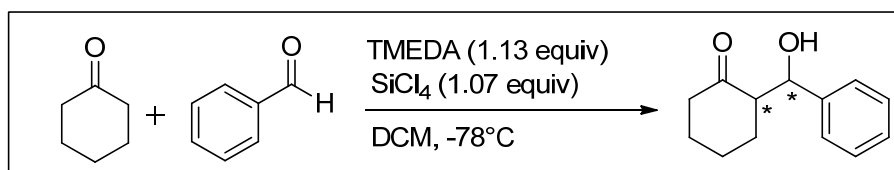
^aIsolated yield ^bDetermined from crude ¹H-NMR spectrum ^cDetermined by HPLC using Chiralcel OD-H column

With the relatively nonpolar solvents such as toluene and diethyl ether, aldol products were obtained in very low yields which may be the result of low solubility of our chiral Lewis base in these solvents. Background reaction dominates so that we obtained the products with poor enantioselectivities and *syn* selectivity also satisfy this (*Entries 1 and 2*). Acetonitrile and propionitrile are highly polar and Lewis basic solvents which provided relatively good yields indeed (*Entries 4 and 6*). However, the reason of low enantiomeric excess and lower diastereomeric ratio obtained with acetonitrile may be the higher operating temperature at which background reaction may interfere. We were supposed to perform the reaction at -20°C, since the melting point of this solvent is -46°C. The polarity indices of 1,2-DCE and DCM are close to each other. The reason of low enantiomeric excess obtained with 1,2-DCE can be again the higher reaction temperature as in the case of acetonitrile (*Entries 4 and 6*).

2.3.5. Further optimization studies

After all these standard optimization studies, we performed many other optimization studies in order to realize whether we can increase the extent of the stereocontrol in our reactions or not.

Finally, we wanted to test the effect of the amounts of additive and silicon tetrachloride. Our current conditions are given in *Figure 16*:

**Figure 16** Reaction conditions adapted after standard optimization studies

The results of these equivalency modification studies were given in *Table 4*. First, we increased and decreased the amount of additive resulting in decrease in the yield, conserving the enantioselectivities. Actually, it was straightforward and already estimated that when we decrease the amount of additive, reaction will slow down and as a result, the yield will decrease and the reverse was expected when we increased the amount of additive. Unexpectedly, the yield and diastereomeric excess were decreased sharply (*Entries 1 and 2*). Then, we increased and decreased the equivalency of silicon tetrachloride resulting in remarkable decrease in yield and diastereomer ratio and slight decrease in enantioselectivity (*Entries 3 and 4*). With the help of these studies, we determined the threshold values of the equivalencies, which are given in *Figure 16*.

Table 4 Equivalency screening studies

Entry	Additive (equiv)	SiCl ₄ (equiv)	Yield ^a (%)	dr ^b (<i>anti</i> : <i>syn</i>)	ee ^c % <i>anti</i> (<i>syn</i>)
1	0.8	1.07	46	90:10	65 (21)
2	1.5	1.07	44	57:43	66 (8)
3	1.13	1.5	39	67:33	60 (3)
4	1.13	0.8	48	50:50	61 (9)

^aIsolated yield ^bDetermined from crude ¹H-NMR spectrum ^cDetermined by HPLC using Chiralcel OD-H column

We have three different concentrations which are enolate concentration, chiral Lewis base concentration and overall reaction concentration. Thus, we thought to find the optimum concentrations for each.

Initially, at the same chiral Lewis base and overall reaction concentration, we increased the concentration at which silyl enol ether forms. We expected an increase in the yield (*Entries 1, 2 and 3, Table 5*). At 1.0M enolate concentration, yield was increased remarkably, without a significant decrease in diastereoselectivity and enantioselectivity. Thus, at this enolate concentration, we altered the concentration of the chiral Lewis base. Upon the increase and the decrease of the chiral Lewis base concentration, the yields were decreased with a slight decrease in the diastereoselectivity and enantioselectivity (*Entries 2, 4 and 5, Table 5*). Moreover, Denmark and coworkers reported that the rate of addition of benzaldehyde is important in terms of diastereoselectivity of the reaction. According to their findings, slow addition of aldehyde results in higher and more reproducible diastereomeric ratios [48]. However, when benzaldehyde added much slower (80 min) than our standard procedure (15 min), we observed slight decrease in diastereomeric ratio (*Entry 7*). Thus, we decided to test the effect of fast aldehyde addition on the diastereoselectivity. Fast addition of aldehyde gave rise to slight increase in diastereomeric ratio without the loss of enantioselectivity, however the yield was decreased (*Entry 6*).

Table 5 Results of concentration, benzaldehyde addition and time studies

Entry	M ₁	M ₂	M ₃	Yield ^a (%)	dr ^b (<i>anti:syn</i>)	ee ^c % <i>anti</i> (<i>syn</i>)
1	0.6	0.35	0.04	46	79:21	63 (21)
2	1.0	0.35	0.04	67	71:29	61 (22)
3	2.0	0.35	0.04	32	45:55	56 (6)
4	1.0	0.35	0.50	40	70:30	65 (18)
5	1.0	0.35	0.02	49	75:25	61 (42)
6 ^d	1.0	0.35	0.04	37	80:20	66 (17)
7 ^e	1.0	0.35	0.04	52	70:30	62 (11)
8 ^f	1.0	0.35	0.04	63	71:29	63 (16)
9 ^h	1.0	0.35	0.04	51	*	62 (15)
10 ^g	1.0	0.35	0.04	48	85:15	61 (12)
11 ⁱ	1.0	0.35	0.04	65	73:27	64 (13)
12 ⁱ	1.0	0.71	0.04	75	82:28	65 (10)
13 ⁱ	1.0	0.35	0.04	70	33:66	51 (9)
14 ⁱ	1.0	0.71	0.04	80	17:83	53 (3)

^aIsolated yield ^bDetermined from crude ¹H-NMR spectrum ^cDetermined by HPLC using Chiralcel OD-H column M₁: Enolate concentration M₂: Reaction concentration M₃: Chiral Lewis base concentration ^dFast addition of aldehyde ^eSlow addition of aldehyde over 80 min. ^fEnolate formation time is increased to 1h from 15 min. ^gReaction time is increased to 30h ^hReaction time is decreased to 15h ⁱChiral Lewis base coordination time is increased. *dr(5h):75:25, dr(21h):76:24, dr(30h):71:29

Following these studies, we decided to focus on enolate formation time. It was 15 min in our standard procedure, and we thought that increase in the time of enolate formation may result in increase in the yield. However, it didn't have a significant effect on the yield, (*Entry 8*). Another possibility to increase the yield of our reaction was the prolonging the reaction time. We increased our reaction time from 21h to 30h, the yield and the diastereomeric excess

were decreased (*Entry 9*). The decrease in the diastereomeric ratio was consistent with our observations during the reaction. During TLC controls, we observed that *anti* product is formed first and *syn* product is formed later, as the reaction proceeds, formation of *syn* product predominates resulting in the decrease in diastereomeric ratio. Thus, we decided to decrease the reaction time hoping to see the reverse trend in diastereoselectivity. We decreased the reaction time to 15h, and the diastereoselectivity was improved as expected while the yield and enantioselectivity were decreased (*Entry 10*).

As a final strategy for concentration and time studies, we increased the time allowed for coordination of chiral Lewis base with silyl enol ether which was also believed to increase the yield of the reaction. First, we increased the time from 15 min to 30 min and this increase had positive effect on yields without the significant loss of enantiomeric excesses (*Entries 11 and 12*). Hoping to see further increase, this coordination time was further increased to 45 min. However, the diastereomeric ratio and enantiomeric excesses were decreased dramatically (*Entries 13 and 14*). This further increase in the coordination time of chiral Lewis base and silyl enol ether reversed the diastereomeric ratio, reaction preferred to proceed through the second pathway (*Figure 15*) in which equilibrium shifts to the cationic trigonal bipyramidal transition state resulting in *syn* product.

Our limiting reagent was cyclohexanone in all optimization studies. Before moving to aldehyde screening studies, we changed the limiting reagent to benzaldehyde. The results of this part was not included in Table 5. The yield was decreased sharply (19%), the diastereoselectivity was in favor of *syn* diastereomer (14:86, *anti:syn*) and poor enantioselectivity was attained (38 (15), *anti (syn)*).

2.3.6. Aldehyde screening studies

To ensure substrate generality, we tested different aromatic aldehydes in the corresponding aldol addition reactions at preoptimized conditions given in *Figure 16*.

The results of aldehyde screening studies were summarized in *Table 6*. Firstly, we can draw such a conclusion that our chiral Lewis base, **POAP-A** is well suited for the corresponding aldol reaction, since it catalyzed the reaction in an *anti* fashion via six-membered cyclic transition state. We proposed that the *p*-bond interaction between the phenyl rings on the chiral Lewis base and the phenyl ring of the aromatic aldehyde may be the reason of this regioselectivity and enantioselectivity. However, we did not perform theoretical studies based on transition state modeling, that is why we couldn't give a transition state structure which satisfies our proposals.

Table 6 Aldehyde screening studies

Entry	R	Yield ^a (%)	dr ^b (<i>anti</i> : <i>syn</i>)	ee ^c % <i>anti</i> (<i>syn</i>)
1	Ph	75	82:18	65 (10)
2	<i>p</i> -MeOPh	39	83:17	64 (35)
3	<i>m</i> -MeOPh	26	54:46	50 (78)
4	<i>o</i> -MeOPh	30	68:32	55 (50)
5	<i>p</i> -CH ₃ Ph	25	64:36	64 (13)
6	2-Naphthyl	25	74:26	68 (67)
7	1-Naphthyl	40	91:9	20 (30)
8	Cinnamyl	27	93:7	44 (8)
9	<i>p</i> -CF ₃ Ph	55	84:16	45 (44)
10	<i>p</i> -NO ₂ Ph	40	72:28	43 (13)
11	<i>m</i> -NO ₂ Ph	24	81:19	43 (41)
12	<i>o</i> -NO ₂ Ph	16	59:41	36 (45)

^a Isolated yield ^b Determined from crude ¹H-NMR spectrum ^c Determined by HPLC

Denmark and coworkers stated that when the steric hinderence is minimum, aldehydes bearing electron donating groups provide better selectivities than benzaldehyde while the aldehydes with electron withdrawing groups provide lower selectivities [60]. As can be inferred from the table, electronic nature of the aromatic aldehydes affected the enantioselectivities which is consistent with the Denmark's conclusion. With *para*-substituted aromatic aldehydes, the steric interactions are minimum and the trend between the aldehydes is in accord with the conclusion stated by Denmark and coworkers [60]. In other words, when the electron donating groups are at *para* positions, enantioselectivities became comparable to the enantioselectivity of the reaction with benzaldehyde (*Entries 2, 5 and 6*). This rule is broken out by 1-naphthaldehyde, for which steric reasons are believed to predominate over electronic factors (*Entry 7*). Moreover, we tested the effect of position of the substituent with anisaldehyde. The results made us propose that steric factors generated from *meta* or *ortho* substitution prevailed the electronic effects of methoxy group such that the coordination of second phosphine oxy group is somewhat prevented and enantioselectivity of *syn* diastereomer become more pronounced than that in *para*-substituted aldehyde. It is noteworthy to state that no conjugate addition product with cinnamaldehyde was observed which is also consistent with the literature [47].

With electron withdrawing groups, enantioselectivities were lower than that of benzaldehyde (*Entries 9-12*). Similarly, steric factors contribute to the formation of boat-like transition state structure leading to higher enantioselectivities of *syn* diastereomer when the position of the substituent on the ring changes (*Entries 10-12*) which is also consistent with our initial observations explained in the previous paragraph.

CHAPTER 3

CONCLUSION

In this work, our previously designed phosphine oxy bearing chiral Lewis bases were synthesized to serve as promoters in silicon tetrachloride mediated asymmetric aldol reactions. We have two different chiral Lewis base families accommodating phosphine oxy subunits in their structures, namely **POFAM** and **POAP** series. **POFAM** series consist of one phosphine oxy group in their structures, whereas **POAP** series bear two phosphine oxy groups in their structures. With these two structurally different chiral Lewis base families, we tried to promote the corresponding aldol reaction. Among 6 different potential chiral Lewis bases, **POAP-A** was able to catalyze the reaction in an expected fashion. With **POAP-A** chiral Lewis base, we performed standard optimization studies involving temperature, concentration, additive and solvent screening studies in order to select the best conditions in favor of yield, diastereomeric ratio and enantioselectivity. After these optimization studies, to see whether we can improve the results or not, we analyzed the reaction conditions in a more detailed way than standard optimization protocols (*Tables 4 and 5*), and unfortunately, a significant improvement cannot be achieved. We observed that background reaction competes with the chiral Lewis base promoted reaction. After determining our best results (75% yield, dr *anti (syn)* = 82:18, and ee *anti (syn)* = 65 (10)), 11 other substrates were selected to ensure substrate generality of our reaction conditions. In those reactions, aldol adducts were obtained with moderate to good yields and enantioselectivities. Although the results were not high or excellent, they are so promising in terms of being comparable to the values as in the works of Nakajima, Kotani and their coworkers and Benaglia and coworkers.

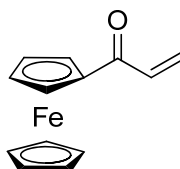
CHAPTER 4

EXPERIMENTAL

4.1. General procedure

All reactions were carried out in predried and vacuumed Schlenk tubes under inert atmosphere of argon or nitrogen. Solvents and chemicals were received from chemical suppliers, dried, purified and stored with the help of standard techniques prior to use. Silica coated plates (250 μ m Silica Gel 60 F₂₅₄ plates) were used to monitor the reactions via visualization by UV light at 254 nm or by TLC stains which are anisaldehyde and ethanolic phosphomolybdic acid. All asymmetric reactions were quenched by saturated NaHCO₃ solution and then extraction was accompanied to obtain crude reaction mixture. The diastereomer ratios of the aldol products were determined from the splitting pattern of hydroxyl bearing methine proton in crude ¹H-NMR spectra. Purification of the products was done by flash column chromatography using E. Merck Silica Gel 60 (particle size: 0.040-0.063 mm, 230-400 mesh ASTM). The mobile phases include hexane and ethyl acetate mixtures, components of which were distilled prior to use. Acetone and methanol were used as received from suppliers. Enantiomeric excess of aldol addition products were determined by HPLC analysis using chiral HPLC columns at predetermined conditions reported in the literature. To make sure about the detection of the retention times, racemic mixtures of the compounds were prepared in the absence of chiral Lewis base before analysis. ¹H, ¹³C and ³¹P NMR spectra were reported on a Bruker spectropin Avance DPX-400 Ultra shield instrument at 400 MHz, 100 MHz and 162 MHz respectively. NMR samples were prepared in 1:1 CDCl₃-CCl₄ solution and TMS was used as internal standard for the NMR analyses. Rudolph Research Analytical Autopol III Polarimeter was used to measure optical rotations. Measurements was done in 1 dm cell and reported as $[\alpha]_D^{25}$ (c in 10mg/ 1 mL solvent).

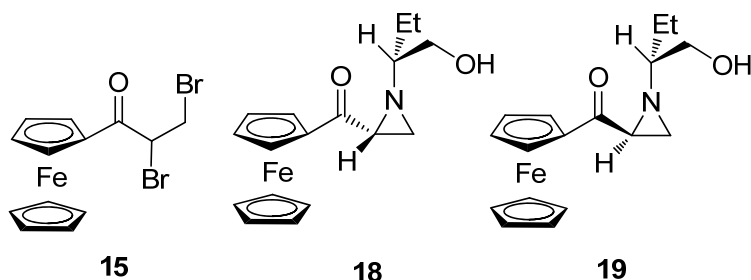
4.2. Synthesis and characterization of acryloyl ferrocene



14

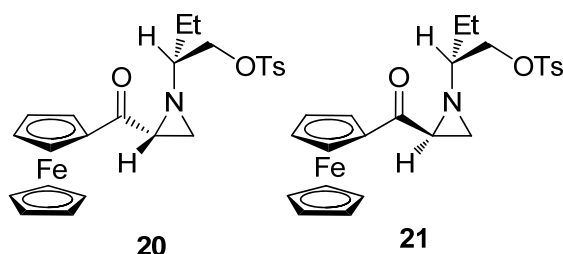
Acryloyl ferrocene, **14** was synthesized following the procedures reported by our group members and obtained as an orange-red solid (5.2 g) in 100% yield [34,55]. ¹H-NMR (400 MHz, CDCl₃) δ 6.81 (dd, *J* = 17.0, 10.2 Hz, 1H), 6.44 (d, *J* = 16.8 Hz, 1H), 5.71 (d, *J* = 10 Hz, 1H), 4.81 (s, 2H), 4.54 (s, 2H), 4.17 (s, 5H).

4.2.1. Synthesis and characterization of aziridino ketones **18** and **19**



1,2-dibromopropionyl ferrocene, **15** was synthesized with procedures reported by our group members and obtained in 95 % yield (8.18 g, 20.5 mmol). From this precursor, the aziridino ketones **18** (3.38 g, 10.32 mmol, 48 % yield, light orange solid) and **19** (3.03 g, 9.26 mmol, 43 % yield, orange solid) were synthesized following the procedures reported [34,55]. **18**: $^1\text{H-NMR}$ (400 MHz, CDCl_3) δ 4.92 (s, 1H), 4.84 (s, 1H), 4.51 (s, 2H), 4.21 (s, 5H), 3.75 (br, 2H), 2.68 (br, 1H), 2.32 (s, 1H), 2.23 (br, 1H) 1.66 (m, 4H), 0.98 (t, $J = 7.2$ Hz, 3H) **19**: $^1\text{H-NMR}$ (400 MHz, CDCl_3) δ 4.82 (d, $J = 12.97$ Hz, 2H, Fc), 4.46 (s, 2H), 4.14 (s, 5H), 3.68 (br, 2H), 2.49 (br, 1H), 2.26 (s, 1H), 2.14 (br, 1H), 1.79 (br, 1H), 1.67 (m, 1H), 1.57 (m, 1H), 1.45 (br, 1H), 0.93 (t, $J = 7.25$ Hz, 3H).

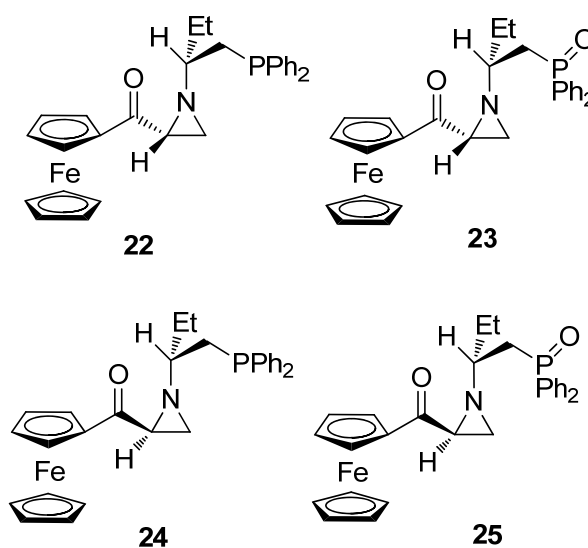
4.2.2. Synthesis and characterization of tosylated aziridino ketones **20** and **21**



Following the literature procedures, tosylated aziridino ketone **20** was obtained as an orange solid (1.92 g, 3.98 mmol) in 97% yield and tosylated aziridino ketone **21** as an orange oily liquid (2.29 g, 4.76 mmol) in 95% yield [34,55]. **20**: $^1\text{H-NMR}$ (400 MHz, CDCl_3) δ 7.63 (d, $J = 8.1$ Hz, 2H), 7.22 (d, $J = 8.0$ Hz, 2H), 5.02 (s, 1H), 4.87 (s, 1H), 4.56 (s, 2H), 4.20 (s, 5H),

4.14 (dd, $J = 10.1, 3.8$ Hz, 1H), 3.98 (dd, $J = 10.0, 7.7$ Hz, 1H), 2.82 (q, $J = 3.1$ Hz, 1H), 2.39 (s, 3H), 2.30 (s, 1H), 1.86 (m, 1H), 1.70 (d, $J = 6.4$, 1H), 1.61 (m, 2H), 0.98 (t, $J = 7.5$ Hz, 3H). **21**: $^1\text{H-NMR}$ (400 MHz, CDCl_3) δ , 7.80 (d, $J = 8.15$ Hz, 2H), 7.35 (d, $J = 7.6$ Hz, 2H), 4.86 (s, 2H), 4.51 (s, 2H), 4.17 (s, 5H), 4.11 (d, $J = 5.7$ Hz, 2H), 2.51 (dd, $J = 6.4, 3.0$ Hz, 1H), 2.45 (s, 3H), 2.22 (s, 1H), 1.91 (d, $J = 6.6$ Hz, 1H), 1.83 (pentet, $J = 5.7$ Hz, 1H), 1.59 (m, 2H), 0.95 (t, $J = 7.3$ Hz, 3H).

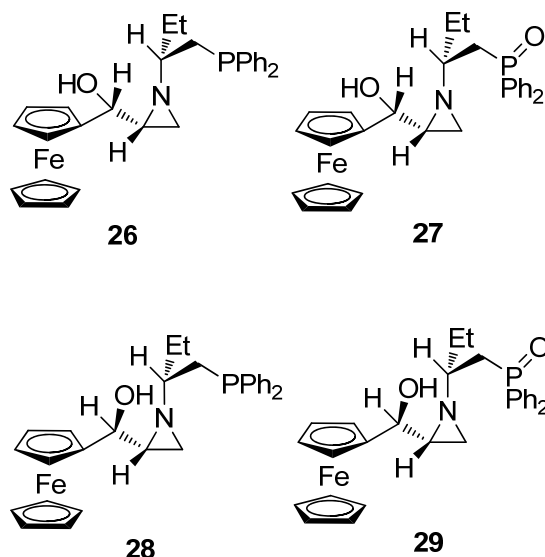
4.2.3. Synthesis and characterization of phosphino aziridines and phosphine oxy aziridines



The phosphino aziridine **22** (0.79 g, 1.60 mmol) was obtained in 78% yield following the procedures reported by our group members [34,55]. The oxidized form, phosphine oxy aziridine **23** (0.16 g, 0.31 mmol) was obtained as a red oily liquid in 15% yield. **22**: $^1\text{H-NMR}$ (400 MHz, CDCl_3) δ 7.34 (m, 4H), 7.23 (m, 6H), 4.77 (s, 2H), 4.43 (s, 2H), 4.08 (s, 5H), 2.32 (t, $J = 7.5$ Hz, 2H), 2.27 (d, $J = 7.1$ Hz, 1H), 1.74 (sextet, $J = 7.2$ Hz, 2H), 1.65 (d, $J = 6.6$ Hz, 1H), 1.38 (sextet, $J = 5.8$ Hz, 1H), 0.94 (t, $J = 7.4$ Hz, 3H). **23**: $^1\text{H-NMR}$ (400 MHz, CDCl_3) δ 7.65 (m, 4H), 7.39 (m, 4H), 7.28 (m, 2H), 5.00 (s, 1H), 4.77 (s, 1H), 4.41 (s, 2H), 4.05 (s, 5H), 2.95 (dd, $J = 3.1, 2.8$ Hz, 1H), 2.51 (m, 2H), 2.31 (s, 1H), 2.04 (m, 1H), 1.81 (d, $J = 6.1$ Hz, 1H), 1.61 (m, 1H), 1.53 (m, 1H), 0.82 (t, $J = 7.4$ Hz, 3H).

The phosphino aziridine **24** was obtained as an orange solid (0.94 g, 1.89 mmol) in 76% yield while its oxidized form, phosphine oxy aziridine **25** (0.26 g, 0.5 mmol) was obtained as a red solid in 20% yield following the same reference procedures [34,55]. **24**: $^1\text{H-NMR}$ (400 MHz, CDCl_3) δ 7.45 (m, 4H), 7.34 (m, 6H), 4.84 (s, 2H), 4.50 (s, 2H), 4.19 (s, 5H), 2.44 (m, 3H), 2.19 (s, 1H), 1.81 (pentet, $J = 7.2$ Hz, 2H), 1.61 (d, $J = 6.7$ Hz, 1H), 1.51 (sextet, $J = 6.3$ Hz, 1H), 1.01 (t, $J = 7.4$ Hz, 3H). **25**: $R_f = 0,35$ EtOAc after treatment of Et_3N for TLC; $^1\text{H-NMR}$ (400 MHz, CDCl_3) δ 7.86 (m, 2H), 7.75 (m, 2H), 7.50 (m, 6H), 4.82 (s, 2H), 4.51 (s, 2H), 4.17 (s, 5H), 2.67 (m, 2H), 2.60 (dd, $J = 6.3, 2.7$ Hz, 1H), 2.15 (septet, $J = 5.5$ Hz, 1H), 1.90 (s, 1H), 1.83 (d, $J = 6.7$ Hz, 1H), 1.69 (pentet, $J = 7.3$ Hz, 2H), 0.94 (t, $J = 7.4$ Hz, 3H).

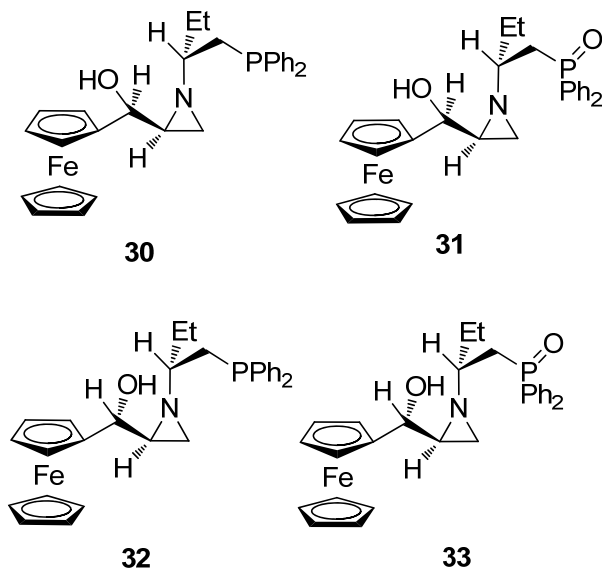
4.2.4. Synthesis and characterization of PFAM and POFAM ligands from phosphino aziridine **22**



From compound **22**, **PFAM3**, **26** was obtained as a light yellow oily liquid (0.24 g, 0.486 mmol) in 60% yield, while its oxidized form, **POFAM3**, **27** was synthesized and obtained as a yellow oily liquid (0.16 g, 0.308 mmol) in 38% yield applying the procedures reported by our group members [34,55]. **26**: ¹H-NMR (400 MHz, CDCl₃) δ 7.34-7.23 (m, 10H), 4.29 (d, *J* = 4.3 Hz, 1H), 4.19 (s, 1H), 4.16 (s, 1H), 4.11 (s, 5H), 4.08 (s, 1H), 2.46 (br, 1H), 2.09 (ddd, *J* = 7.7, 6.3, 5.1 Hz, 2H), 1.81 (d, *J* = 3.3, 1H), 1.66 (sextet, *J* = 6.2 Hz, 1H), 1.59 (sextet, *J* = 7.1 Hz, 1H), 1.53 (m, 1H), 1.33 (sextet, *J* = 7.5 Hz, 1H), 1.23 (d, *J* = 6.4 Hz, 1H), 0.89 (t, *J* = 7.4 Hz, 3H) **27**: ¹H-NMR (400 MHz, CDCl₃) δ 7.57 (q, *J* = 7.4 Hz, 4H), 7.43-7.37 (m, 6H), 4.23 (s, 1H), 4.18 (s, 1H), 4.14 (s, 5H), 4.11 (s, 2H), 3.97 (s, 1H), 2.50 (br, 1H), 2.32-2.13 (m, 2H), 1.81 (s, 1H), 1.66 (m, 1H), 1.33 (d, *J* = 6.3 Hz, 2H), 1.23 (d, *J* = 6.2 Hz, 1H), 1.19 (s, 1H), 0.84 (t, *J* = 7.4 Hz, 3H).

From the compound **22**, pure chiral **PFAM4**, **28** (0.164 g, 0.33 mmol) was synthesized and obtained as an air sensitive pale yellow oily liquid in 42% yield and its oxidized form **POFAM4**, **29** (0.21 g, 0.41 mmol) was obtained as yellow oily liquid in 52% yield by the procedures reported by our group members [34,55]. **28**: ¹H-NMR (400 MHz, CDCl₃) δ 7.34 (m, 4H), 7.25 (m, 6H), 4.23 (s, 1H), 4.12 (s, 5H), 4.10 (s, 2H), 4.08 (s, 1H), 4.06 (s, 1H), 2.20 (m, 2H), 1.72 (d, *J* = 3.2, 1H), 1.59 (m, 1H), 1.52 (pentet, *J* = 7.3, 1H), 1.40 (q, *J* = 6.0 Hz, 1H), 1.27 (d, *J* = 6.4 Hz, 1H), 1.19 (m, 1H), 0.88 (t, *J* = 7.3 Hz, 3H). **29**: ¹H-NMR (400 MHz, CDCl₃) δ 7.64 (dd, *J* = 10.7, 4.7 Hz, 4H), 7.41 (m, 6H), 4.24 (s, 1H), 4.17 (s, 5H), 4.13 (s, 1H), 4.07 (s, 2H), 3.90 (d, *J* = 6.0 Hz, 1H), 2.55 (m, 1H), 2.37 (m, 1H), 1.70 (br, 1H), 1.55 (m, 2H), 1.29 (d, *J* = 7.1 Hz, 2H), 1.20 (s, 1H), 0.81 (t, *J* = 7.0 Hz, 3H).

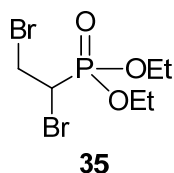
4.2.5. Synthesis and characterization of PFAM and POFAM ligands from phosphino aziridine 24



Starting from the compound **24**, **PFAM5**, **30** was synthesized and afforded as an air sensitive light yellow oily liquid (0.20 g, 0.41 mmol) in 50% yield and its oxidized form **POFAM5**, **31** as a yellow oily liquid (0.16 g, 0.32 mmol) in 39% yield by the procedures reported by our group members [34, 55]. **30**: ¹H-NMR (400 MHz, CDCl₃) δ 7.35 (m, 4H), 7.23 (m, 6H), 4.39 (s, 1H), 4.12 (s, 1H), 4.08 (s, 5H), 4.05 (s, 2H), 4.05 (s, 1H), 2.57 (s, 1H), 2.26 (d, *J* = 6.4 Hz, 2H), 1.60 (m, 4H), 1.44 (sextet, *J* = 6.1 Hz, 1H), 1.09 (d, *J* = 6.2 Hz, 1H), 0.86 (t, *J* = 7.3 Hz, 3H) **31**: ¹H-NMR (400 MHz, CDCl₃) δ 7.75 (dd, *J* = 10.5, 3.5 Hz, 2H), 7.67 (dd, *J* = 10.3, 3.6 Hz, 2H), 7.40 (m, 6H), 4.48 (s, 1H), 4.17 (s, 1H), 4.11 (s, 1H), 4.08 (s, 5H), 4.05 (s, 1H), 4.03 (s, 1H), 2.54 (m, 2H), 1.98 (pentet, *J* = 5.4 Hz, 2H), 1.78 (br, 1H), 1.54 (m, 2H), 1.23 (d, *J* = 6.2 Hz, 1H), 1.05 (d, *J* = 6.0 Hz, 1H), 0.80 (t, *J* = 7.4 Hz, 3H).

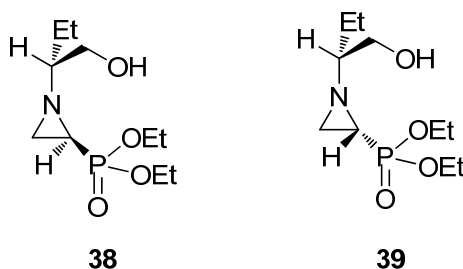
Starting from the compound **24**, **PFAM6**, **32** (0.27 g, 0.55 mmol) was obtained as pale yellow oily liquid in 50 % yield and its oxidized form **POFAM6**, **33** (0.27 g, 0.52 mmol) was obtained as a yellow oily liquid in 47 % yield by the procedures reported by our group members [34, 55]. **32**: ¹H-NMR (400 MHz, CDCl₃) δ 7.37 (s, 4H), 7.23 (s, 6H), 4.15 (s, 1H), 4.09 (s, 5H), 4.05 (s, 3H), 3.93 (d, *J* = 5.1 Hz, 1H), 2.29 (m, 3H), 1.57 (t, *J* = 7.3 Hz, 2H), 1.54 (s, 2H), 1.32 (m, 1H), 1.18 (d, *J* = 6.0 Hz, 1H), 0.87 (t, *J* = 7.3 Hz, 3H) **33**: ¹H-NMR (400 MHz, CDCl₃) δ 7.82 (dd, *J* = 7.4, 3.3 Hz, 2H), 7.73 (dd, *J* = 7.0, 3.3 Hz, 2H), 7.46 (ddd, *J* = 7.6, 8.5 and 3.7 Hz, 6H), 4.22 (s, 1H), 4.15 (s, 5H), 4.10 (s, 3H), 3.93 (d, *J* = 5.8 Hz, 1H), 2.65 (br, 1H), 2.56 (q, *J* = 5.9 Hz, 2H), 1.97 (pentet, *J* = 6.8 Hz, 1H), 1.71 (ddd, *J* = 3.7, 2.6 and 3.4 Hz, 1H), 1.50 (pentet, *J* = 7.1 Hz, 2H), 1.45 (d, *J* = 6.6 Hz, 1H), 1.31 (d, *J* = 3.4 Hz, 1H), 0.89 (t, *J* = 7.3 Hz, 3H).

4.3. Synthesis and characterization of 1,2-dibromoethyl phosphonate



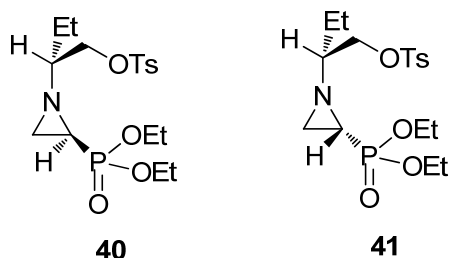
Starting from diethyl vinylphosphonate, diethyl 1,2-dibromoethyl phosphonate, **35** was synthesized and obtained as a light yellow oily liquid (4.00 g) in 100% yield following the procedure reported by our group [34]. $^1\text{H-NMR}$ δ 4.18 (m, 4H), 3.96 (m, 2H), 3.55 (m, 1H), 1.33 (t, $J = 7.0$ Hz, 6H).

4.3.1. Synthesis and characterization of aziridines **38** and **39**



Starting from the compound **35**, diethyl (1-(1-hydroxybutan-2-yl) aziridin-2-yl) phosphonates **38** and **39** were synthesized and obtained as a colorless oily liquid in 42% yield (1.31 g, 5.22 mmol) and as a colorless oily liquid in 40% yield (1.25 g, 4.97 mmol), respectively following the procedures reported in the literature by our group [34]. **38**: $^1\text{H-NMR}$ δ 4.11 (m, 4H), 3.60 (m, 2H), 3.33 (s, 1H), 2.01 (dd, $J = 8.9, 3.6$ Hz, 1H), 1.72 (ddd, $J = 20.5, 6.6$ and 3.6 Hz, 1H), 1.57 (t, $J = 7.1$ Hz, 1H), 1.46 (m, 2H), 1.34 (m, 1H), 1.30 (t, $J = 7.1$ Hz, 3H), 1.26 (t, $J = 7.1$ Hz, 3H), 0.88 (t, $J = 7.5$ Hz, 3H). **39**: $^1\text{H-NMR}$ δ 4.08 (m, 4H), 3.62 (m, 2H), 2.37 (s, 1H), 2.09 (dd, $J = 9.1, 3.6$ Hz, 1H), 1.67 (t, $J = 7.1$ Hz, 1H), 1.60 (m, 1H), 1.49 (m, 2H), 1.34 (m, 1H), 1.31–1.28 (m, 3H), 1.26 (m, 3H), 0.89 (t, $J = 7.5$ Hz, 3H).

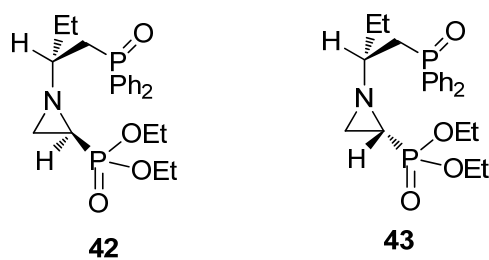
4.3.2. Synthesis and characterization of tosylated aziridines **40** and **41**



Starting from the compound **38**, we synthesized 2-(2-(diethoxyphosphoryl) aziridin-1-yl) butyl 4-methylbenzenesulfonate **40** and obtained it as a light yellow oily liquid in 67% yield (1.42 g, 4.7 mmol) by the procedure reported by our group [34]. $^1\text{H-NMR}$ δ 7.80 (d, $J = 8$ Hz, 2H), 7.35 (d, $J = 8$ Hz, 2H), 4.10 (m, 4H), 4.07 (m, 2H), 2.46 (s, 3H), 2.15 (dd, $J = 5.4, 1.8$ Hz, 1H), 2.03 (d, $J = 4.4$ Hz, 1H), 1.67 (ddd, $J = 18.4, 6.8, 4$ Hz, 1H), 1.61 (t, $J = 2.4$ Hz, 1H), 1.58 (m, 2H), 1.32 (t, $J = 7.2$ Hz, 3H), 1.31 (t, $J = 7.2$ Hz, 3H), 0.91 (t, $J = 7.6$ Hz, 3H)

Starting from the compound **39**, we synthesized 2-(2-(diethoxyphosphoryl) aziridin-1-yl) butyl 4-methylbenzenesulfonate **41** and obtained it as a light yellow oily liquid in 86% yield (1.73 g, 4.27 mmol) by the procedure reported by our group [34]. $^1\text{H-NMR}$ δ 7.78 (d, $J = 8.4$ Hz, 2H), 7.35 (d, $J = 8$ Hz, 2H), 4.08 (m, 4H), 4.05 (m, 2H), 2.46 (s, 3H), 2.06 (dd, $J = 8.8, 4.0$ Hz, 1H), 1.75 (t, $J = 7.2$ Hz, 1H), 1.62 (d, $J = 2.4$ Hz, 1H), 1.58 (m, 2H), 1.49 (ddd, $J = 19.0, 6.8$ and 4 Hz, 1H), 1.31 (t, $J = 7.0$ Hz, 3H), 1.30 (t, $J = 7.0$ Hz, 3H), 0.93 (t, $J = 7.2$ Hz, 3H).

4.3.3. Synthesis and characterization of phosphine oxy aziridines **42** and **43**



Starting from the tosylated product **40**, diethyl 1-(1-(diphenylphosphoryl) butan-2-yl) aziridin-2-yl phosphonate **42** was obtained as a light yellow oily liquid in 88% yield (1.80 g, 4.14 mmol) by adapting the procedure reported by our group [34]. $^1\text{H-NMR}$ δ 7.77 (m, 4H), 7.49 (m, 6H), 4.13 (m, 4H), 2.70 (m, 1H), 2.57 (m, 1H), 2.14 (dd, $J = 9.6, 3.6$ Hz, 1H), 1.67 (m, 1H), 1.38 (m, 1H), 1.33 (m, 1H), 1.31 (t, $J = 7.2$ Hz, 3H), 1.30 (t, $J = 7.0$ Hz, 3H), 0.90 (t, $J = 7.4$ Hz, 3H). $^{13}\text{C-NMR}$ (100 MHz, CDCl_3) δ 134.04 (Cq, ArC-P), 133.75 (Cq, ArC-P), 131.65 (CH, 2C, Ph), 130.89 (CH, Ph), 130.80 (CH, Ph), 130.70 (CH, Ph), 130.61 (CH, Ph), 128.69 (CH, Ph), 128.63 (CH, Ph), 128.57 (CH, Ph), 128.51 (CH, Ph), 65.75 (CH, d, $J = 7.08$ Hz), 62.51 (OCH_2CH_3 , $J = 6.68$ Hz), 62.35 (OCH_2CH_3 , d, $J = 6.10$ Hz), 35.17 (CH_2 , aziridine), 33.77 (CH_2 , $\text{CH}_2\text{-P}$, d, $J_{\text{C-P}} = 6.5$ Hz), 29.81 (CH, aziridine, d, $J_{\text{C-P}} = 216.32$ Hz), 28.92 (CH_2CH_3), 16.42, t, $J = 5.25$ Hz, OCH_2CH_3), 9.70 (CH_3).

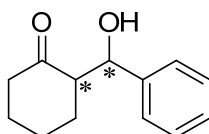
Starting from the tosylated product **41**, diethyl 1-(1-diphenylphosphoryl) butan 2-yl) aziridin-2-ylphosphonate **43** was obtained as a white solid in 84% yield (1.56 g, 3.60 mmol) by adapting the procedure reported by our group [34]. ¹H-NMR δ 7.82 (ddd, *J* = 11.5, 8.0 and 1.6 Hz, 2H), 7.70 (ddd, *J* = 11.5, 8.0 and 1.6 Hz, 2H), 7.47 (m, 6H), 4.06 (m, 4H), 2.57 (m, 2H), 1.89 (p, *J* = 5.2 Hz, 1H), 1.65 (m, 2H), 1.61 (m, 2H), 1.53 (ddd, *J* = 19.1, 6.7 and 3.8 Hz, 1H), 1.29 (t, *J* = 7.2 Hz, 3H), 1.27 (t, *J* = 7.2 Hz, 3H), 0.94 (t, *J* = 7.4 Hz, 3H). ¹³C-NMR (100 MHz, CDCl₃) δ 131.66 (Cq, ArC-P, 2C), 130.78 (CH, 2C, Ph), 130.38 (CH, Ph, 2C), 128.66 (CH, Ph, 3C), 128.55 (CH, Ph, 3C), 65.52 (CH, d, *J* = 7.48 Hz), 62.40 (CH, d, *J* = 6.27 Hz), 62.24 (OCH₂CH₃, d, *J* = 6.27 Hz), 32.52 (CH, aziridine, d, *J* = 218.19 Hz), 31.92 (CH₂, CH₂-P, d, *J*_{C-P} = 5.07 Hz), 28.52 (CH₂, aziridine, *J* = 6.91 Hz), 25.20 (CH₂CH₃), 16.41 (O CH₂CH₃, d, *J* = 9.69 Hz), 9.13 (CH₃).

4.4. Asymmetric studies

4.4.1. General procedure for silicon tetrachloride mediated asymmetric Aldol addition⁴⁸

Cyclohexanone (0.104 mL, 1.00 mmol) was added to the heat-gun dried, degassed Schlenk tube containing DCM (2.4 mL) under argon at room temperature. After that, silicon tetrachloride (0.123 mL, 1.07 mmol) was added dropwise at the same temperature. Stirring continued for another 10 minutes and tetramethylethylenediamine (0.170 mL, 1.13 mmol) was also added dropwise. After stirring the reaction mixture for 15 minutes chiral Lewis base (0.1 mmol, 43.5 mg, in 1.2 mL DCM) was added dropwise and stirred for 20 minutes. Then the reaction mixture was brought to -78°C and aldehyde (in 2.4 mL DCM, 1.33 mmol) was added. The reaction mixture was allowed to stir for 21 h at -78°C. Then, it was hydrolyzed by adding saturated NaHCO₃ solution (5 mL) and stirred for 1h. After this time period, two phases were separated and the aqueous phase was extracted with EtOAc (20 mL x 3). The combined organic phase was washed with 10% HCl solution (20 mL), saturated NaHCO₃ solution (20 mL) and saturated NaCl solution (20 mL), respectively. After drying over Na₂SO₄, it was concentrated and purified by flash column chromatography on silica gel (10:1 Hexane: EtOAc). The aldol products were obtained as a mixture of *anti* and *syn* isomers (82:18) in 75% total yield (153.2 mg, 0.75 mmol).

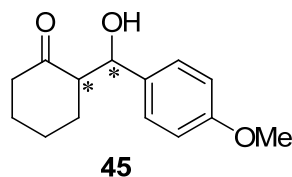
4.4.1.1. 2-(Hydroxy(phenyl)methyl) cyclohexan-1-one⁵⁴



44

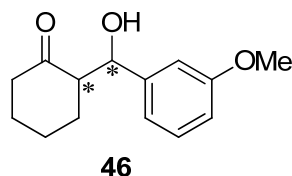
R_f = 0.28 (*syn*), 0.22 (*anti*) Hexane/EtOAc 5:1, dyed red with anisaldehyde. ¹H-NMR (400 MHz, CDCl₃) δ (ppm) 7.38-7.21 (m, 5H), 5.39 (brs, 1H, *syn*), 4.78 (d, *J* = 9.03 Hz, 1H, *anti*), 3.96 (brs, 1H, *anti*), 3.03 (brs, 1H, *syn*), 2.67-2.56 (m, 1H), 2.12-2.01 (m, 1H), 1.70-1.48 (m, 4H), 1.35-1.21 (m, 1H), HPLC analysis Chiralcel OD-H (Hexane/ⁱPrOH = 98/2, 0.8 mL/min), *anti*: *t_R* (major) = 33.4 min and *t_R* (minor) = 23.2 min, *syn*: *t_R* (major) = 16.3 min and *t_R* (minor) = 18.9 min.

4.4.1.2. 2-(Hydroxy(4-methoxyphenyl)methyl) cyclohexan-1-one⁶⁵



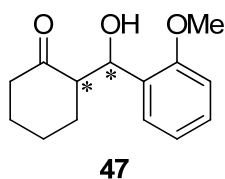
R_f =0.52 (*syn*), 0.41 (*anti*) Hexane/EtOAc 5:1, dyed red with anisaldehyde. ¹H-NMR (400 MHz, CDCl₃) δ (ppm) 7.27-7.21 (m, 2H), 6.91-6.85 (m, 2H), 5.32 (brs, 1H, *syn*) 4.74 (dd, J = 8.89, 2.43 Hz, 1H, *anti*), 3.93 (d, J = 2.59 Hz, 1H, *anti*), 3.80 (s, 3H), 2.99 (d, J =3.53 Hz, 1H, *syn*), 2.65-2.53 (m, 1H), 2.52-2.44 (m, 1H), 2.41-2.30 (m, 1H), 2.13-2.03 (m, 1H), 1.83-1.73 (m, 1H), 1.73-1.47 (m, 3H), 1.33-1.22 (m, 1H). HPLC analysis Chiralpak AS-H (Hexane/ⁱPrOH = 90/10, 0.5 mL/min), *anti*: t_R (major) = 62.1 min and t_R (minor) = 52.8 min, *syn*: t_R (major) = 48.8 min and t_R (minor) = 45.1 min.

4.4.1.3. 2-(Hydroxy(3-methoxyphenyl)methyl) cyclohexan-1-one⁶⁶



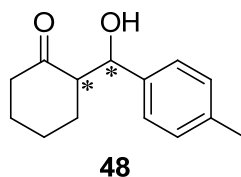
R_f =0.38 (*syn*), 0.30 (*anti*) Hexane/EtOAc 5:1, dyed red with anisaldehyde. ¹H-NMR (400 MHz, CDCl₃) δ (ppm) 7.31-7.21 (m, 1H), 6.95-6.77 (m, 3H), 5.40-5.34 (brs, 1H, *syn*), 4.76 (dd, J = 8.80, 2.40 Hz, 1H, *anti*), 3.96 (d, J = 2.7 Hz, 1H, *anti*), 3.84 (s, 3H), 3.07-3.03 (d, J = 3.2 Hz, 1H, *syn*), 2.68-2.30 (m, 3H), 2.15-2.03 (m, 1H), 1.90-1.46 (m, 4H), 1.40-1.22 (m, 1H). HPLC analysis Chiralpak AS-H (Hexane/ⁱPrOH = 90/10, 0.5 mL/min), *anti*: t_R (major) = 71.5 min and t_R (minor) = 55.6 min, *syn*: t_R (major) = 49.1 min and t_R (minor) = 38.0 min.

4.4.1.4. 2-(Hydroxy(2-methoxyphenyl)methyl) cyclohexan-1-one⁶⁷



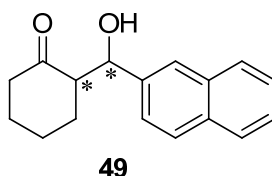
R_f =0.35 (*syn*), 0.32 (*anti*) Hexane/EtOAc 5:1, dyed red with anisaldehyde. ¹H-NMR (400 MHz, CDCl₃) δ (ppm) 7.43-7.38 (dd, J = 7.6, 1.7 Hz, 1H), 7.28-7.22 (dd, J = 7.5, 1.7 Hz, 1H), 6.98 (td, J = 7.5, 0.9 Hz, 1H), 6.86 (d, J = 7.8 Hz, 1H, *syn*), 5.29-5.24 (dd, J = 8.6, 4.4 Hz, 1H, *anti*), 3.81 (s, 3H), 2.78-2.69 (m, 1H, *syn*), 2.51-2.43 (m, 1H), 2.41-2.29 (m, 1H), 2.11-1.97 (m, 1H), 1.84-1.39 (m, 5H). HPLC analysis Chiralpak AS-H (Hexane/ⁱPrOH = 90/10, 1.0 mL/min), *anti*: t_R (major) = 27.5 min and t_R (minor) = 35.7 min, *syn*: t_R (major) = 14.5 min and t_R (minor) = 12.2 min.

4.4.1.5. 2-(Hydroxy(4-methylphenyl)methyl) cyclohexan-1-one⁶⁸



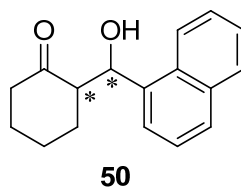
R_f =0.67 (*syn*), 0.59 (*anti*) Hexane/EtOAc 5:1, dyed red with anisaldehyde. ¹H-NMR (400 MHz, CDCl₃) δ (ppm) 7.21-7.12 (m, 4H), 5.35 (m, 1H, *syn*), 4.75-4.73 (dd, J = 8.9, 2.74 Hz, 1H, *anti*), 3.90 (d, J = 2.79 Hz, 1H, *anti*), 2.95 (d, J = 3.30 Hz, 1H, *syn*), 2.65-2.55 (m, 1H), 2.51-2.30 (m, 2H), 2.12-2.04 (m, 1H), 1.87-1.48 (m, 4H), 1.34-1.22 (m, 4H). HPLC analysis Chiralcel OD-H (Hexane/ⁱPrOH = 97/3, 1.0 mL/min), *anti*: t_R (major) = 19.3 min and t_R (minor) = 14.0 min, *syn*: t_R (major) = 10.9 min and t_R (minor) = 10.2 min.

4.4.1.6. 2-(Hydroxy(naphthalen-2-yl)methyl) cyclohexan-1-one⁶⁹



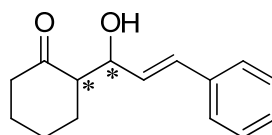
R_f =0.40 (*syn*), 0.35 (*anti*) Hexane/EtOAc 5:1, dyed red with anisaldehyde. ¹H-NMR (400 MHz, CDCl₃) δ (ppm) 7.88-7.80 (m, 3H), 7.76 (s, 1H), 7.53-7.44 (m, 3H), 4.97 (d, J = 8.8 Hz, 1H, *anti*), 4.07 (s, 1H, *anti*), 2.77-2.67 (m, 1H), 2.56-2.46 (m, 1H), 2.44-2.32 (m, 1H), 2.13-2.04 (m, 1H), 1.81-1.28 (5H, m). HPLC analysis Chiralpak AS-H (Hexane/ⁱPrOH = 90/10, 1.0 mL/min), *anti*: t_R (major) = 29.6 min and t_R (minor) = 26.3 min, *syn*: t_R (major) = 18.1 min and t_R (minor) = 23.2 min.

4.4.1.7. 2-(Hydroxy(naphthalen-1-yl)methyl) cyclohexan-1-one⁶⁹



R_f =0.63 (*syn*), 0.52 (*anti*) Hexane/EtOAc 5:1, dyed red with anisaldehyde. ¹H-NMR (400 MHz, CDCl₃) δ (ppm) 8.27-8.24 (m, 1H), 7.89-7.84 (m, 1H), 7.81 (d, J = 8.1 Hz, 1H), 7.57 (d, J = 6.3 Hz, 1H), 7.53-7.45 (m, 3H), 5.58 (dd, J = 8.78, 2.96 Hz, 1H, *syn*), 4.14 (d, J = 3.11 Hz, 1H, *anti*), 3.68 (brs, 1H, *anti*), 3.10 (d, J = 3.42, 1H, *syn*), 3.05-2.94 (m, 1H), 2.56-2.47 (m, 1H), 2.46-2.36 (m, 1H), 2.13-2.05 (m, 1H), 1.76-1.61 (m, 2H), 1.49-1.33 (m, 3H), HPLC analysis Chiralpak AD (Hexane/ⁱPrOH = 90/10, 0.8 mL/min), *anti*: t_R (major) = 22.5 min and t_R (minor) = 26.8 min, *syn*: t_R (major) = 14.7 min and t_R (minor) = 19.4 min.

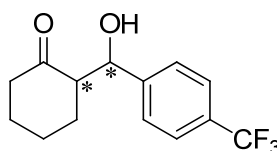
4.4.1.8. 2-(1-Hydroxy-3-phenyl-2-propenyl) cyclohexan-1-one⁵⁴



51

R_f =0.52 (*syn*), 0.48 (*anti*) Hexane/EtOAc 5:1, dyed red with anisaldehyde. ¹H-NMR (400 MHz, CDCl₃) δ (ppm) 7.43-7.36 (m, 2H), 7.28-7.22 (m, 1H), 6.62 (dd, J = 15.92, 1.16 Hz, 1H), 6.22 (dd, J = 12.22, 3.55 Hz, 1H), 4.76 (brs, 1H, *syn*), 4.40 (d, J = 7.2 Hz, 1H, *anti*), 3.67 (brs, 1H, *anti*), 2.97 (brs, 1H, *syn*), 2.59-2.30 (m, 3H), 2.18-2.04 (m, 2H), 1.95-1.87 (m, 1H), 1.77-1.59 (m, 3H). HPLC analysis Chiralpak AD (Hexane/ ¹PrOH = 97/3, 0.5 mL/min), *anti*: t_R (major) = 83.1 min and t_R (minor) = 72.3 min, *syn*: t_R (major) = 66.1 min and t_R (minor) = 54.5 min.

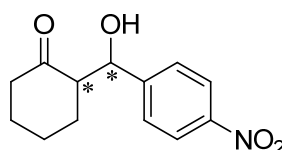
4.4.1.9. 2-(Hydroxy(4-trifluoromethyl)phenyl)methyl cyclohexan-1-one⁶⁹



52

R_f =0.59 (*syn*), 0.52 (*anti*) Hexane/EtOAc 5:1, dyed red with anisaldehyde. ¹H-NMR (400 MHz, CDCl₃) δ (ppm) 7.61 (d, J = 8.23 Hz, 2H), 7.44 (d, J = 8.03 Hz, 2H), 5.44 (brs, 1H, *syn*), 4.85 (dd, J = 8.71, 2.85 Hz, 1H, *anti*), 4.03 (d, J = 2.99 Hz, 1H, *anti*), 3.11 (d, J = 3.30 Hz, 1H, *syn*), 2.55-2.64 (m, 1H), 2.44-2.53 (m, 1H), 2.31-2.41 (m, 1H), 2.06-2.15 (m, 1H), 1.77-1.85 (m, 1H), 1.49-1.75 (m, 3H), 1.24-1.40 (m, 1H). HPLC analysis Chiralpak AD (Hexane/ ¹PrOH = 90/10, 0.5 mL/min), *anti*: t_R (major) = 22.6 min and t_R (minor) = 28.9 min, *syn*: t_R (major) = 17.2 min and t_R (minor) = 14.7 min.

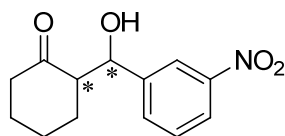
4.4.1.10. 2-(Hydroxy(4-nitrophenyl)methyl) cyclohexan-1-one⁶⁹



53

R_f =0.41 (*syn*), 0.33 (*anti*) Hexane/EtOAc 5:1, dyed red with anisaldehyde. ¹H-NMR (400 MHz, CDCl₃): δ (ppm) 8.21 (dd, J = 8.89, 2.04 Hz, 2H), 7.50 (t, J = 8.15 Hz, 2H), 5.49 (brs, 1H *syn*), 4.90 (dd, J = 8.48, 3.05 Hz, 1H *anti*), 4.07 (d, J = 3.28 Hz, 1H *anti*), 3.17 (d, J = 3.35 Hz, 1H *syn*), 2.55-2.66 (m, 1H), 2.46-2.53 (m, 1H), 2.32-2.44 (m, 1H), 2.08-2.16 (m, 1H), 1.80-1.90 (m, 1H), 1.35-1.45 (m, 1H), 1.49-1.76 (m, 3H). HPLC analysis Chiralpak AD (Hexane/ ¹PrOH = 90/10, 1.0 mL/min), *anti*: t_R (major) = 28.7 min and t_R (minor) = 38.6 min, *syn*: t_R (major) = 20.7 min and t_R (minor) = 26.0 min.

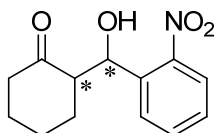
4.4.1.11. 2-(Hydroxy(3-nitrophenyl)methyl) cyclohexan-1-one⁶⁹



54

R_f =0.33 (*syn*), 0.26 (*anti*) Hexane/EtOAc 5:1, dyed red with anisaldehyde. ¹H-NMR (400 MHz, CDCl₃): δ (ppm) 8.21-8.15 (m, 2H), 7.67 (d, J = 7.62 Hz, 1H), 7.56-7.50 (m, 1H), 5.48 (brs, 1H, *syn*), 4.90 (d, J = 8.53 Hz, 1H, *anti*), 4.12 (brs, 1H, *anti*), 3.20 (brs, 1H, *syn*), 2.69-2.46 (m, 1H), 2.43-2.33 (m, 1H), 2.17-2.07 (m, 1H), 1.90-1.78 (m, 1H), 1.78-1.52 (m, 4H), 1.45-1.37 (m, 1H). HPLC analysis Chiralpak AD (Hexane/ *i*PrOH = 95/5, 0.7 mL/min), *anti*: t_R (major) = 66.6 min and t_R (minor) = 51.7 min, *syn*: t_R (major) = 45.8 min and t_R (minor) = 40.1 min.

4.4.1.12. 2-(Hydroxy(2-nitrophenyl)methyl) cyclohexan-1-one⁶⁹



55

R_f =0.30 (*syn*), 0.25 (*anti*) Hexane/EtOAc 5:1, dyed red with anisaldehyde. ¹H-NMR (400 MHz, CDCl₃) δ (ppm) 7.85 (dd, J = 8.2, 1.2 Hz, 1H), 7.77 (dd, J = 7.9, 1.2 Hz, 1H), 7.67 – 7.61 (m, 1H), 7.46-7.39 (m, 1H), 5.96 (d, J = 1.8 Hz, 1H, *syn*), 5.45 (d, J = 7.0 Hz, 1H, *anti*), 4.15 (brs, 1H, *anti* and *syn*), 2.99-2.82 (m, 1H), 2.80-2.68 (m, 1H), 2.48-2.38 (m, 1H), 2.34 (td, J = 13.5, 7.1 Hz, 1H), 2.16-2.04 (m, 1H), 1.92-1.54 (m, 4H). HPLC analysis Chiralcel OD-H (Hexane/ *i*PrOH = 95/5, 1.0 mL/min), *anti*: t_R (major) = 23.9 min and t_R (minor) = 20.2 min, *syn*: t_R (major) = 14.6 min and t_R (minor) = 13.6 min.

4.4.2. Preparation of racemic compounds

In the absence of **POAP-A**, cyclohexanone (0.150 mL, 1.50 mmol) was reacted with benzaldehyde (0.102 mL, 1.00 mmol) in the presence of silicon tetrachloride (0.173 mL, 1.07 mmol) and tetramethylethylenediamine (0.170 mL, 1.13 mmol) at 0°C. The aldol products were obtained as a mixture of *anti* and *syn* isomers (72:28) in 40% total yield (78 mg, 0.60 mmol). This procedure was applied to all other substrates in *Table 6*.

BIBLIOGRAPHY

1. Ebens, R. H. E. *Acetals of 1-Aryl-2,2-dimethyl 1,3-propanediols Synthesis and Use as Chiral Auxiliary*, PhD thesis, **1993**.
2. Trost, B.M. *PNAS*, **2004**, *101*, 5348–5355.
3. KSA Faculty Members' website, <http://faculty.ksu.edu.sa>, last visited on January 2013.
4. Arya, P.; Qin, H. *Tetrahedron*, **2000**, *56*, 917–947.
5. Gawley, R. E.; & Aubé, J. *Principles of Asymmetric Synthesis*. Oxford: Pergamon, 1996.
6. Breuer, M.; Ditrich, K., Habicher, T.; Hauer, B.; Keßeler, M., Stürmer, R.; and Zelinski, T. *Angew. Chem. Int. Ed.* **2004**, *43*, 788–824.
7. Sarker, D. S.; Nahar, L. *Chemistry for pharmacy students: general, organic and natural product chemistry*. Chichester, England: John Wiley & Sons, **2007**.
8. Enders, D. *Asymmetric synthesis with chemical and biological methods*. Weinheim: WILEY-VCH, **2007**.
9. Kalsi, P. S. *Stereochemistry conformation and mechanism*. New Delhi: New Age International, **2006**.
10. Seyden-Penne, J. *Chiral auxiliaries and ligands in asymmetric synthesis*. New York [u.a.]: Wiley, **1995**.
11. Narasaka, K. *Pure & Appl. Chem.*, **1992**, *64*, 1889-1896.
12. Gruttadauria, M.; Giacalone, F.; & Wiley InterScience (Online service). *Catalytic methods in asymmetric synthesis: Advanced materials, techniques, and applications*. Hoboken, N.J: Wiley, **2011**.
13. Patti, A. *Green approaches to asymmetric catalytic synthesis*. Dordrecht [etc.]: Springer, **2011**.
14. Jacobsen, E. N.; Pfaltz, A.; Yamamoto, H. *Comprehensive Asymmetric Catalysis III*. Springer-Verlag, **2000**.
15. Halpern, J.; Trost, B. M.. *PNAS*, **2004**, *101*, 5347
16. Sih, C. J.; Gu, Q.; Holdgrün, X.; Harris, K. *Chirality*, **1992**, *4*, 91-97.

17. Hayashi, T.; Kumada, M. *Acc. Chem. Res.* **1982**, *15*, 395-401.
18. Pfaltz, A. and Drury, W. J. *PNAS*, **2004**, *101*, 5723-5726.
19. Trost, B. M.; and Crawley, M. L. *Chem. Rev.* **2003**, *103*, 2921-2943.
20. Institut des Biomolécules Max Mausseron, <http://www.ibmm.univ-montp1.fr>, last visited on January 2013.
21. Louis S. Hegedus, *J. Am. Chem. Soc.*, **2009**, *131*, 17995–17997.
22. Bergin, E. *Annu. Rep. Prog. Chem., Sect. B: Org. Chem.*, **2012**, *108*, 353-371.
23. Benaglia, M.; Guizzetti, S.; Pignataro, L. *Coordination Chemistry Reviews*, **2008**, *252*, 492–512.
24. Dilman, A. D.; and Ioffe, S. L. *Chem. Rev.*, **2003**, *103*, 733-772.
25. Sereda, O.; Tabassum, S.; Wilhelm, R. *Top Curr Chem*, **2010**, *291*, 349–393.
26. Denmark, S.E. *Chimia*, **2008**, *62*, 37–40.
27. Denmark, S. E.; Barsanti, P. A.; Wong, K. T.; Stavenger, R. A. *J. Org. Chem.*, **1998**, *63*, 2428-2429.
28. Denmark, S. E.; Barsanti, P. A.; Beutner, G. L.; Wilson, T. W. *Adv. Synth. Catal.*, **2007**, *349*, 567–582.
29. Tao, B.; Lo, M. M. C.; Fu, G. C. *J. Am. Chem. Soc.*, **2001**, *123*, 353-354.
30. Tokunaga, E.; Kotani, S.; Matsunaga, H.; Ishizuka, T.; Hashimoto, S. and Nakajima, M. *Tetrahedron: Asymmetry*, **2005**, *16*, 2391–2392.
31. Pu, X.; Qi, X.; Ready, J. M. *J. Am. Chem. Soc.*, **2009**, *131*, 10364–10365.
32. Samanta S. and Zhao C. *J Am Chem Soc.*, **2006**, *128*, 7442–7443.
33. Nakanishi, K.; Kotani, S.; Sugiura, M.; Nakajima, M. *Tetrahedron*, **2008**, *64*, 6415–6419.
34. Isci, M. *Synthesis and use of new phosphine oxy aziridinylphosphonates (POAP) as organocatalysts in asymmetric phosphorylation of aldehydes*, MSc thesis, **2012**.
35. Kobayashi, S.; Nishio, K. *J. Am. Chem. Soc.*, **1995**, *117*, 6392-6393.
36. Iseki, K.; Kuroki, Y.; Kobayashi, Y. *Tetrahedron: Asymmetry*, **1998**, *9*, 2889–2894.
37. Nakajima, M.; Saito, M.; Hashimoto, S. *Tetrahedron: Asymmetry*, **2002**, *13*, 2449–2452.
38. Hosomi, A. *Acc. Chem. Res.*, **1988**, *21*, 200-206.

39. Kobayashi, S.; Nishio, K. *J. Org. Chem.*, **1994**, *59*, 6620-6628.
40. Denmark, S. E.; Fu, *Chem. Commun. (Focus)*, **2003**, 167-170.
41. Denmark, S. E.; Coe, D. M.; Pratt, N. E.; Griedel, B. D. *J. Org. Chem.*, **1994**, *59*, 6161-6163.
42. Iseki, K.; Mizuno, S.; Kuroki, Y.; Kobayashi, Y. *Tetrahedron Letters*, **1998**, *39*, 2767-2770.
43. Nakajima, M.; Saito, M.; Shiro, M.; Hashimoto, S. *J. Am. Chem. Soc.* **1998**, *120*, 6419-6420.
44. Shimada, T.; Kina, A.; Ikeda, S.; Hayashi, T. *Organic Letters*, **2002**, *4*, 2799-2801.
45. Nakajima, M.; Kotani, S.; Ishizukaa, T.; Hashimoto, S. *Tetrahedron Letters*, **2005**, *46*, 157-159.
46. Simonini, V.; Benaglia, M.; Benincori, T. *Adv. Synth. Catal.*, **2008**, *350*, 561-564.
47. Denmark, S. E.; Winter, S. B. D.; Su, X.; Wong, K. *J. Am. Chem. Soc.*, **1996**, *118*, 7404-7405.
48. Denmark, S. E.; Stavenger, R. A.; Wong, K.; Su, X. *J. Am. Chem. Soc.*, **1999**, *121*, 4982-4991.
49. Denmark, S. E.; Stavenger, R. A. *Acc. Chem. Res.*, **2000**, *33*, 432-440.
50. Nakajima, M.; Yokota, T.; Saito, M.; Hashimoto, S. *Tetrahedron Letters*, **2004**, *45*, 61-64.
51. Kotani, S.; Hashimoto, S.; Nakajima, M. *Tetrahedron*, **2007**, *63*, 3122-3132.
52. Kotani, S.; Shimoda, Y.; Sugiura, M.; Nakajima, M. *Tetrahedron Letters*, **2009**, *50*, 4602-4605.
53. Kotani, S.; Shimoda, Y.; Aoki, S.; Sugiura, M.; Nakajima, M. *Tetrahedron Letters*, **2011**, *52*, 2834-2836.
54. Rossi, S.; Benaglia, M.; Genoni, A.; Benincori, T.; Celentano, G. *Tetrahedron*, **2011**, *67*, 158-166.
55. Eroksuz, S. *A New P-FAM-Silver Catalyst for Asymmetric 1,3-Dipolar Cycloaddition Reactions of Azomethine Ylides*, MSc thesis, **2008**.
56. Dogan, O.; Zeytinci, S.; Bulut, A. *Synth. Commun.*, **2005**, *35*, 1067.

57. Gabriel, S. S. *Chem. Ber.*, **1888**, 21, 1049.
58. Williams, G. D.; Wade, C. E.; Clarkson, G. J.; Wills, M. *Tetrahedron: Asymmetry*, **2007**, 18, 664–670.
59. Yun, J. M.; Sim, T. B.; Hahm, H. S.; Lee, W. K.; Ha, H. *J. Org. Chem.*, **2003**, 68, 7675.
60. Denmark, S. E.; Stavenger, R. A.; Wong, K. *Tetrahedron*, **1998**, 54, 10389–10402.
61. Benaglia, M.; Rossi, S. *Org. Biomol. Chem.*, **2010**, 8, 3824–3830.
62. Malkov, A. V.; Kocovský, P. *Eur. J. Org. Chem.*, **2007**, 29–36.
63. Denmark, S. E.; Eklov, B. M.; Yao, P. J.; Eastgate, M. D. *J. Am. Chem. Soc.*, **2009**, 131, 11770–11787.
64. Denmark, S. E.; Beutner, G. L.; Wynn, T.; Eastgate, M. D. *J. Am. Chem. Soc.*, **2005**, 127, 3774–3789.
65. Maya, V.; Raj, M.; Singh, V. K. *Org. Lett.*, **2007**, 9, 2593–2595.
66. Wu, X.; Jiang, Z.; Shen, H.; Lu, Y. *Adv. Synth. Catal.*, **2007**, 349, 812–816.
67. Rodríguez, B.; Rantanen, T.; Bolm, C. *Angew Chem Int Ed Engl.*, **2006**, 45, 6924–6926.
68. Chen, J.; Lu, H.; Li, X.; Chen, L.; Wan, J.; Xiao, W. *Org. Lett.*, **2005**, 7, 4543–4545.
69. Wu, Y.; Zhang, Y.; Yu, M.; Zhao, G.; Wang, S. *Org. Lett.*, **2006**, 8, 4417–4420.

APPENDIX

NMR SPECTRA and HPLC CHROMATOGRAMS

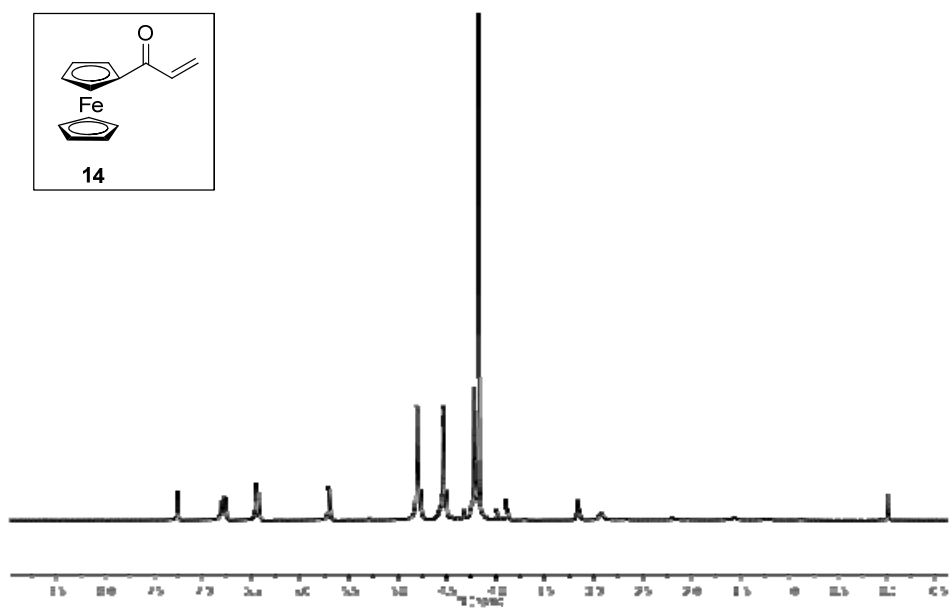


Figure A. ¹H-NMR spectrum of compound 14

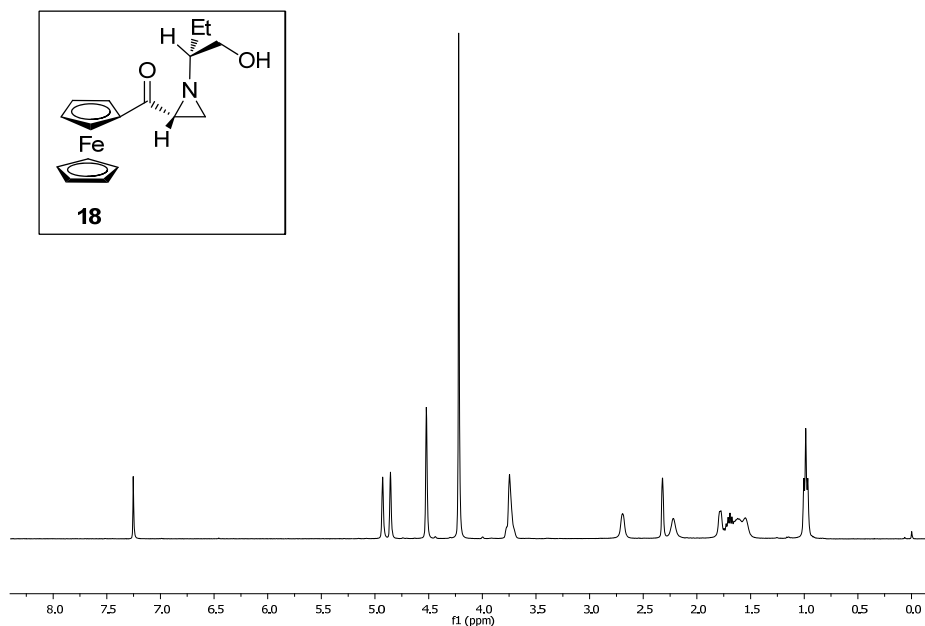


Figure A. 2 $^1\text{H-NMR}$ spectrum of compound 18

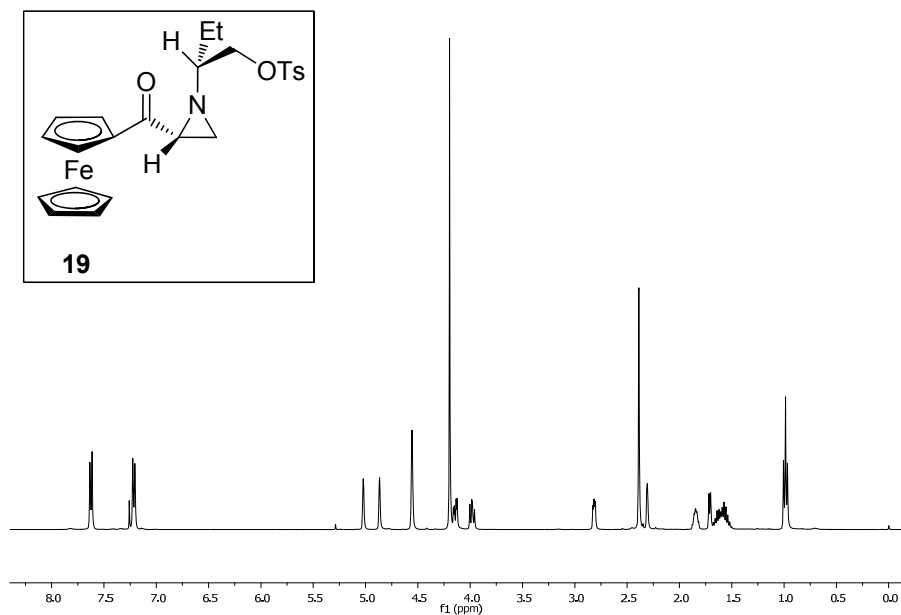


Figure A. 3 $^1\text{H-NMR}$ spectrum of compound 20

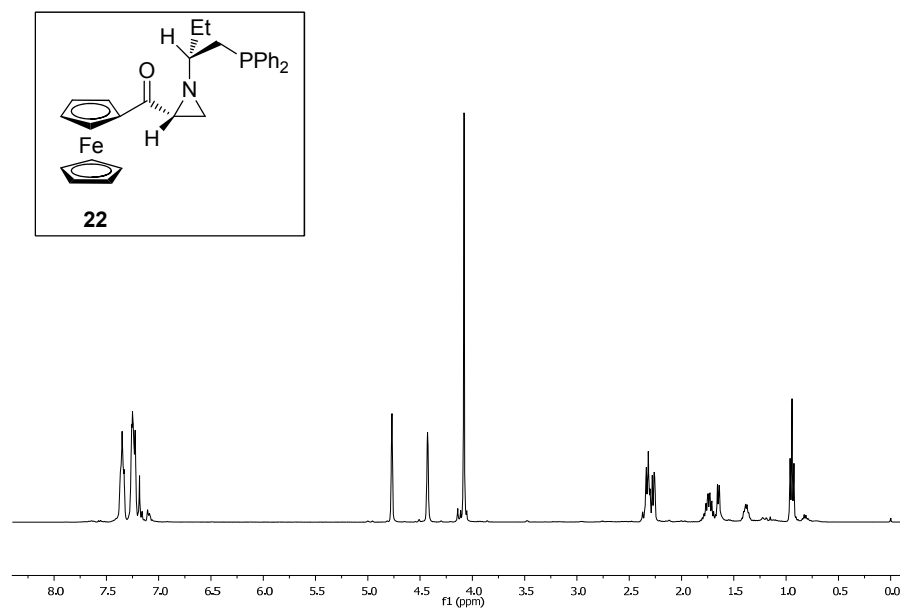


Figure A. 4 ¹H-NMR spectrum of compound 22

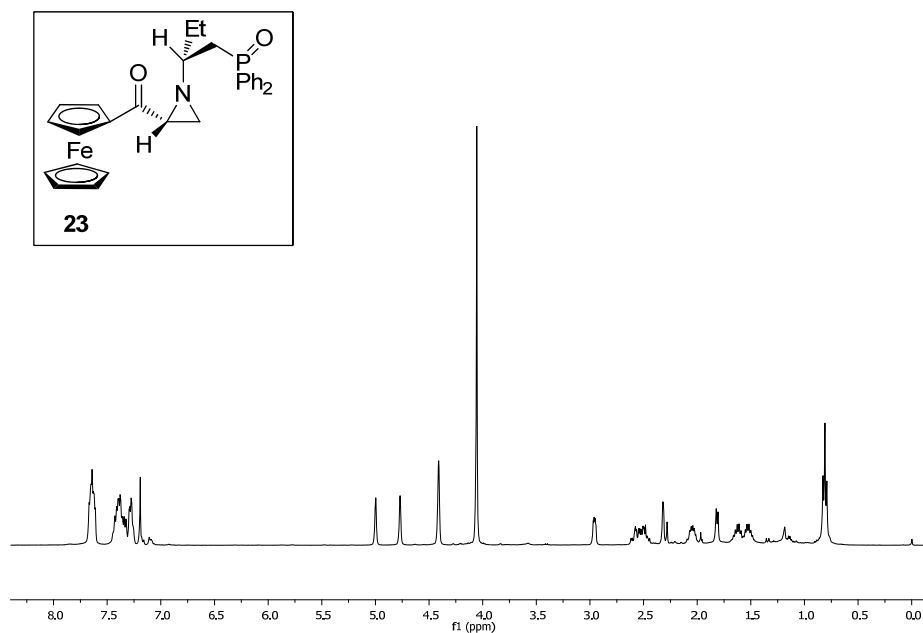


Figure A. 5 ¹H-NMR spectrum of compound 23

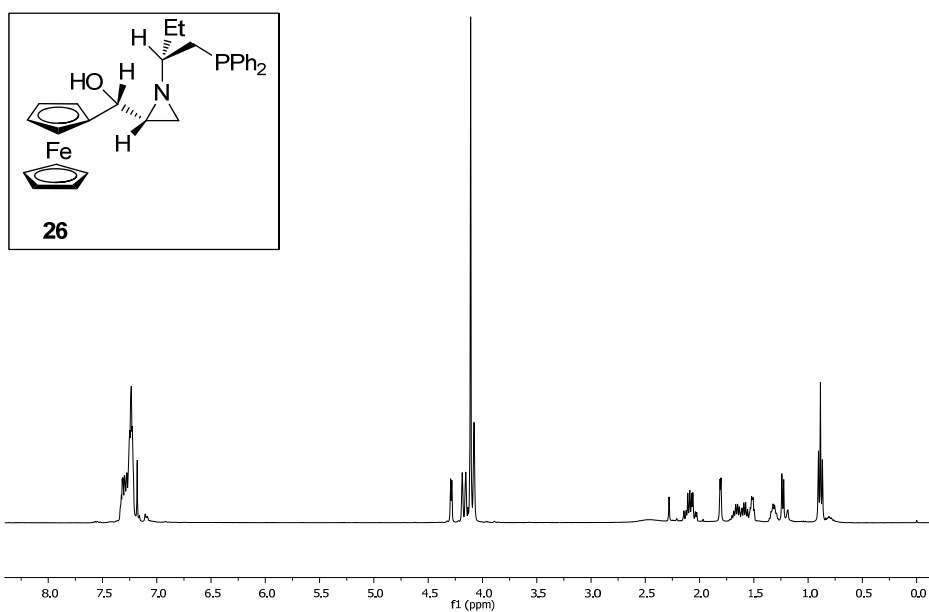


Figure A. 6 $^1\text{H-NMR}$ spectrum of compound 26

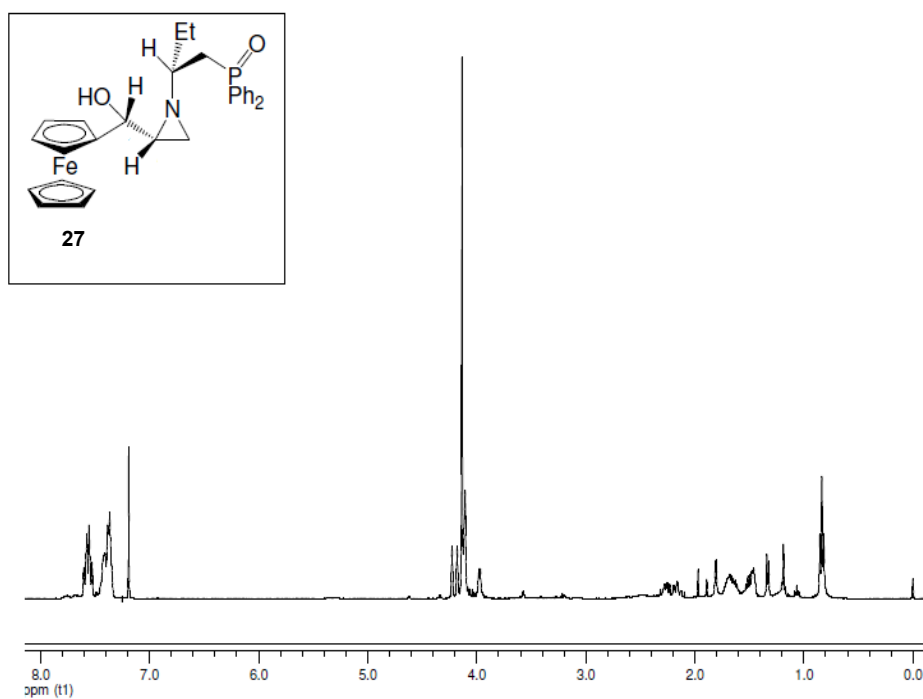


Figure A. 7 $^1\text{H-NMR}$ spectrum of compound 27

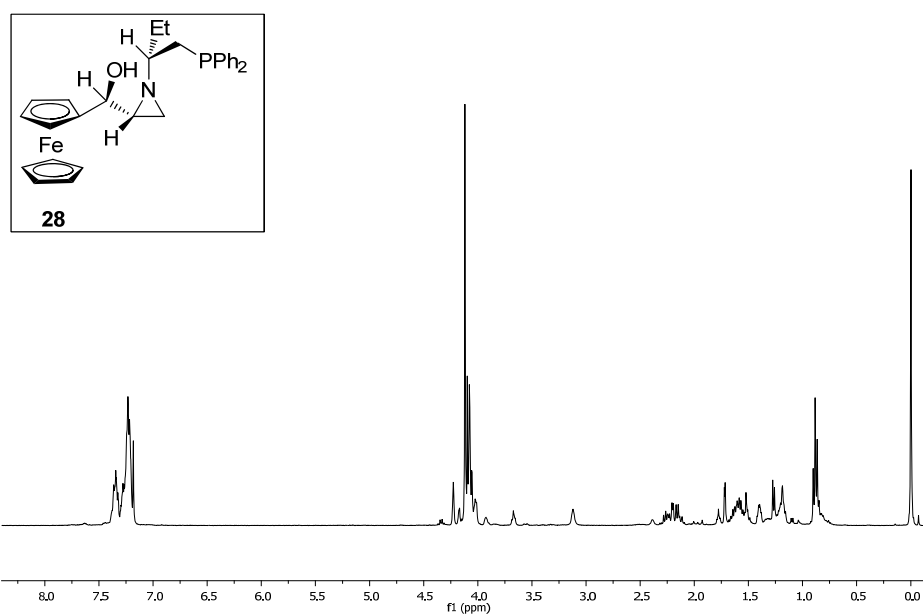


Figure A. 8 $^1\text{H-NMR}$ spectrum of compound **28**

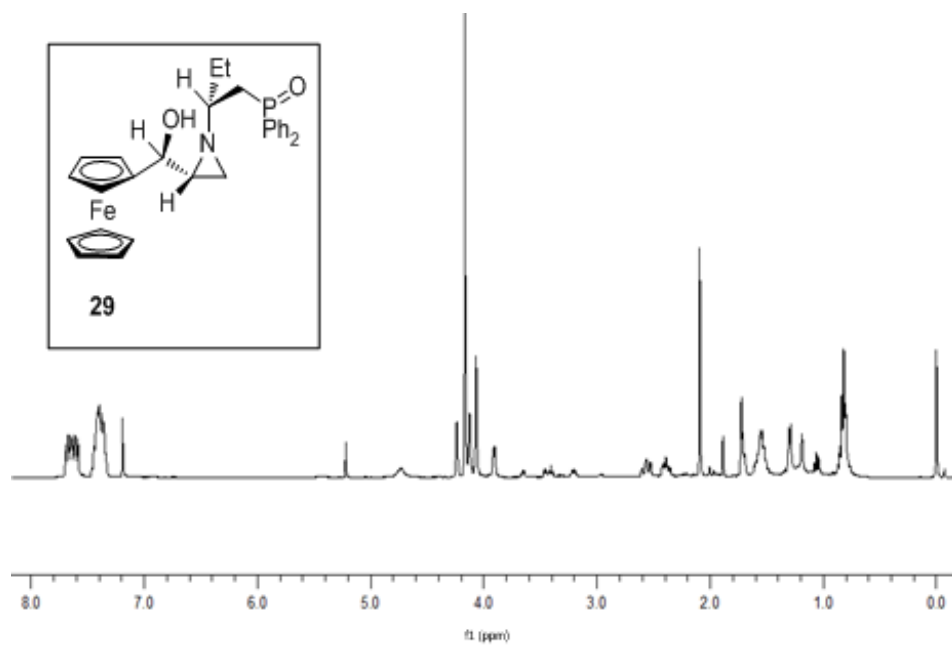


Figure A. 9 $^1\text{H-NMR}$ spectrum of compound **29**

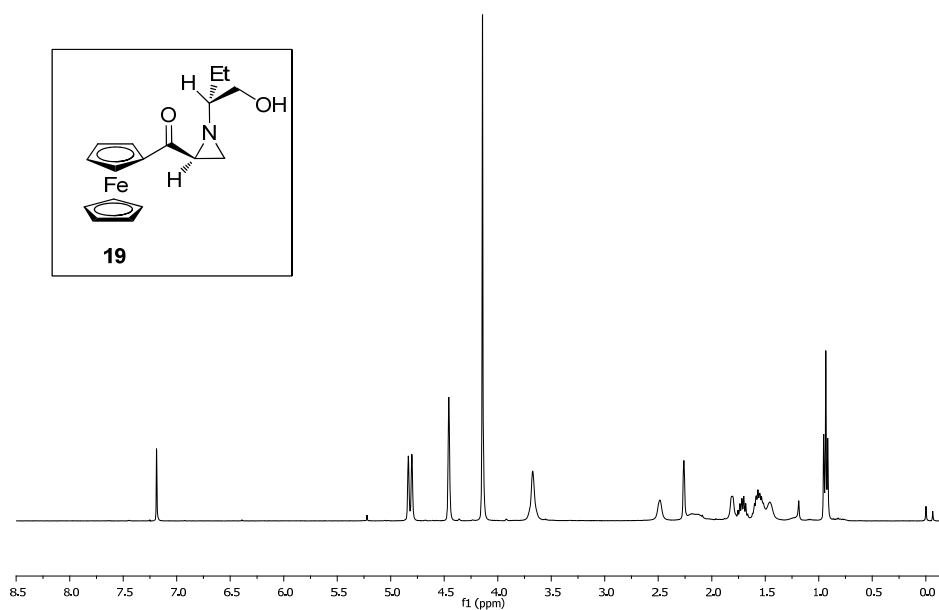


Figure A. 10 ¹H-NMR spectrum of compound 19

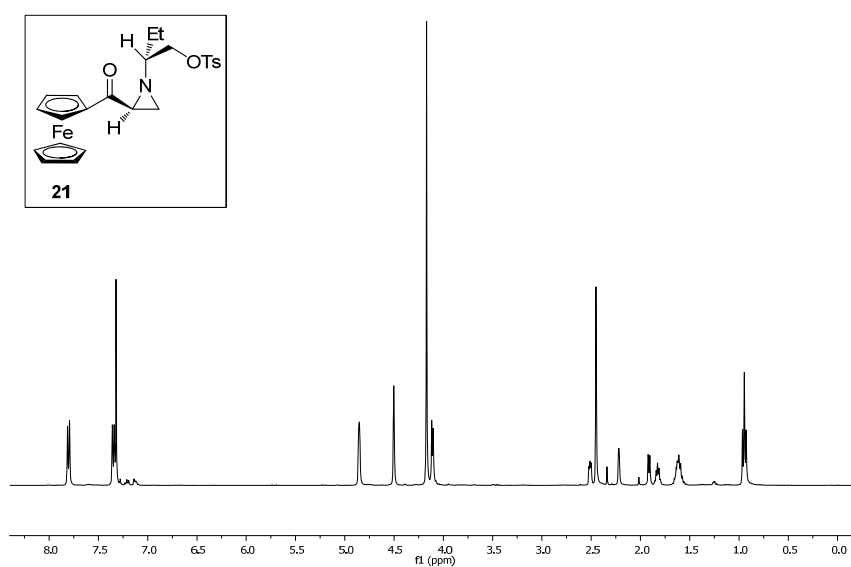


Figure A. 11 ¹H-NMR spectrum of compound 21

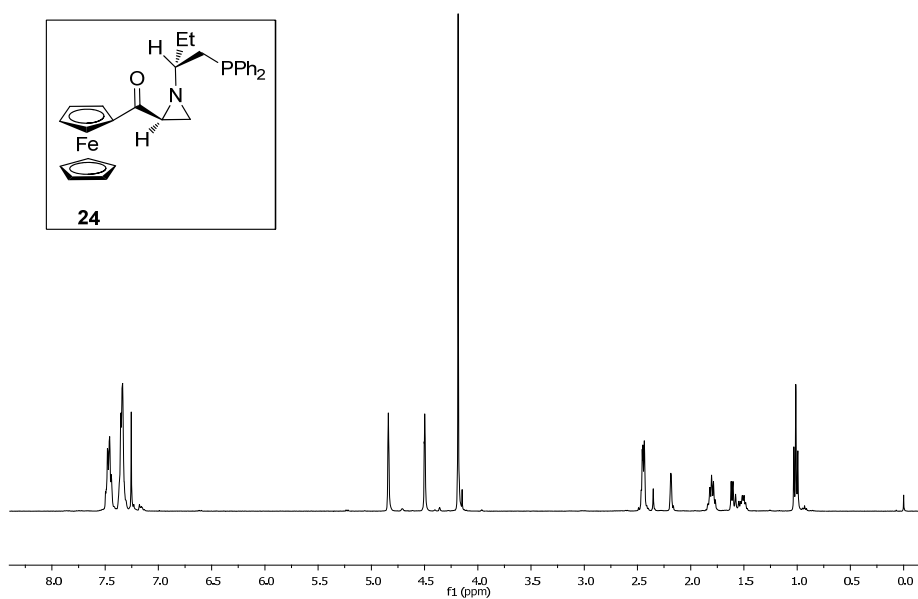


Figure A. 12 ¹H-NMR spectrum of compound 24

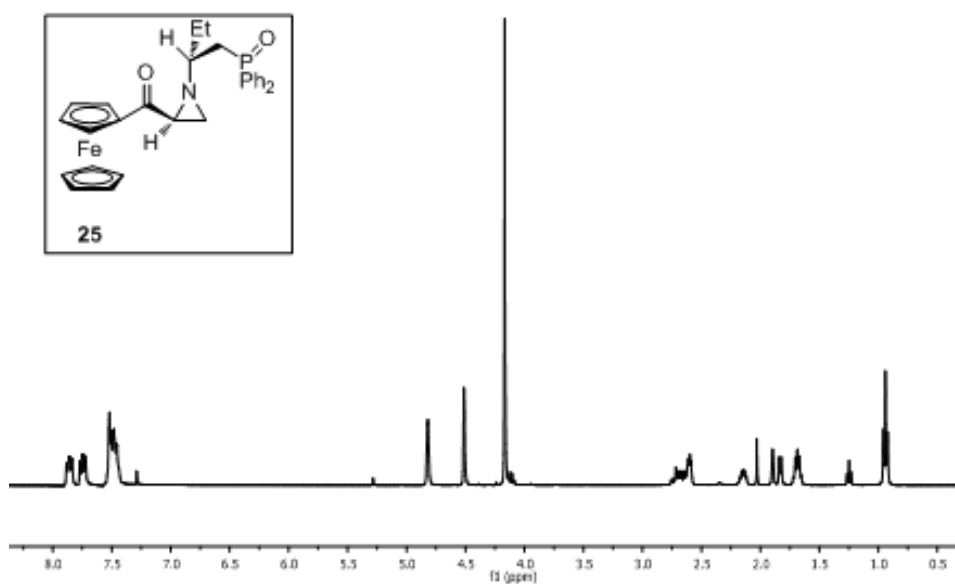


Figure A. 13 ¹H-NMR spectrum of compound 25

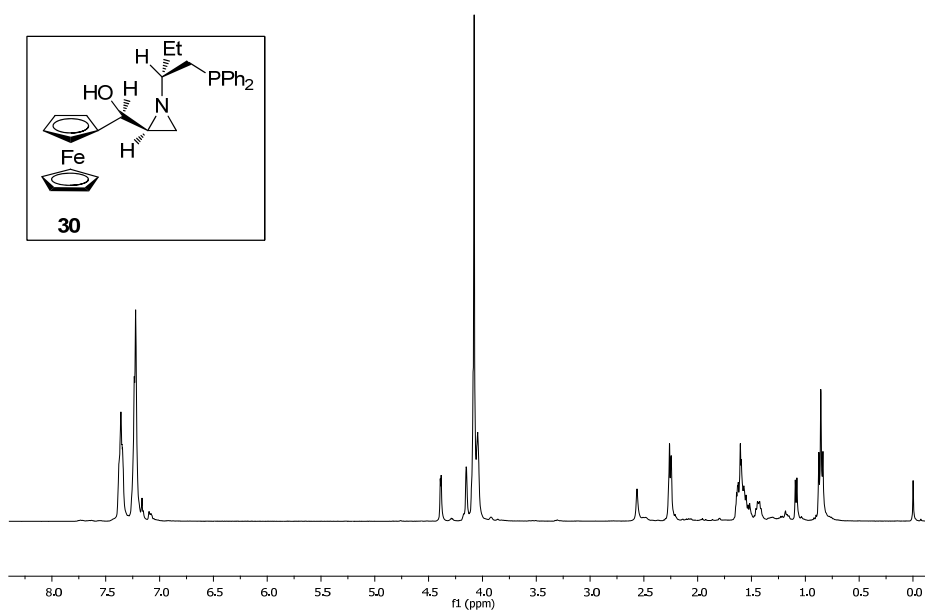


Figure A. 14 $^1\text{H-NMR}$ spectrum of compound **30**

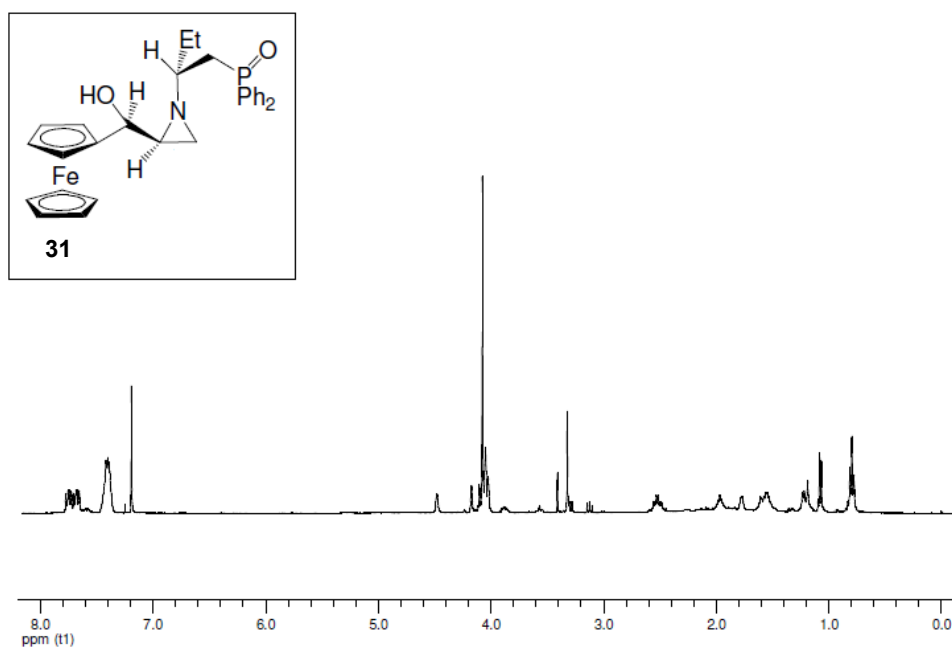


Figure A. 15 $^1\text{H-NMR}$ spectrum of compound **31**

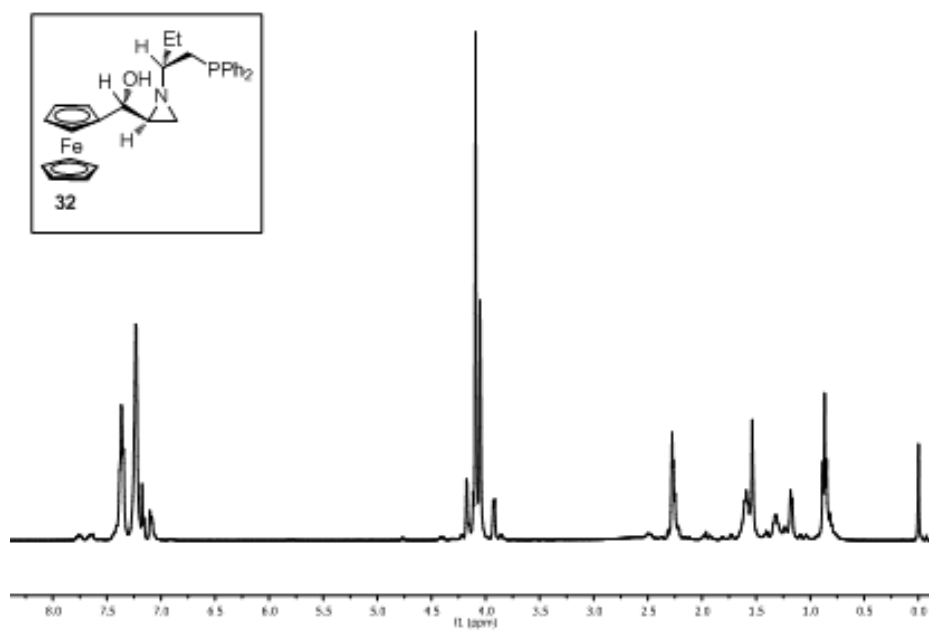


Figure A. 16 ^1H -NMR spectrum of compound **32**

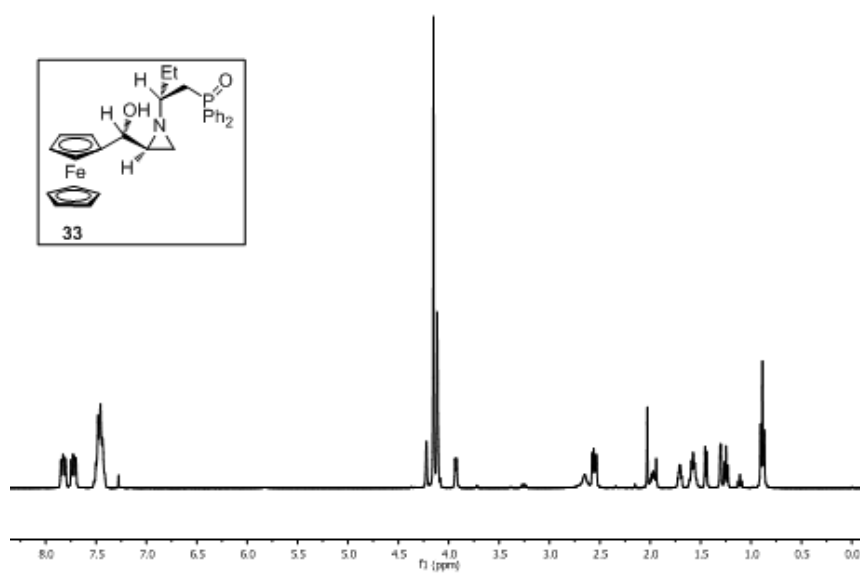


Figure A. 17 ^1H -NMR spectrum of compound **33**

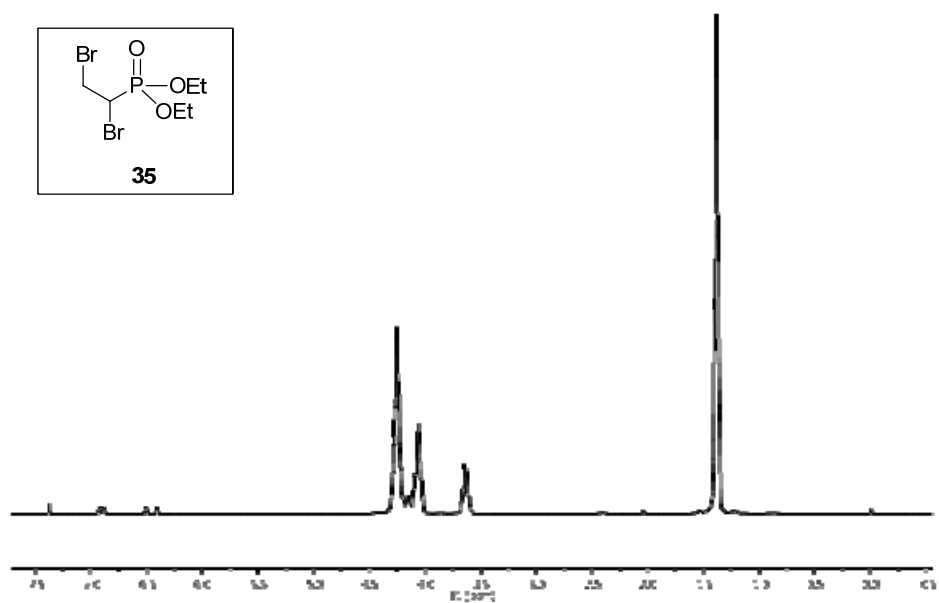


Figure A. 18 $^1\text{H-NMR}$ spectrum of compound 35

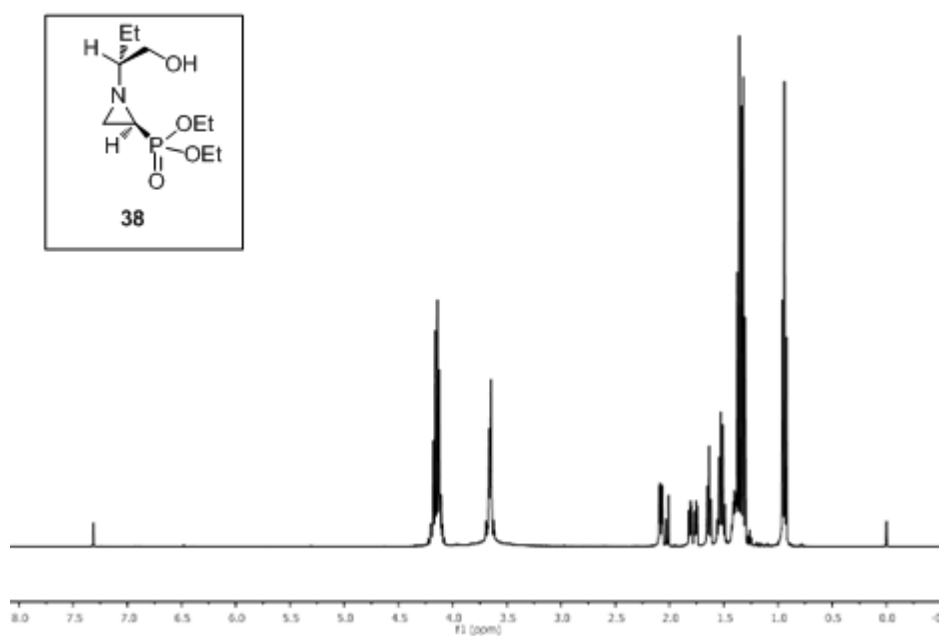


Figure A. 19 $^1\text{H-NMR}$ spectrum of compound 38

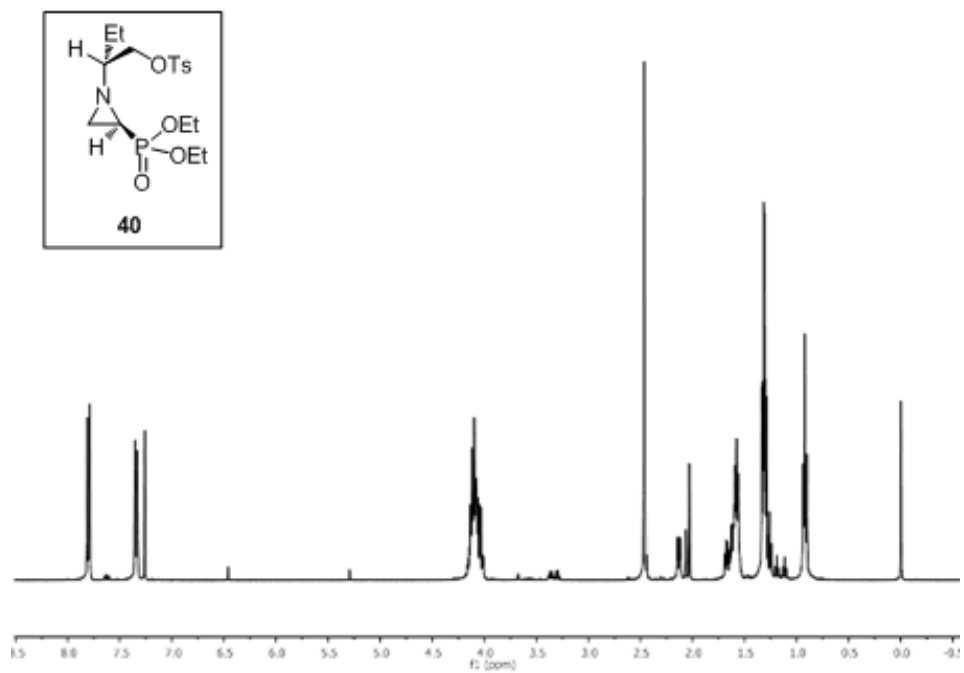


Figure A. 20 $^1\text{H-NMR}$ spectrum of compound 40

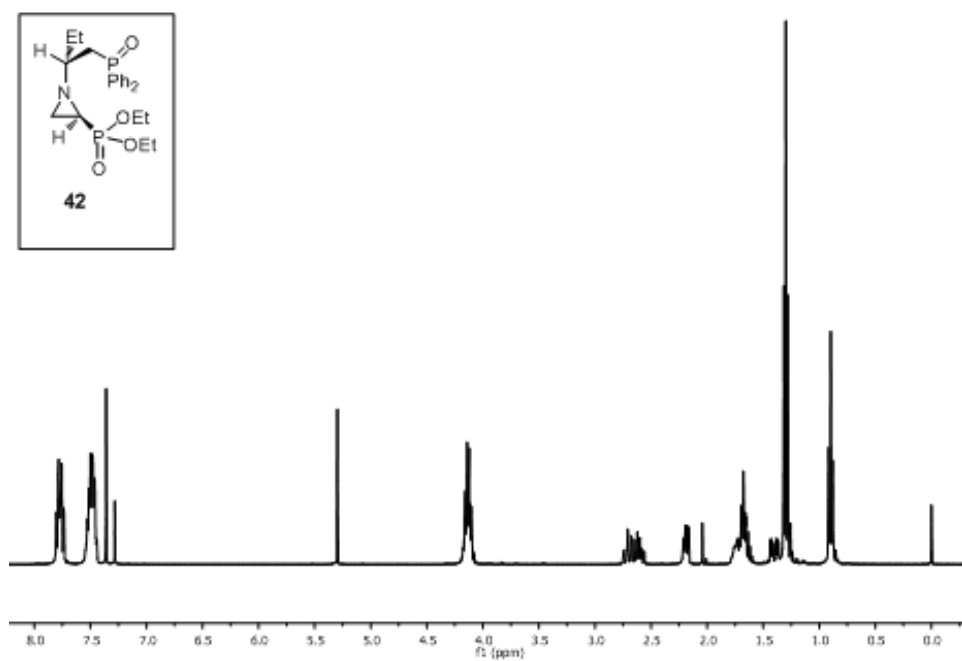


Figure A. 21 $^1\text{H-NMR}$ spectrum of compound 42

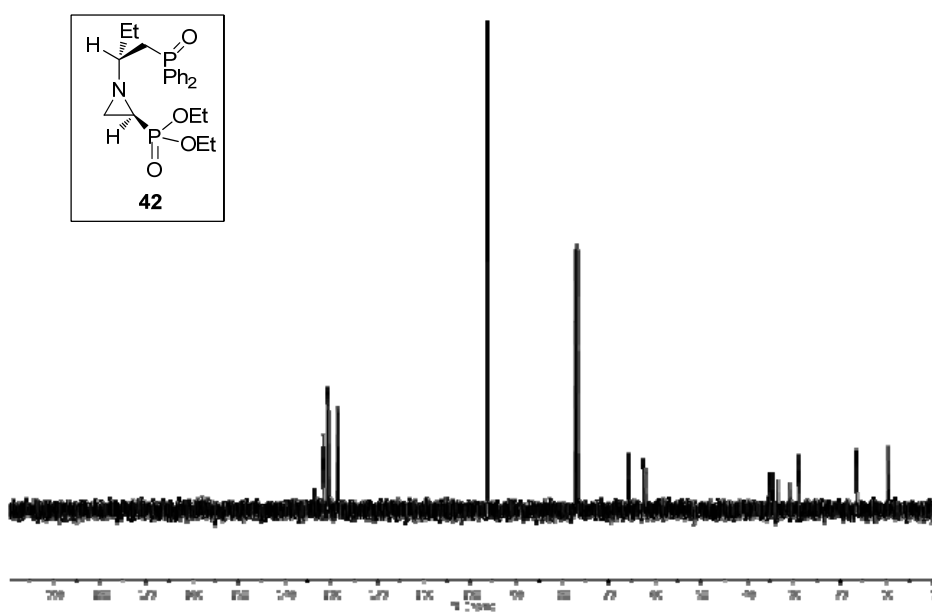


Figure A. 22 ^{13}C -NMR spectrum of compound 42

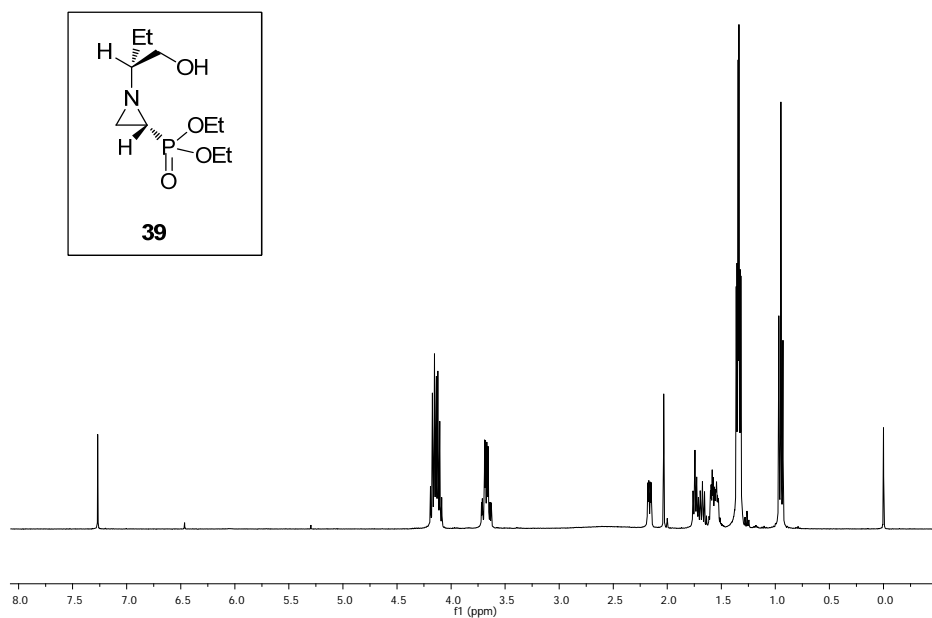


Figure A. 23 ^1H -NMR spectrum of compound 39

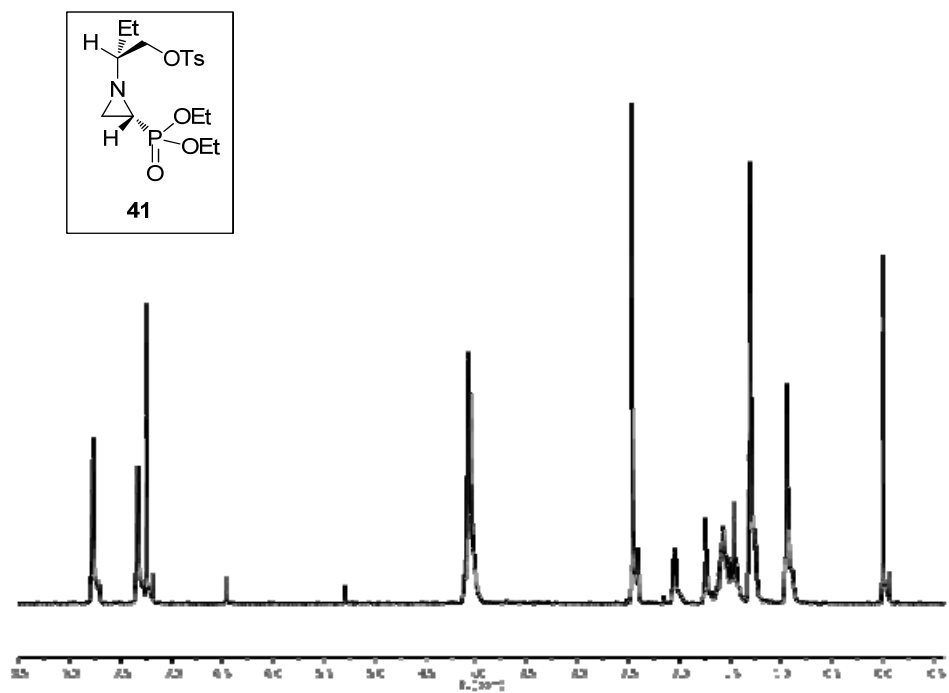


Figure A. 24 $^1\text{H-NMR}$ spectrum of compound 41

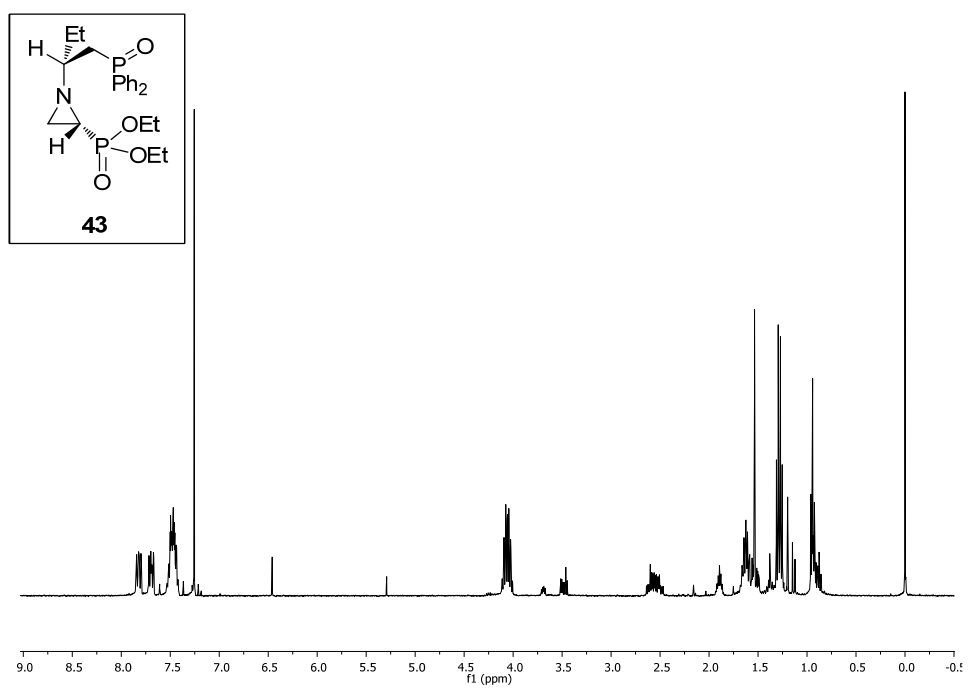


Figure A. 25 $^1\text{H-NMR}$ spectrum of compound 43

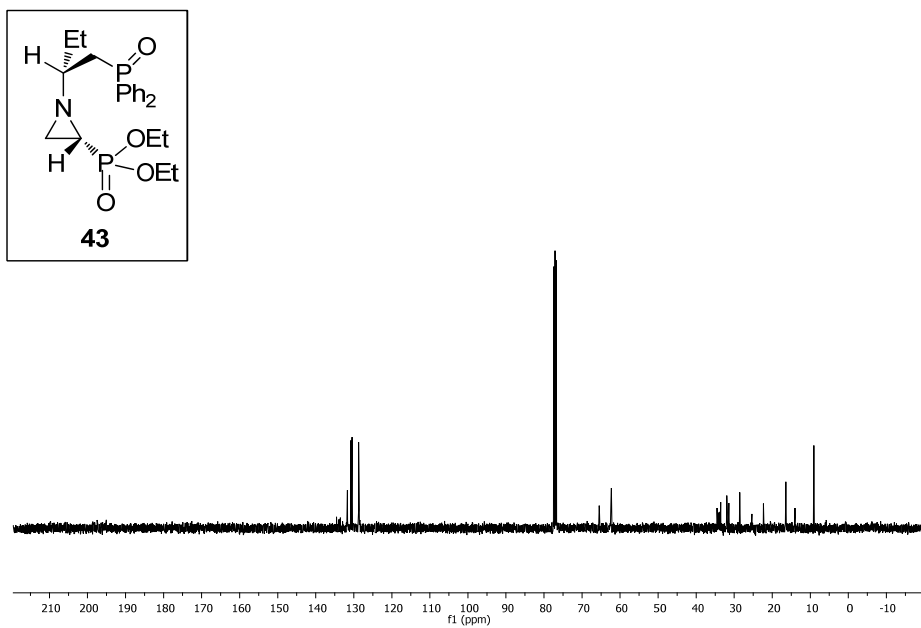


Figure A. 26 ^{13}C -NMR spectrum of compound **43**

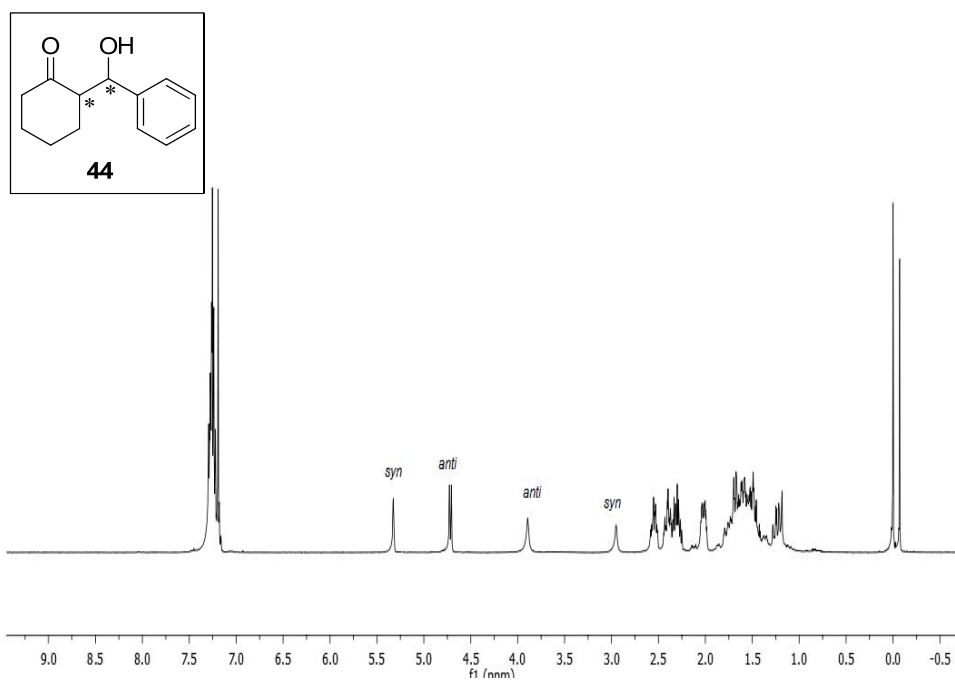


Figure A. 27 ^1H -NMR spectrum of compound **44**

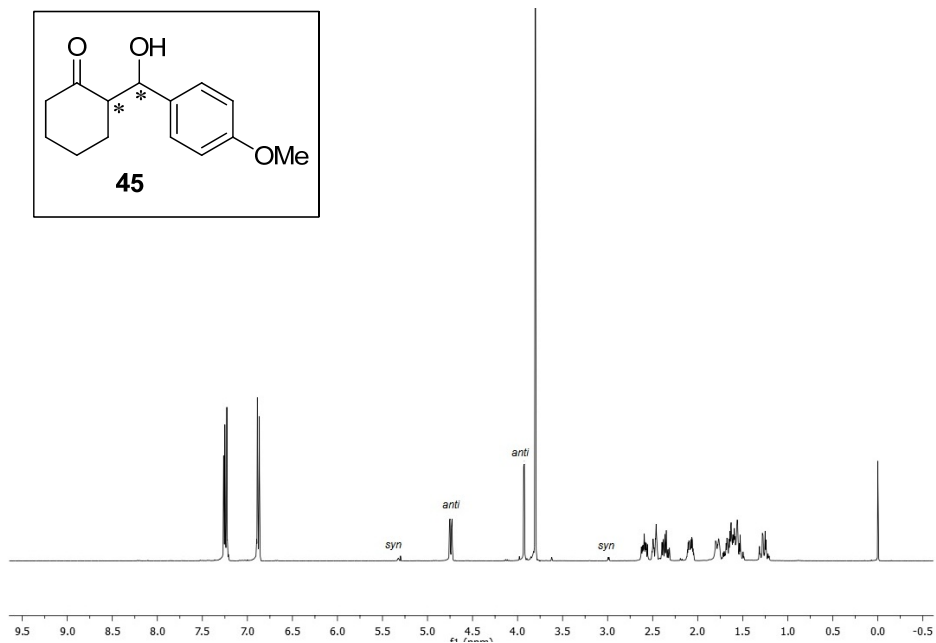


Figure A. 28 ¹H-NMR spectrum of compound **45**

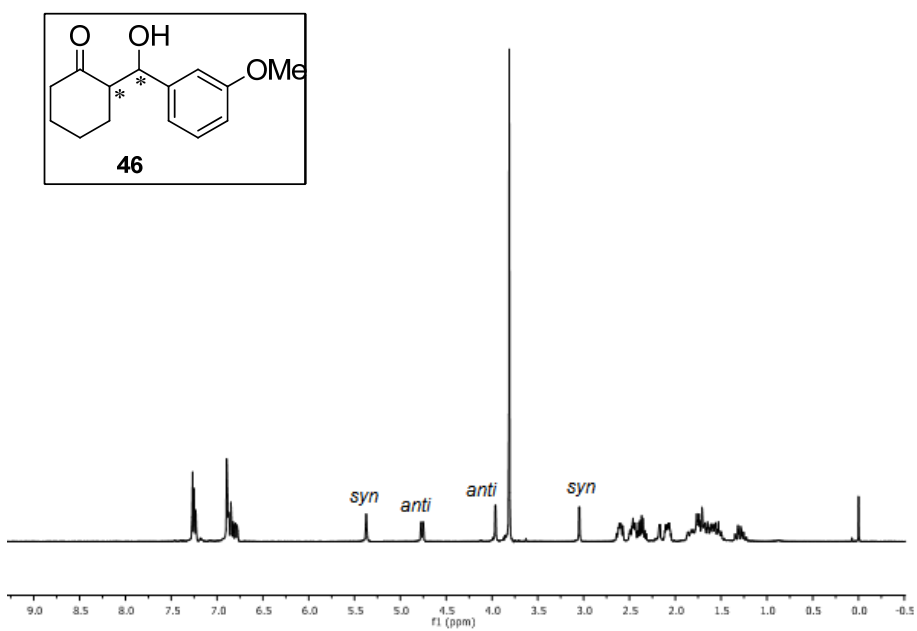


Figure A. 29 ¹H-NMR spectrum of compound **46**

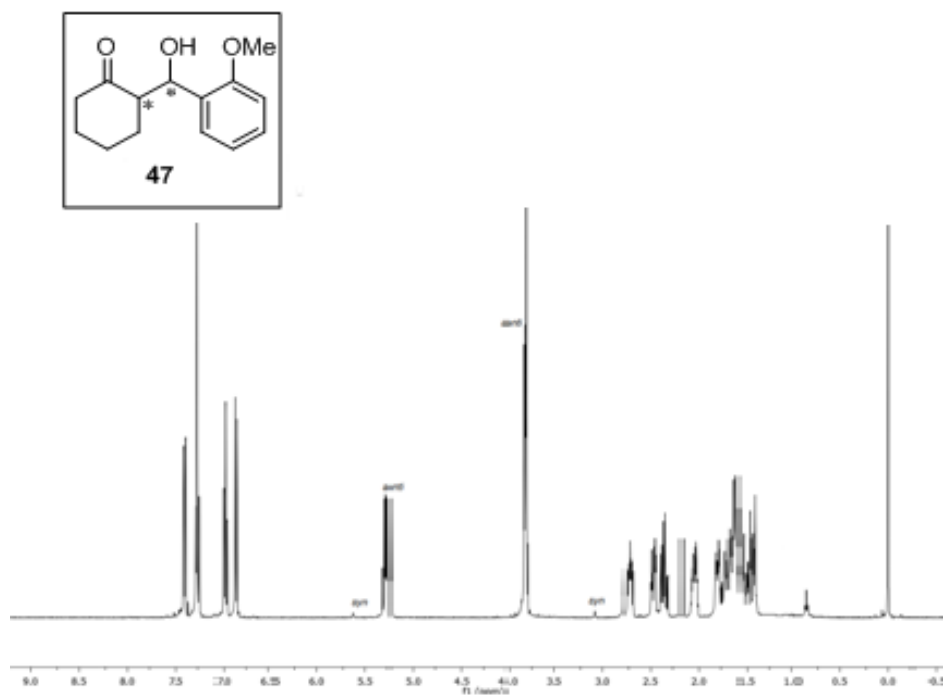


Figure A. 30 ¹H-NMR spectrum of compound 47

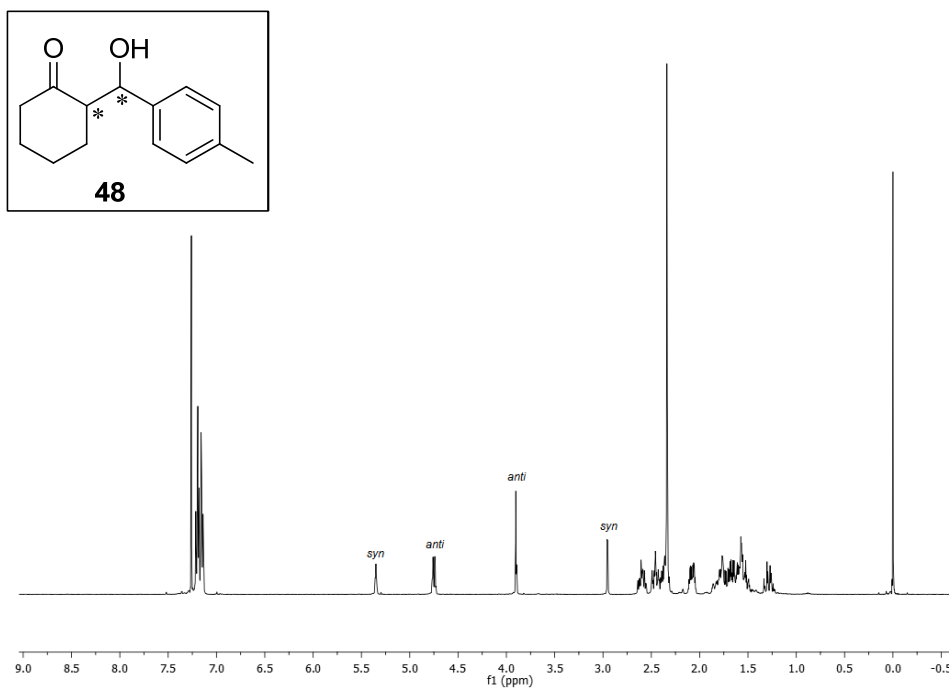


Figure A. 31 ¹H-NMR spectrum of compound 48

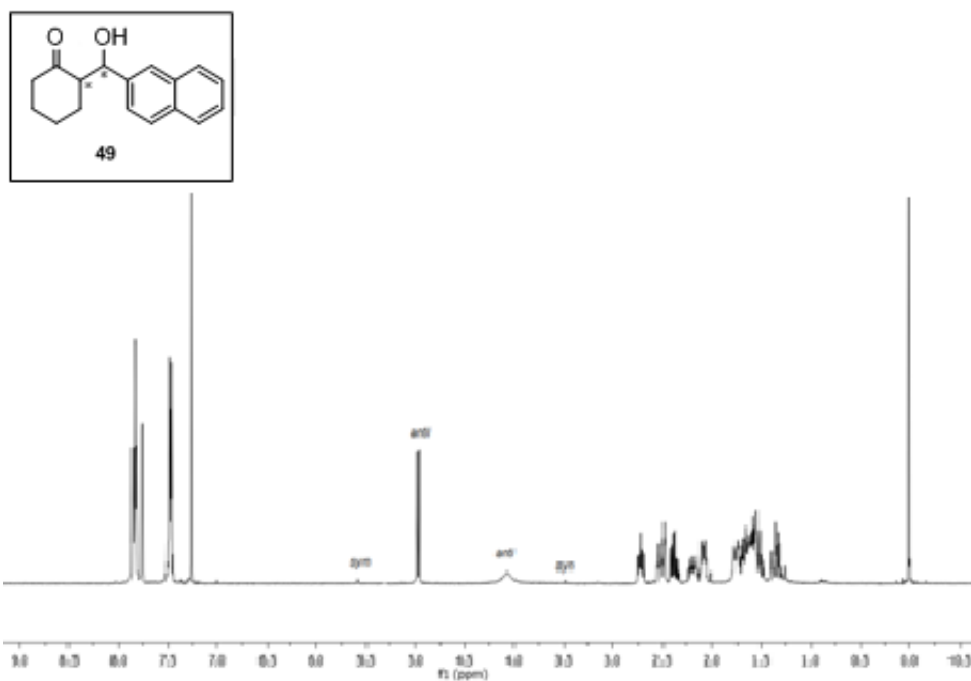


Figure A. 32 $^1\text{H-NMR}$ spectrum of compound 49

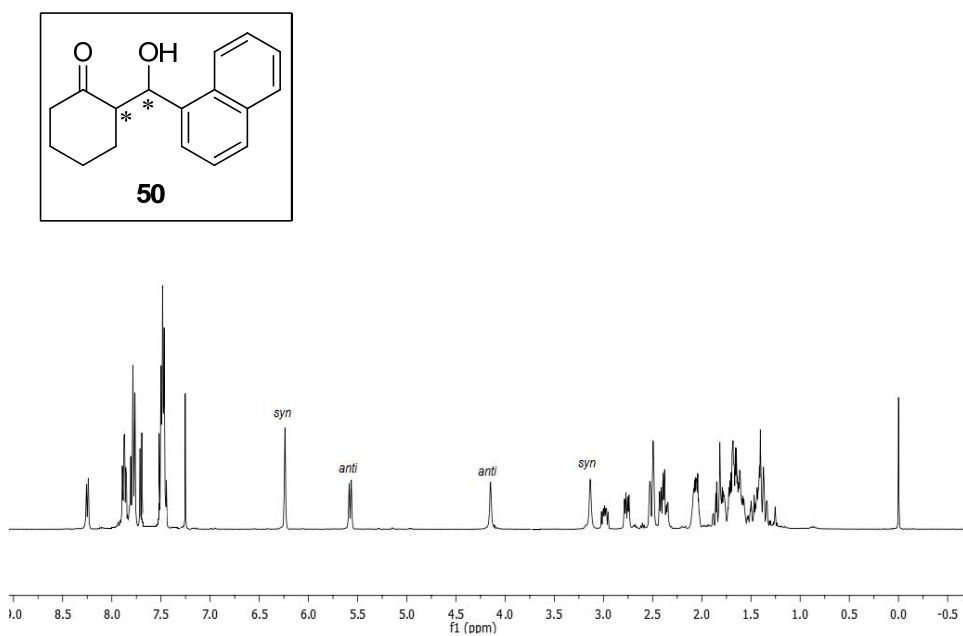


Figure A. 33 $^1\text{H-NMR}$ spectrum of compound 50

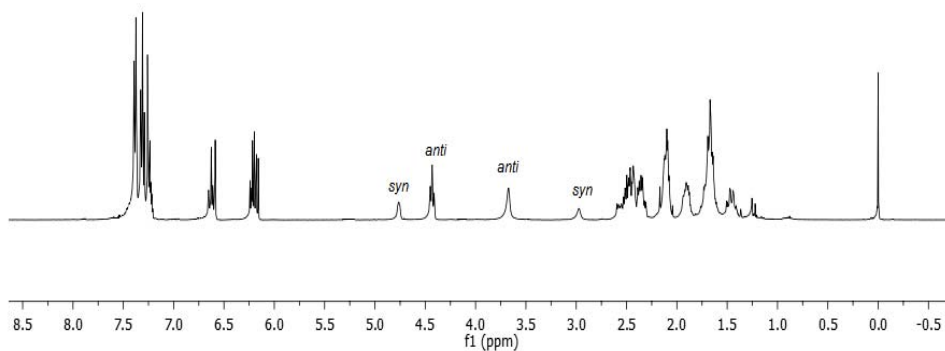
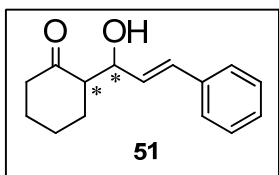


Figure A. 34 ¹H-NMR spectrum of compound 51

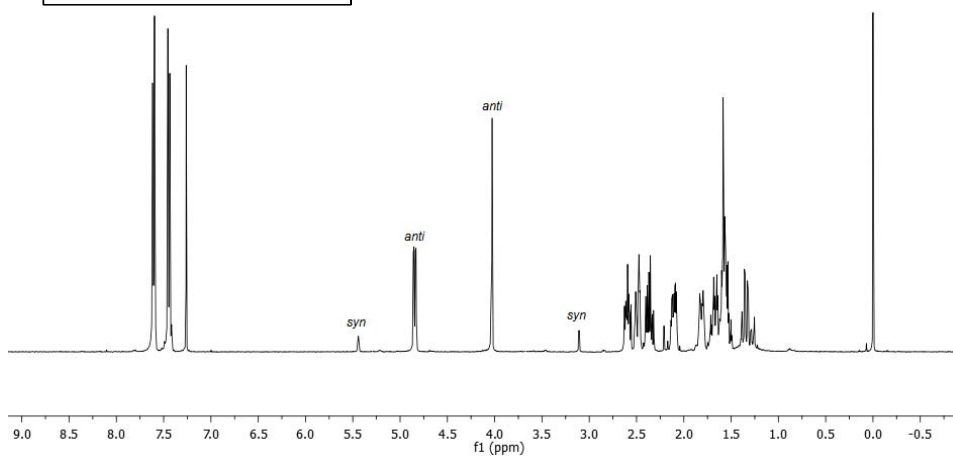
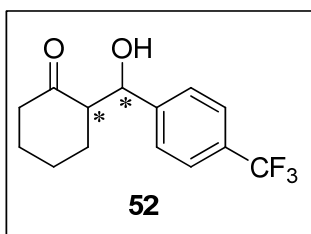


Figure A. 35 ¹H-NMR spectrum of compound 52

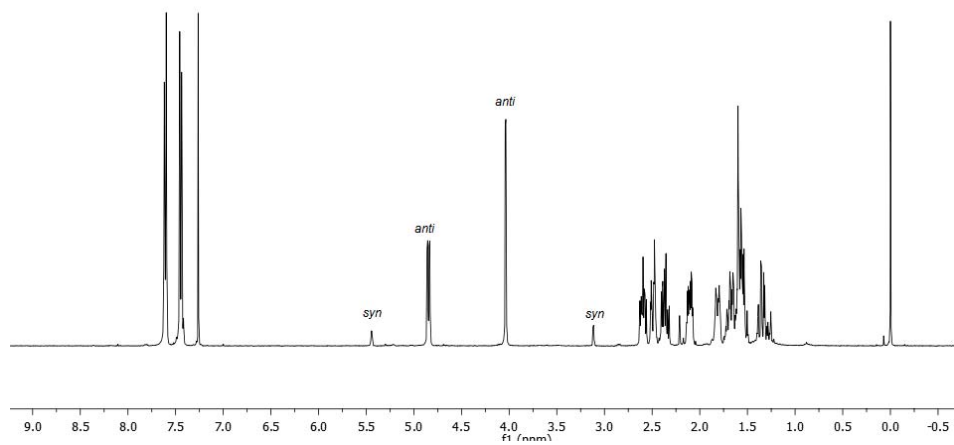
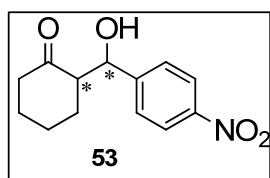


Figure A. 36 $^1\text{H-NMR}$ spectrum of compound **53**

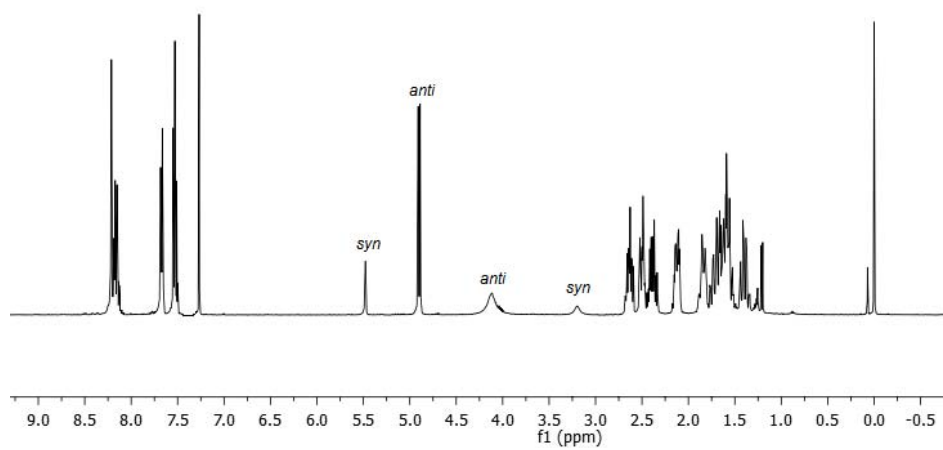
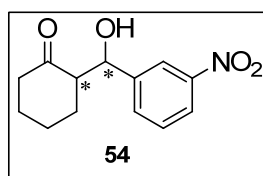


Figure A. 37 $^1\text{H-NMR}$ spectrum of compound **54**

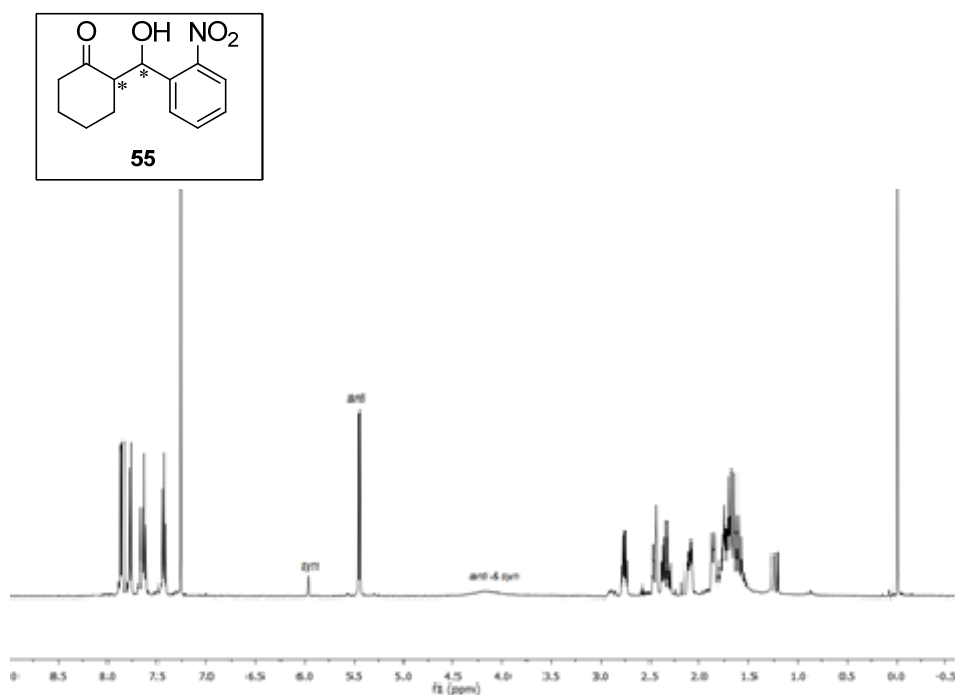


Figure A. 38 $^1\text{H-NMR}$ spectrum of compound 55

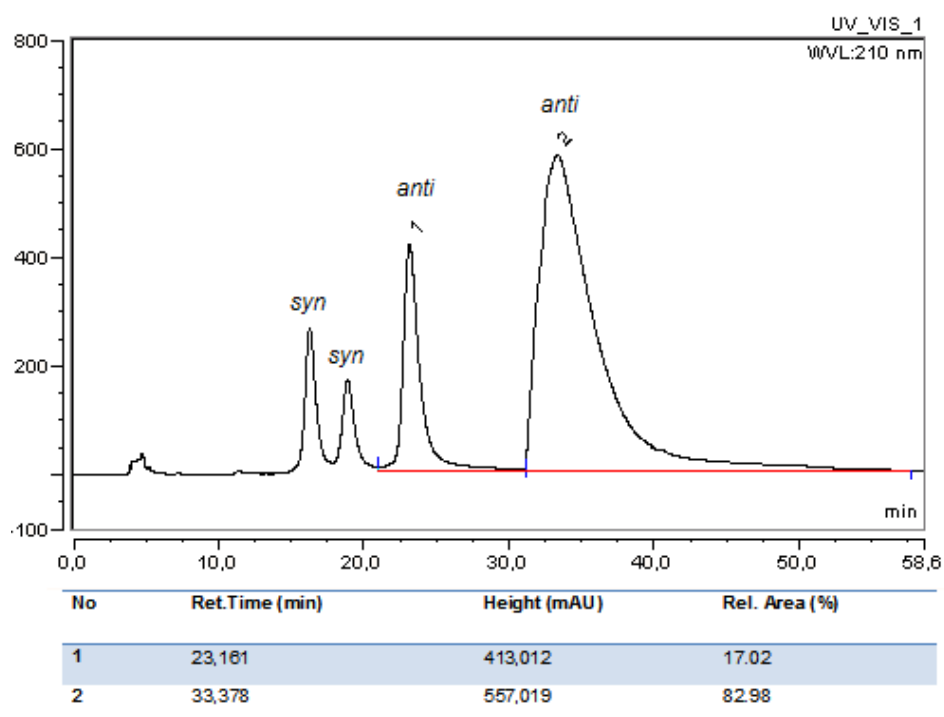


Figure A. 39 HPLC chromatogram of 44

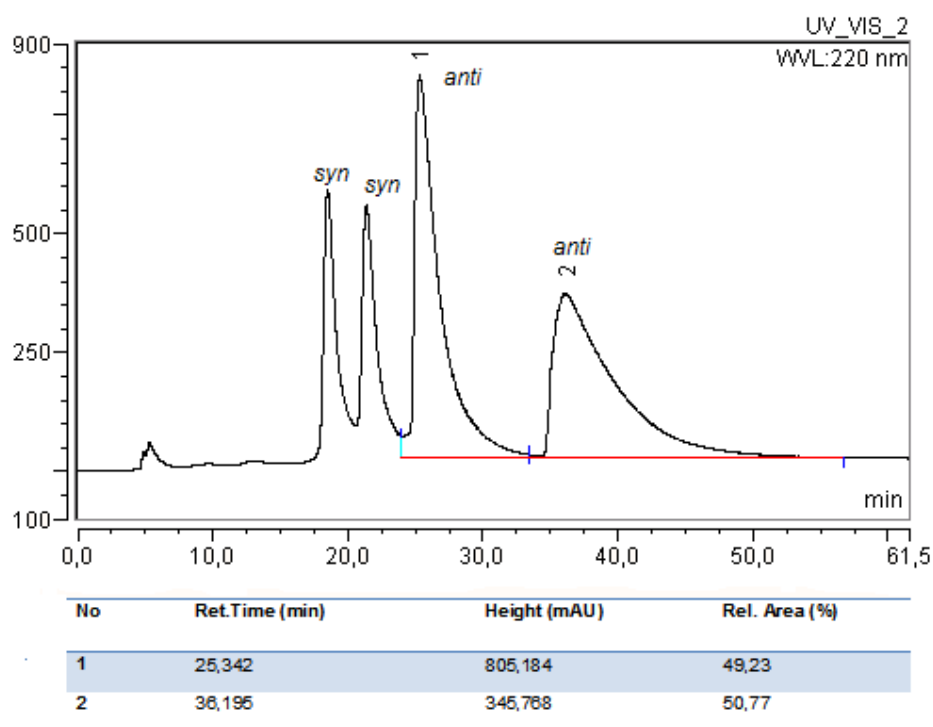


Figure A. 40 HPLC chromatogram of racemic mixture of **44**

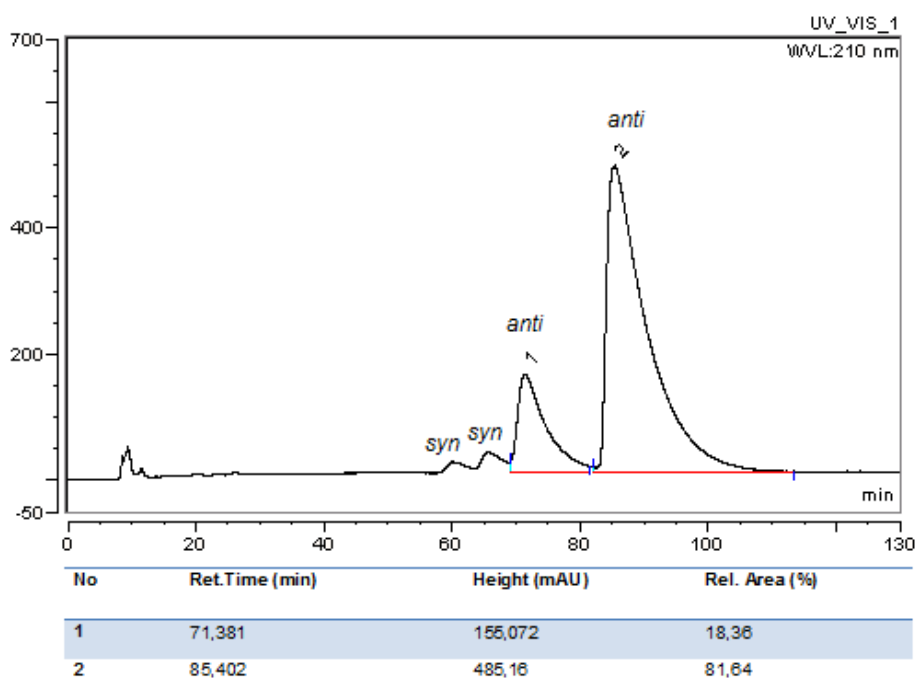


Figure A. 41 HPLC chromatogram of **45**

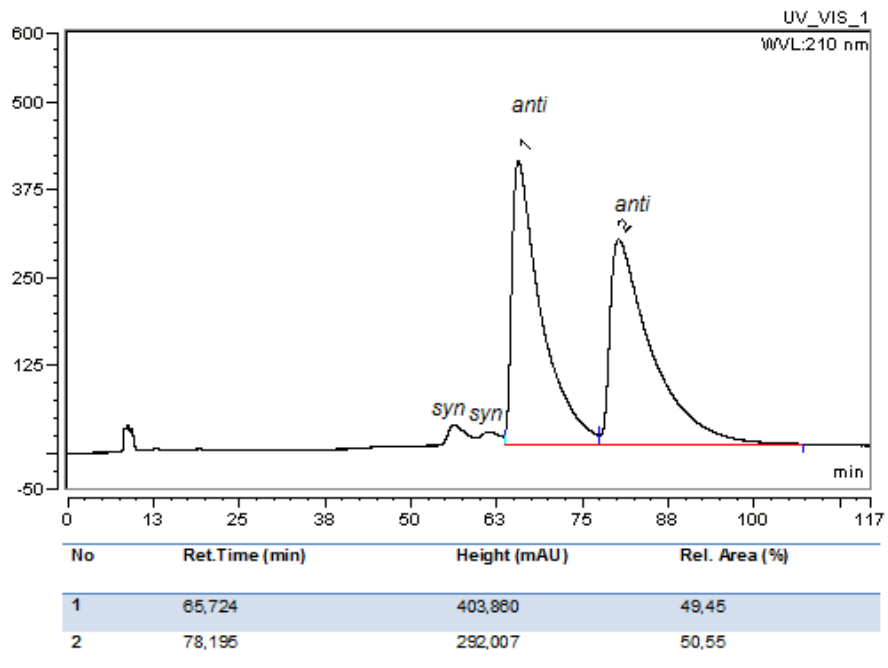


Figure A. 42 HPLC chromatogram of racemic mixture of **45**

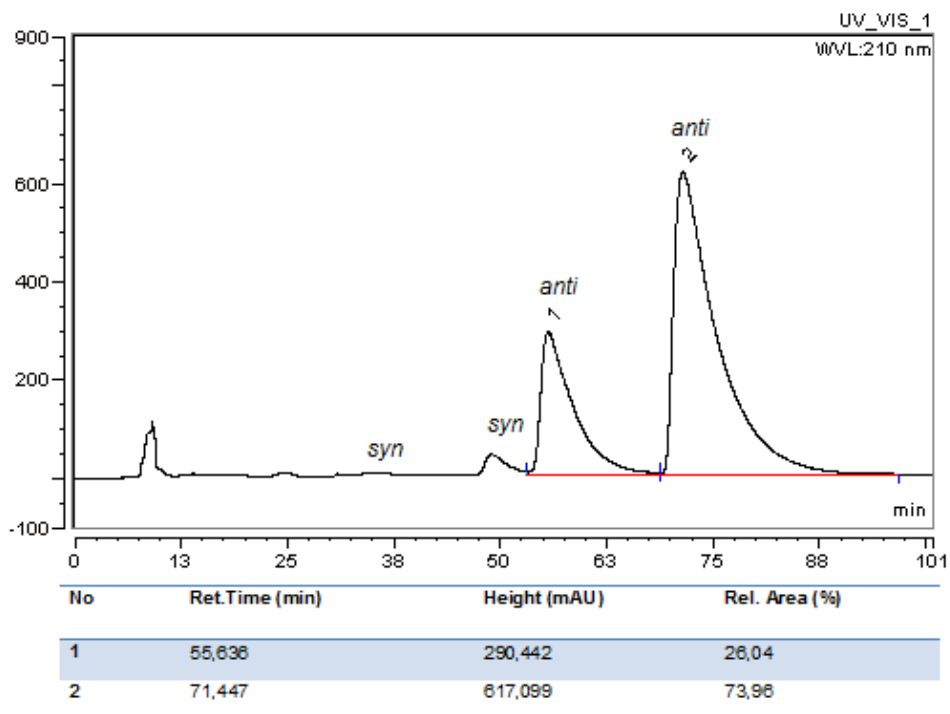


Figure A. 43 HPLC chromatogram of **46**

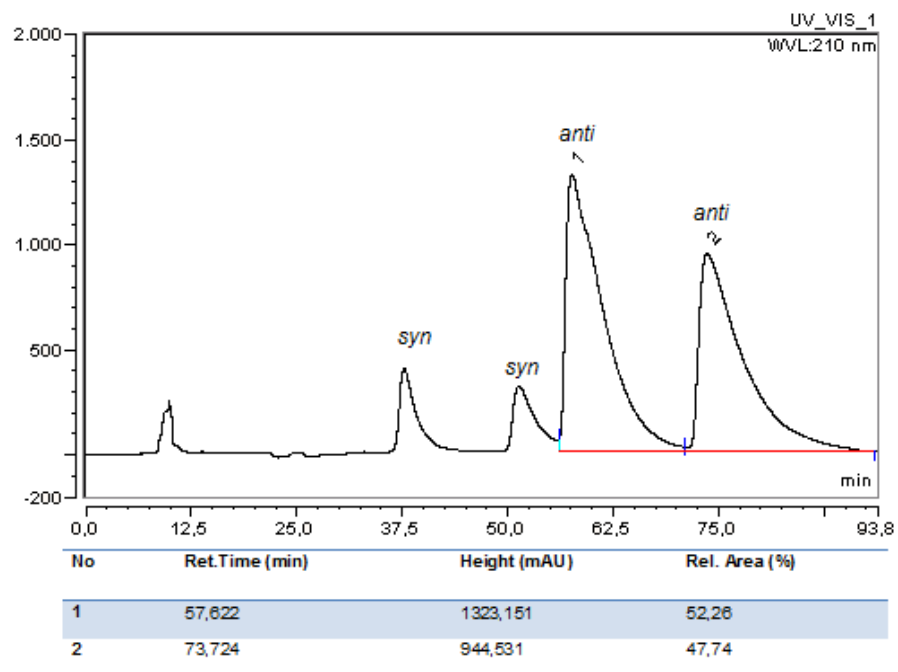


Figure A. 44 HPLC chromatogram of racemic mixture of 46

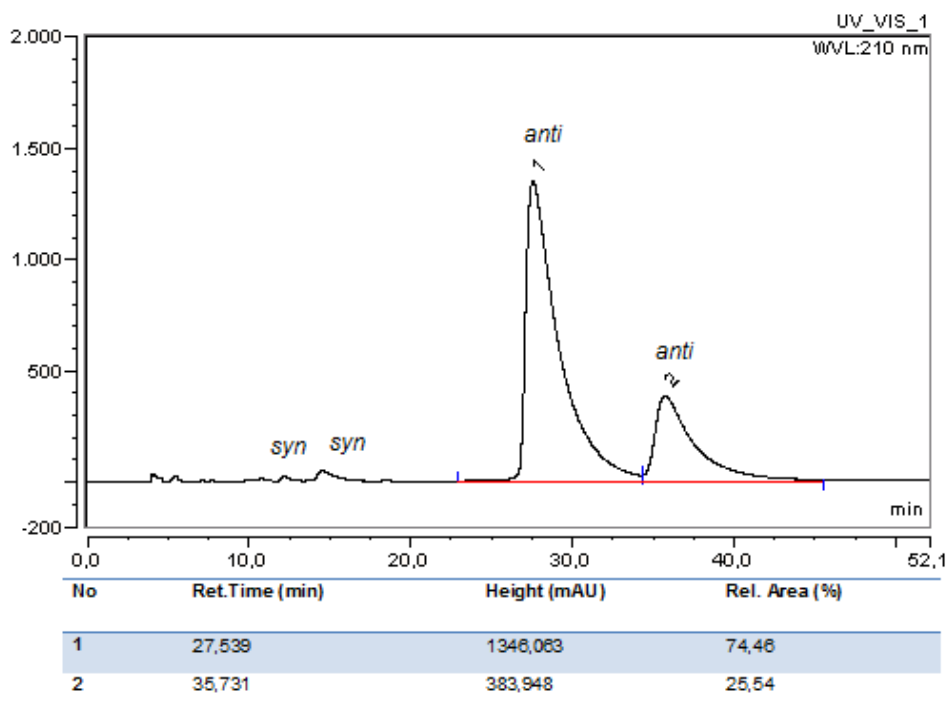


Figure A. 45 HPLC chromatogram of 47

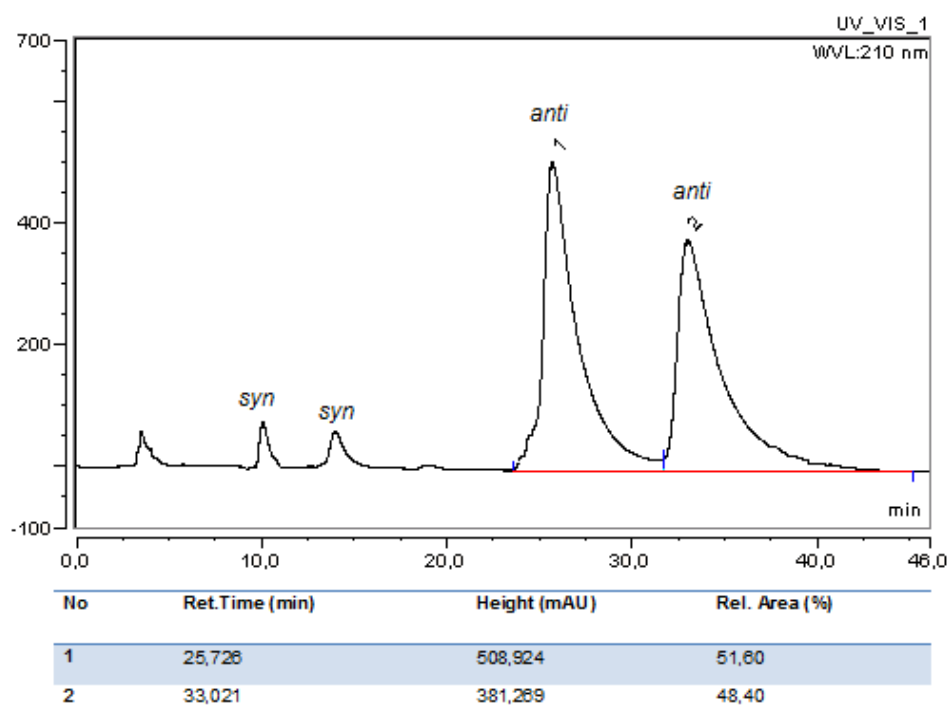


Figure A. 46 HPLC chromatogram of racemic mixture of **47**

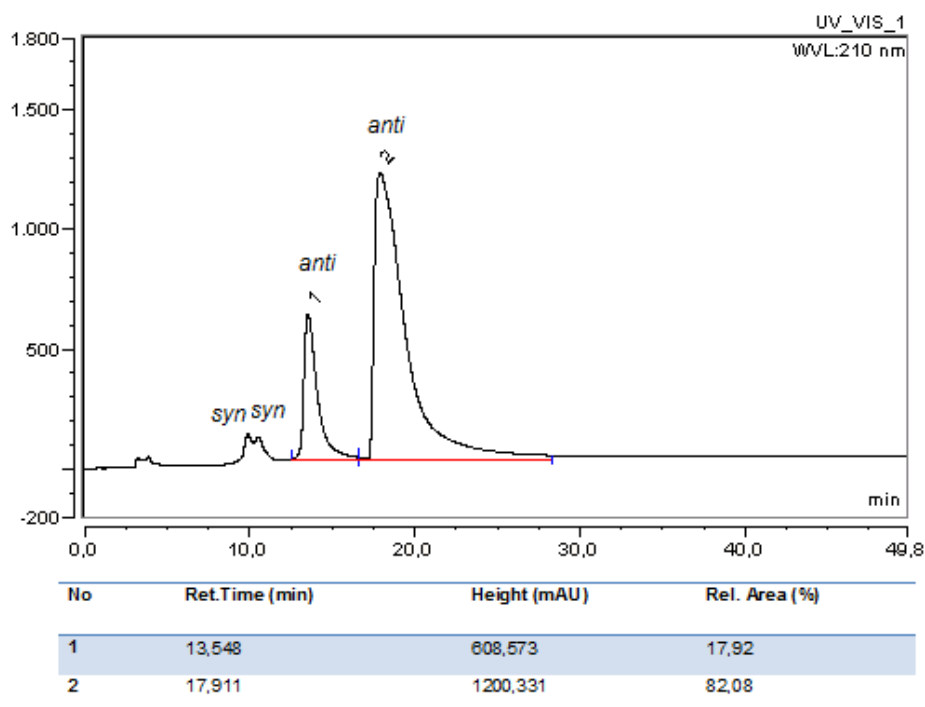


Figure A. 47 HPLC chromatogram of **48**

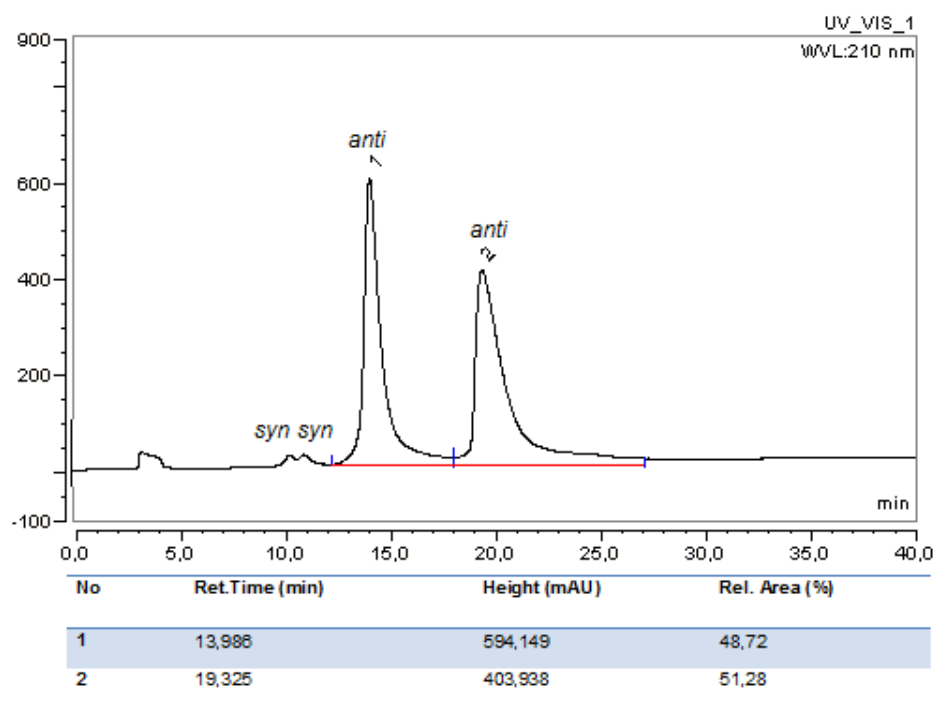


Figure A. 48 HPLC chromatogram of racemic mixture of 48

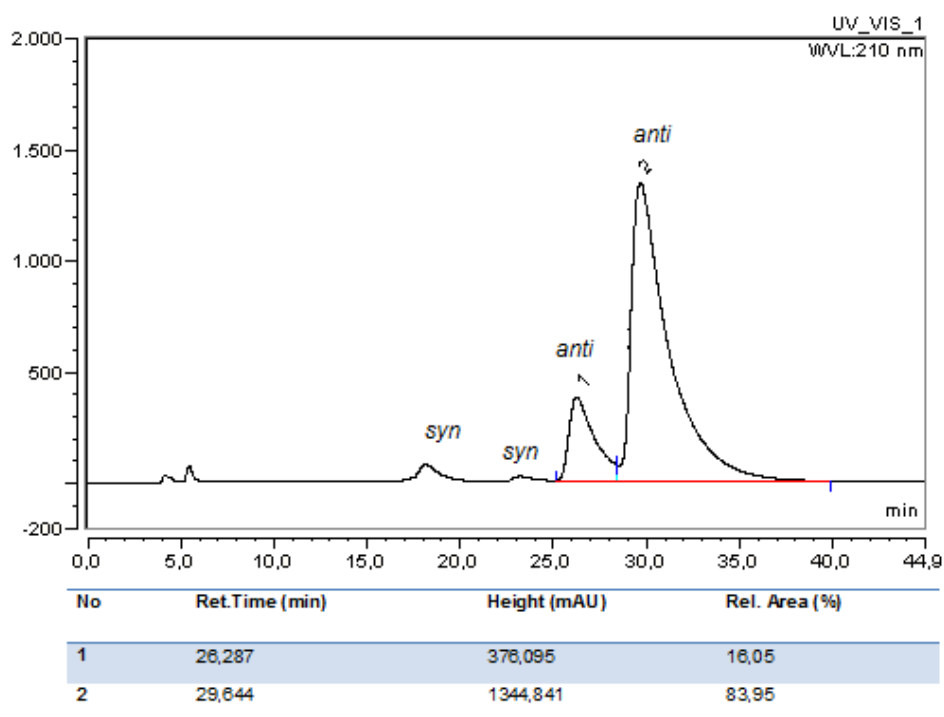


Figure A. 49 HPLC chromatogram of 49

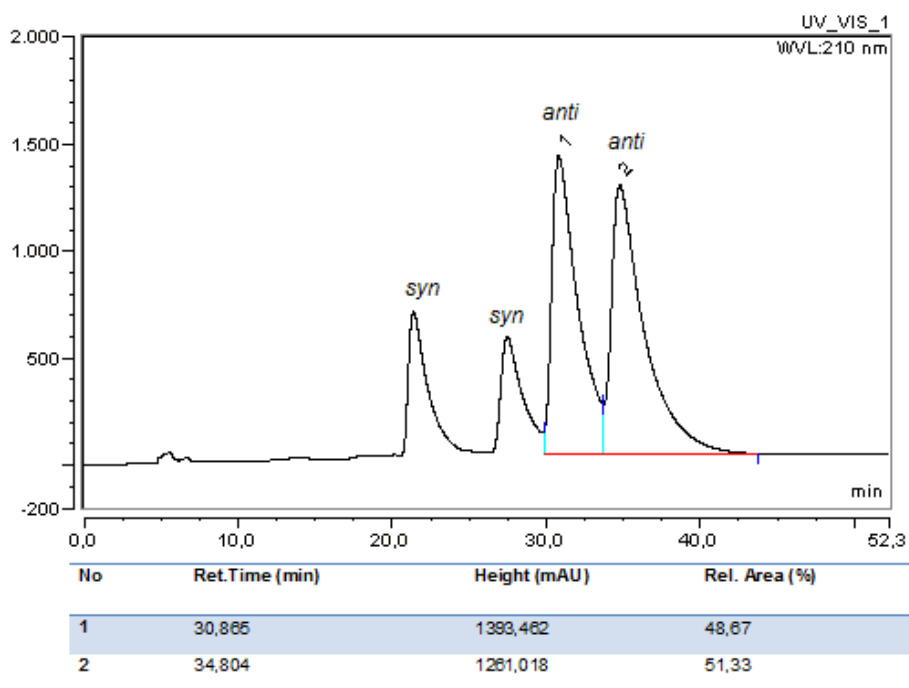


Figure A. 50 HPLC chromatogram of racemic mixture of **49**

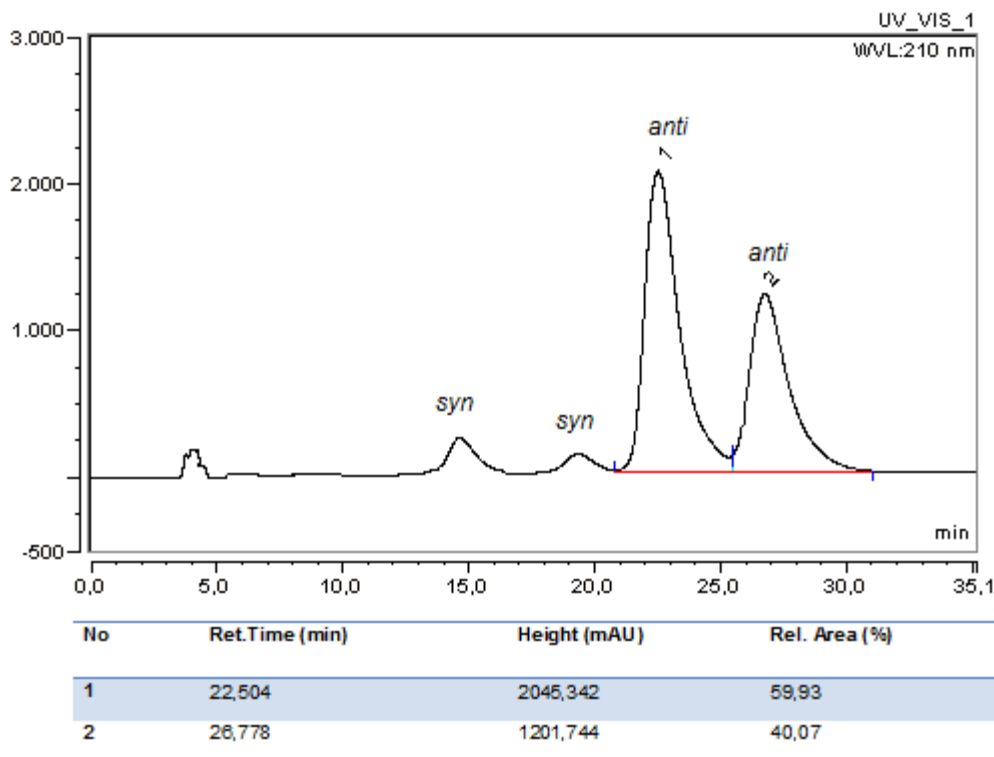


Figure A. 51 HPLC chromatogram of **50**

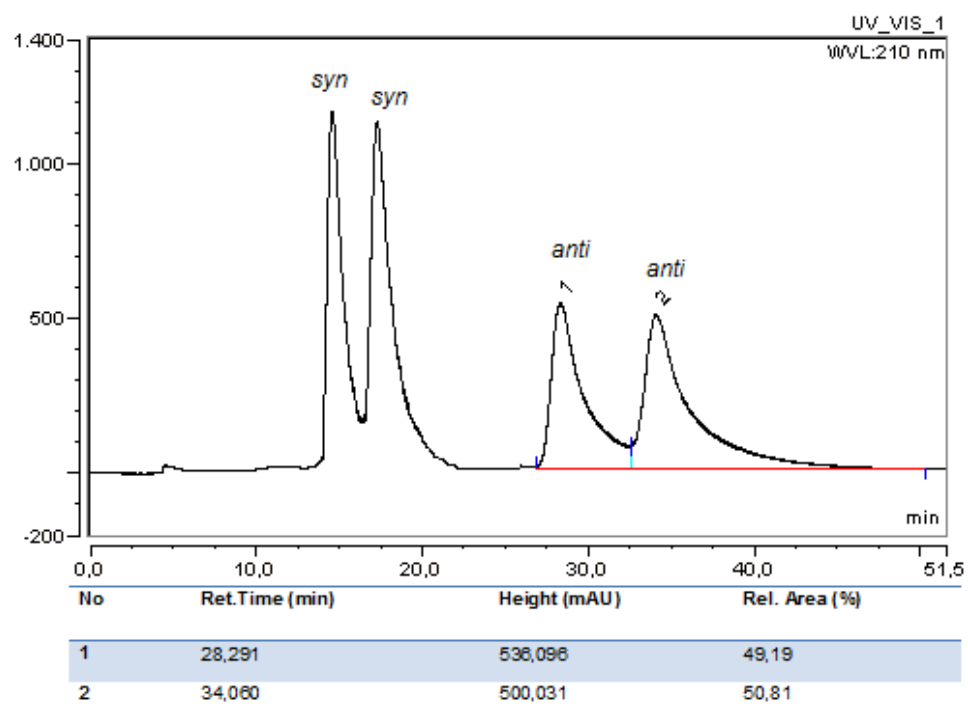


Figure A. 52 HPLC chromatogram of racemic mixture of **50**

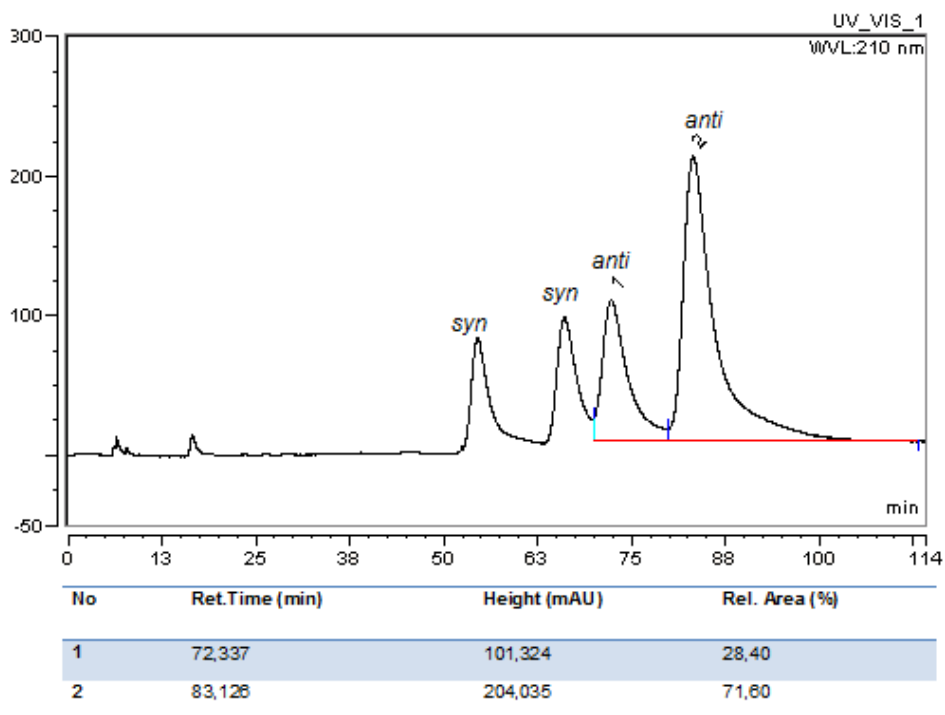


Figure A. 53 HPLC chromatogram of **51**

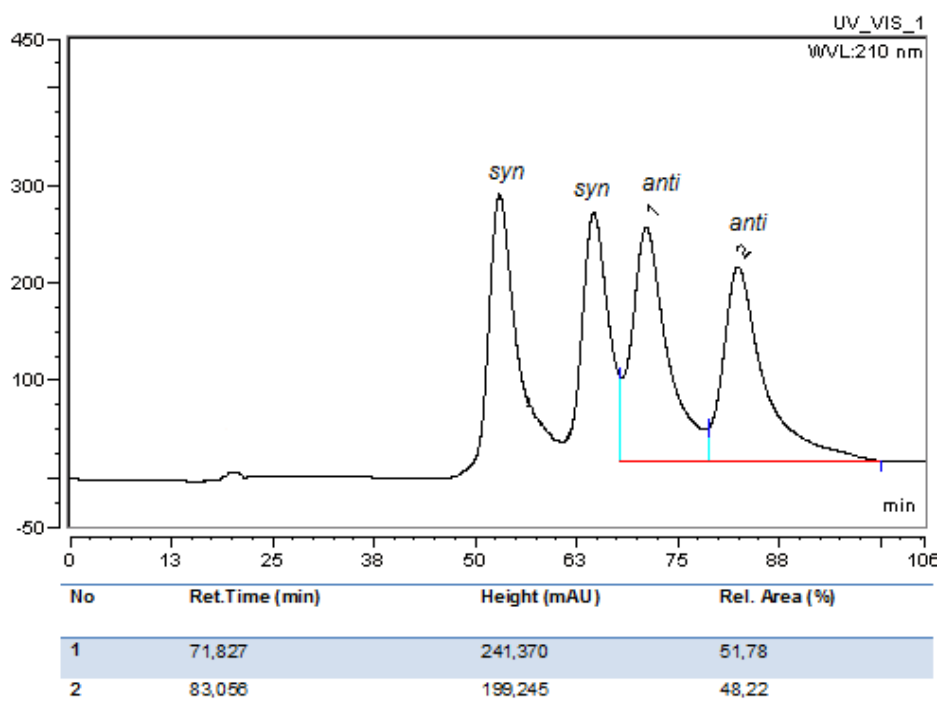


Figure A. 54 HPLC chromatogram of racemic mixture of **51**

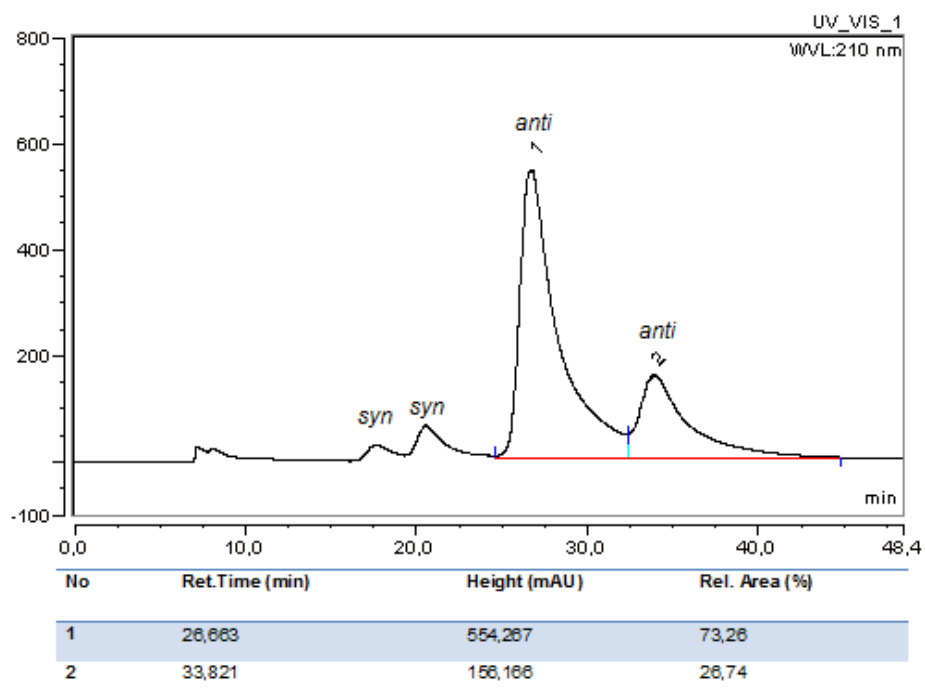


Figure A. 55 HPLC chromatogram of **52**

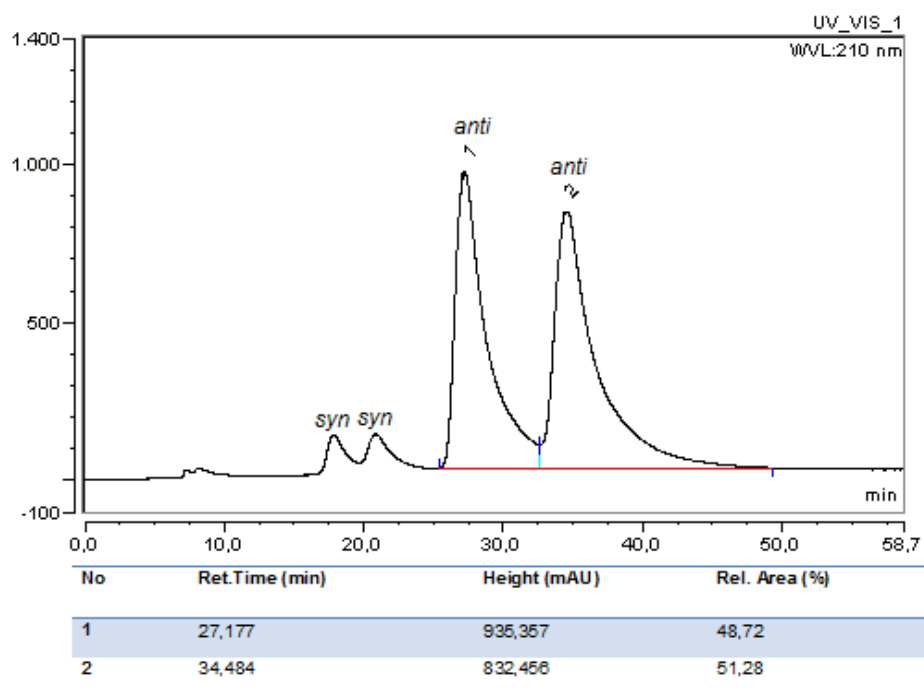


Figure A. 56 HPLC chromatogram of racemic mixture of **52**

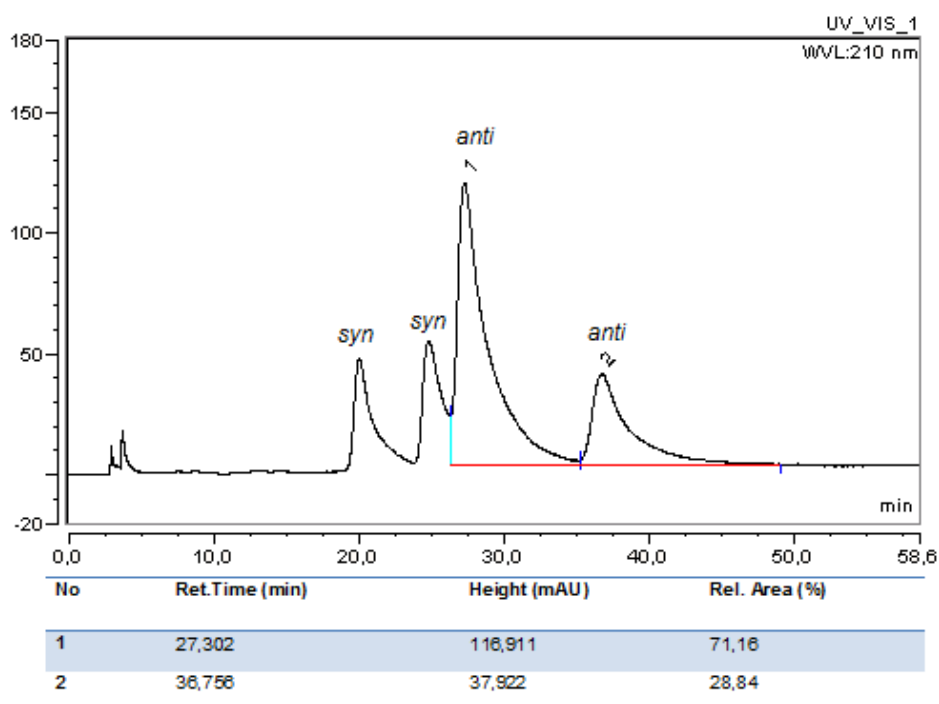


Figure A. 57 HPLC chromatogram of **53**

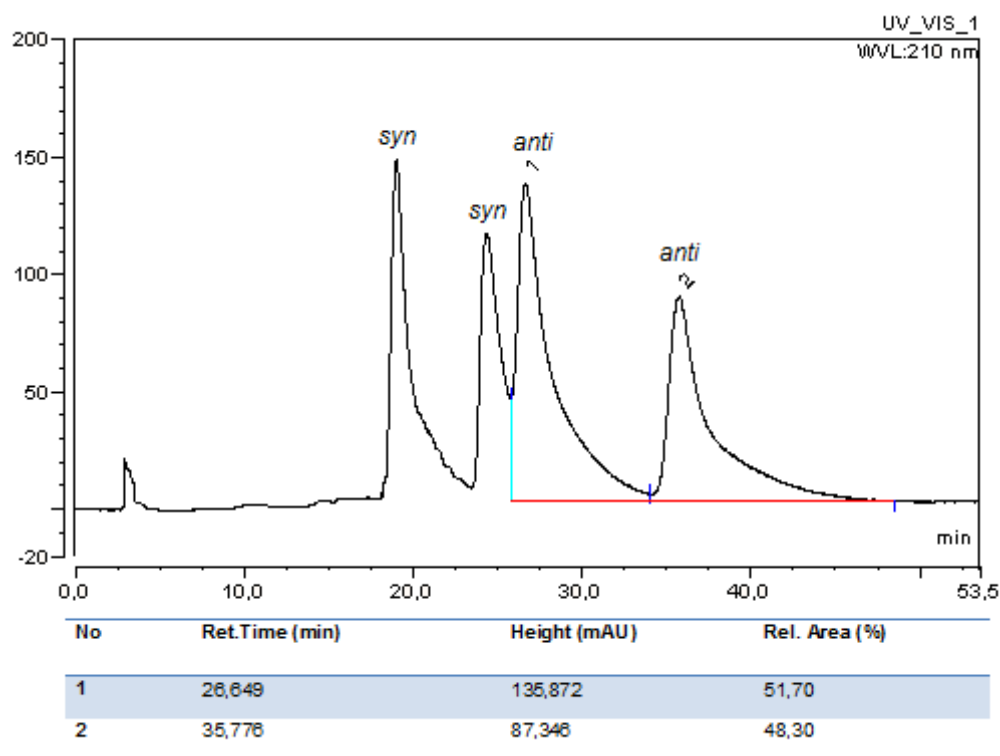


Figure A. 58 HPLC chromatogram of racemic mixture of **53**

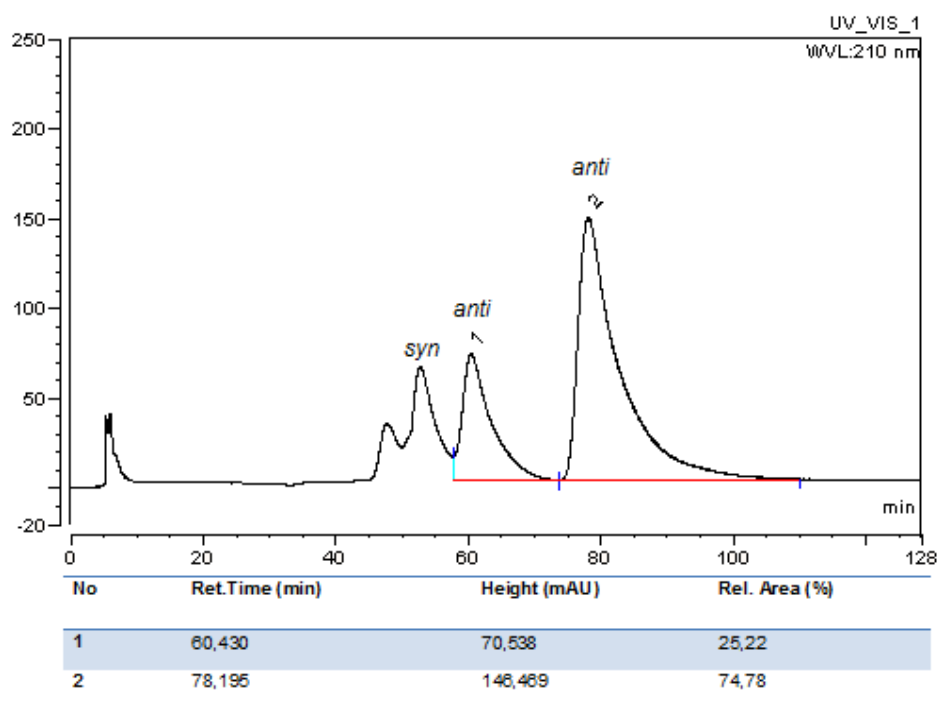


Figure A. 59 HPLC chromatogram of **54**

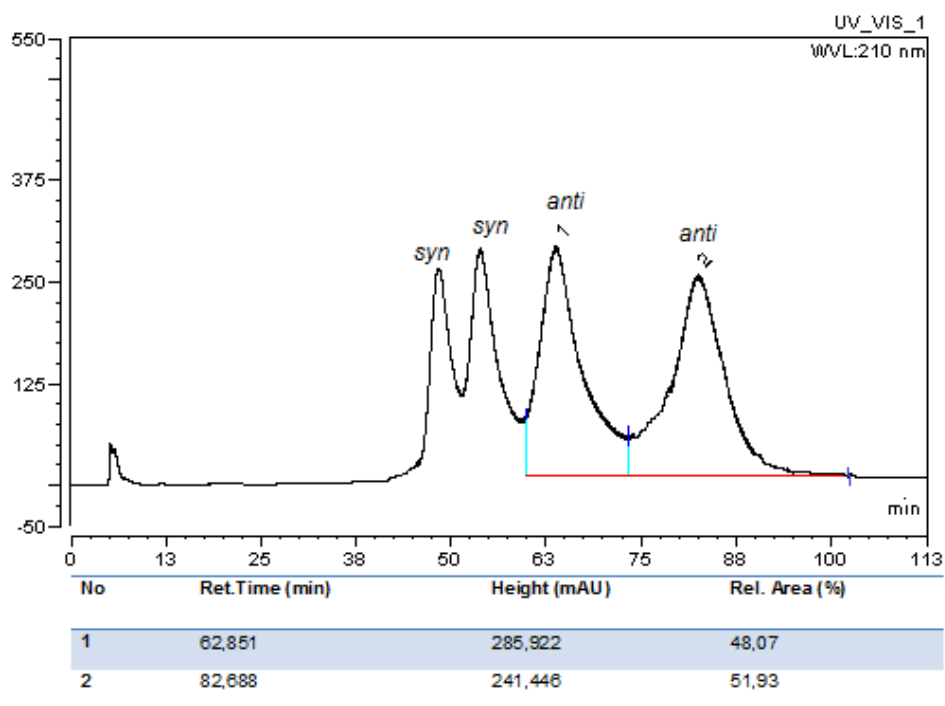


Figure A. 60 HPLC chromatogram of racemic mixture of **54**

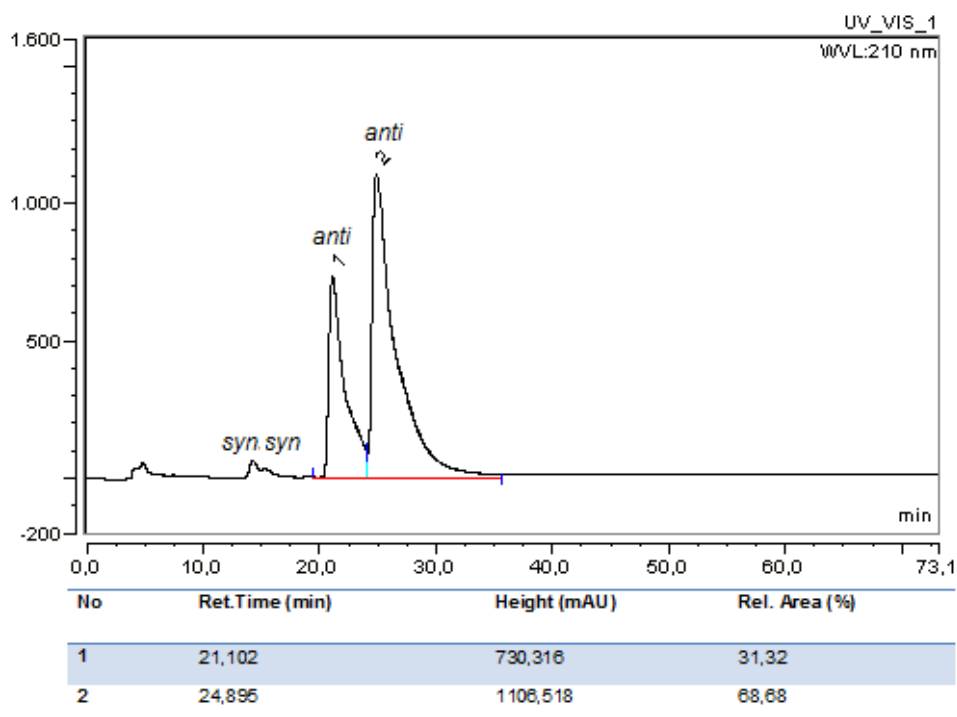


Figure A. 61 HPLC chromatogram of **55**

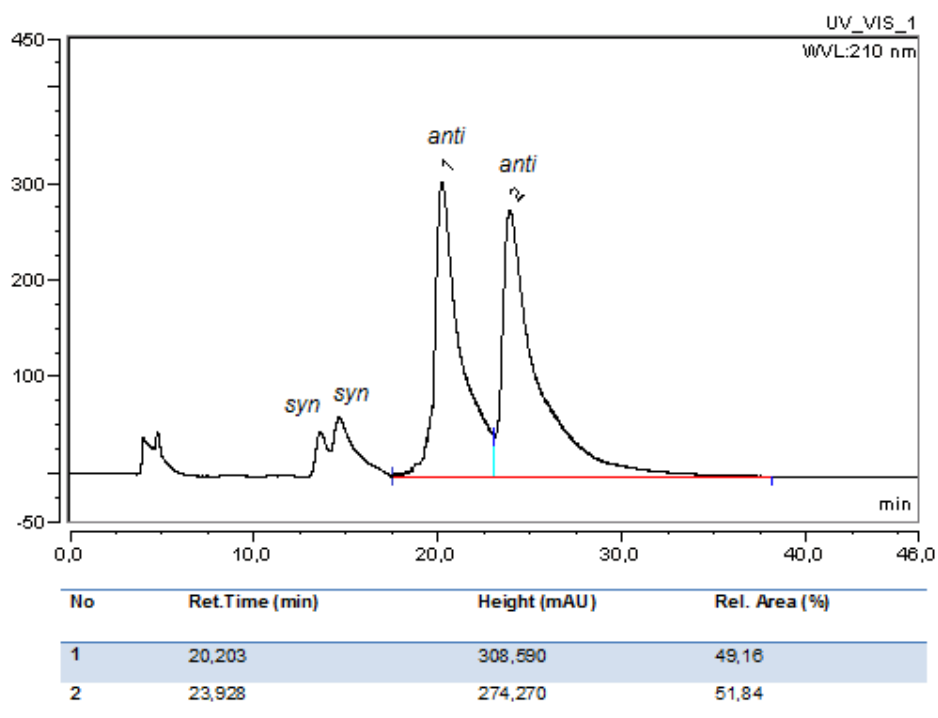


Figure A. 62 HPLC chromatogram of racemic mixture of **55**